Supplementary Information

# HeliDye1: helquat fluorogenic probe specific for AT-rich DNA duplexes

Erika Kužmová, [a] Vishwas D. Joshi, [a] Jaroslav Kozák, [a] Lukáš Severa, [a] Lucie Bednárová, [a] Yevgen Yurenko, [a] Juraj Dobiaš, [a] Adam Pecina, [a] Cemal Köprülüoğlu, [a,b] Petr Jurečka, [c] Martin Lepšík, [a] Pavel Hobza, [a,b] Ivana Císařová, [d] Radek Pohl, [a] Piotr Jurkiewicz, [e] Marek Cebecauer, [e] Radek Trojanec, [f] Petr Džubák, [f] Marián Hajdúch, [f] Filip Teplý, * [a] Paul E. Reyes-Gutiérrez,* [a] and Zbigniew Zawada* [a,g]

## Table of contents

## 1. General information

All reactions were carried out under an inert atmosphere of dry argon. Glassware was dried in an oven or by heat-gun in vacuum shortly before the experiments. Liquids and solutions were transferred *via* needle and syringe under inert atmosphere unless stated otherwise. Melting points were determined on a Wagner & Munz PolyTherm A micro melting point apparatus and are uncorrected. Thin-layer chromatography (TLC) analysis was performed on silica gel plates (Silica gel 60 $F_{254}$-coated aluminum sheets, Merck, cat. no. 1.05554.0001) and visualized by UV (UV lamp 254/365 nm, Spectroline® Model ENF– 240C/FE). TLC analysis of dications was achieved using Stoddart's magic mixture[1] (MeOH : $NH_4Cl$ aq. (2 M) : $MeNO_2$, 7 : 2 : 1) as eluent on silica gel plates. Sonication was conducted with a BANDELIN SONOREX sonicator. Chemical shifts are given in δ-scale as parts per million (ppm); coupling constants (*J*) are given in Hertz (Hz). Peaks in $^1$H and $^{13}$C NMR spectra in acetone-$d_6$ were referenced relative to the solvent residual peak ($CHD_2COCD_3$, $\delta_H$ = 2.09 ppm) and $CD_3COCD_3$ ($\delta_C$ = 29.80 ppm); in $CDCl_3$ relative to the solvent peak $\delta_H$ = 7.26 ppm and $\delta_C$ = 77.00 ppm; and in DMSO-$d_6$ $\delta_H$ = 2.50 ppm and $\delta_C$ = 39.50 ppm. IR spectra were obtained at the NMR and Molecular Spectroscopy Facility operated by the Institute of Organic Chemistry and Biochemistry, Czech Academy of Sciences (IOCB CAS). They were recorded on a Nicolet 6700 spectrometer in KBr pellets. Abbreviations for intensities of IR bands are as follows: s for strong, vs for very strong, m for medium, w for weak, vw for very weak, br for broad, sh for shoulder. Mass spectral data were obtained at the Mass Spectrometry Facility operated by the Institute of Organic Chemistry and Biochemistry, Czech Academy of Sciences (IOCB CAS). ESI mass spectra were recorded using a Thermo Scientific LCQ Fleet mass spectrometer equipped with an electrospray ion source and controlled by Xcalibur software. The mobile phase consisted of MeOH: water (9 : 1) at a flow rate of 200 μL/min. The sample was dissolved, diluted with the mobile phase and injected using a 5 μL loop. Spray voltage, capillary voltage, tube lens voltage and capillary temperature were 5.5kV, 5V, 80V and 275°C, respectively. HR MS spectra were obtained with the ESI instrument.

The instruments used are listed below:

- NMR spectrometers: Bruker Avance 600 (600 MHz for $^1$H, 151 MHz for $^{13}$C) or Bruker Avance 400 (400 MHz for $^1$H, 100.6 MHz for $^{13}$C).
- For imaging of well plates: ChemiDoc UV-transilluminator (BIO-RAD) imaging device using $\lambda_{excitation}$ = 302 nm.
- For fluorescent imaging in cuvettes: 3UV™ transilluminator with $\lambda_{excitation}$ = 312 nm.
- Microplate reader: TECAN infinite M1000 series.
- UV-vis and fluorescence spectrometer: Varian Cary 5000 series UV-vis spectrometer; Fluoromax-4 spectrofluorometer (HORIBA Scientific).
- Cell cytometry: BD FACS Aria™ cell sorter.
- Fluorescence microscopy: Zeiss Axio Observer A1, 10x objective microscope; Zeiss LSM 780 confocal microscope.
- Super-resolution microscopy: Zeiss Elyra PS.1, 100x/1.46 Oil DIC M27 Elyra Objective alpha Plan-Apochromat, Tube Lens 1.6x, FWFOVPosition TIRF_HP, Axio Observer Andor1
- Viscometer: Lovis 2000 M/ME rolling-ball viscometer, Anton Paar GmbH.
- Centrifuge: Biosan LMC3000 series.
- CD spectroscopy: Jasco-815 spectropolarimeter.
- IR spectroscopy: Nicolet 6700.
- Visualization of gels: Typhoon FLA 9500 fluorescence scanner, GE Healthcare, USA.
- *NanoDrop*™ 1000 spectrophotometer, Thermo Scientific.
- Fluorescence lifetime: IBH 5000 U Time Resolved Fluorescence spectrometer.

## 2. Materials

All starting materials, reagents and solvents were obtained from commercial suppliers and used without further purification unless stated otherwise. MeOH and EtOH were dried by distilling from the respective magnesium alcoholates prepared by dissolving Mg turnings in crude solvents.

Acetonitrile (Sigma-Aldrich, 675415).
BPES buffer [$Na_2HPO_4$ (6 mM), $NaH_2PO_4$ (2 mM), $Na_2EDTA$ (1 mM), and NaCl (150 mM)], pH = 7.2.
Coumarin 153 (Sigma-Aldrich, 546186).
Deoxyribonucleic acid sodium salt from calf thymus (Sigma-Aldrich, D1501).
Diethyl ether (Penta chemicals, 12180).
Diisopropyl ether (Sigma-Aldrich, 296856).
DMSO (Sigma Life sciences, D2650).
DNA Oligonucleotides (Generi Biotech) and RNA oligonucleotide (Sigma Life sciences).

| | *Sequence (5'-3')* | *Generic name* |
|---|---|---|
| 1 | ds(CAATCGGATCGAATTCGATCCGATTG) | ds26 |
| 2 | ds(AAAATTTTAAAATTTT) | |
| 3 | ds(AATTAATTAATTAATT) | |
| 4 | ds(GCAAATTTGCGCAAATTTGC) | |
| 5 | ds(CGAATTCGCGAATTCG) | |
| 6 | ds(CGCGAATTCGCGCGCGAATTCGCG) | |
| 7 | ds(ATCCGGATATCCGGAT) | |
| 8 | ds(CAATCGGATCGAATTCGATCCGATTG) | |
| 9 | ds(GGCAAAAACGCGGTCCGCGTTTTTGCC) | |
| 10 | ds(GGCAAAACCGCGGTCCGCGGTTTTGCC) | |
| 11 | ds(GGCAAAGCCGCGGTCCGCGGCTTTGCC) | |
| 12 | ds(GGCAACGCCGCGGTCCGCGGCGTTGCC) | |
| 13 | ds(GGCAGCGCCGCGGTCCGCGGCGCTGCC) | |
| 14 | ds(GGCCGCGCCGCGGTCCGCGGCGCGGCC) | |
| 15 | ds(CCCCGGGGCCCCGGGG) | |
| 16 | ds(CCGGCCGGCCGGCCGG) | |
| 17 | ss(CCAGTTCGTAGTAACCC) | |
| 18 | ss(AAAAAAAAAAAAAAAA) | |
| 19 | ss(TTTTTTTTTTTTTTTT) | |
| 20 | ds(CAAUCGGAUCGAAUUCGAUCCGAUUG) | ds26-dsRNA |

3,4-Dimethoxybenzaldehyde (Sigma-Aldrich, 143758).
1,4-Dimethylpyridinium iodide (compound **8**, Sigma-Aldrich, 376434).
3-Ethoxy-4-methoxybenzaldehyde (Sigma-Aldrich, 252751).
4-Ethoxy-3-methoxybenzaldehyde (Sigma-Aldrich, 516406).
EtOH (Penta Chemicals, 70390).
EtOH for UV-vis spectroscopy (Lach-ner, 20025-U99).
GelRed™ (Biotium, 41003).
Hoechst 33258 (Thermo Scientific, H1398).

MeOH (Penta Chemicals, 21190).
Nuclease free water (Qiagen, 129114).
Nunc™ F96 MicroWell™ black polystyrene plate (Thermo Scientific, 137103).
Propidium iodide (Life Technologies, P3566).
Pyrrolidine (Sigma-Aldrich, 83240).
Stoddart's magic mixture[1] = MeOH : $NH_4Cl$ (2 M) : $MeNO_2$ = 7 : 2 : 1.
Tetra-*n*-butylammonium bromide (Sigma-Aldrich, 818839).

## 3. Abbreviations

ds = double stranded
ECD = electronic circular dichroism
equiv. = equivalents
FACS = fluorescence activated cell sorting
PI = propidium iodide
RT = room temperature
ss = single stranded
$TfO^-$ = trifluoromethanesulfonyl anion
TLC = thin-layer chromatography

# 4. Experimental procedures and analytical data

## *4.1. General procedure for the synthesis of helquat dyes HeliDye1, 6a and 6b:*

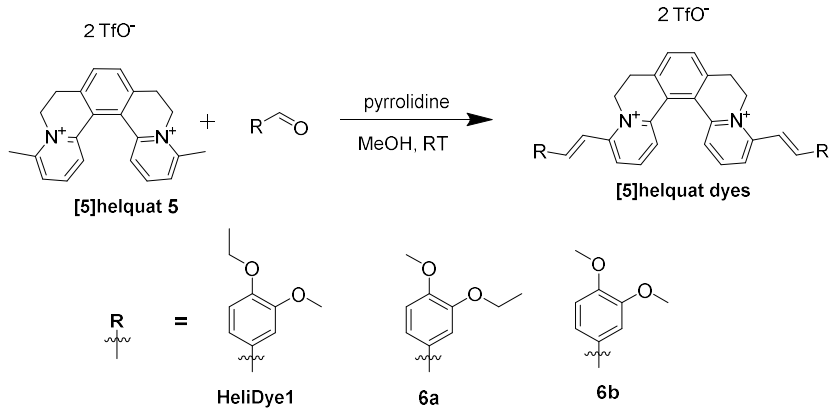


[5]Helquat **5** (0.082 mmol) and respective aldehyde (1.230 mmol, 15 equiv.) were placed into an oven dried Schlenk flask equipped with a rubber septum and a stirring bar. Content of the Schlenk flask was placed under argon atmosphere. Dry MeOH (5 mL) and pyrrolidine (1.230 mmol) were added and the resulting mixture was stirred at RT. The flask was protected from ambient light using Alufoil cover. A color change was observed immediately after addition of pyrrolidine. Progress of the reaction was monitored by TLC analysis with the first TLC typically after 30 minutes (mobile phase: Stoddart's magic mixture, see *Materials Section*). After complete consumption of starting helquat was detected by TLC analysis**,** $Et_2O$ (40 mL) was added to the reaction mixture to precipitate crude product, which was separated from supernatant after sonication and centrifugation. Isolated crude solid was further purified using re-precipitation from its acetonitrile solution (6 mL) by addition of $Et_2O$ (36 mL). This dissolution/precipitation procedure was repeated two times. Each time, solid and liquids were sonicated together to get a free-flowing suspension followed by centrifugation to settle down the solid. After final separation of supernatants, the solid pellet was re-suspended in $Et_2O$ (8-10 mL) and transferred into a pre-weighed vial for storage. After separation of $Et_2O$, the solid product was dried under high vacuum to remove the residual solvents.

## *HeliDye1*

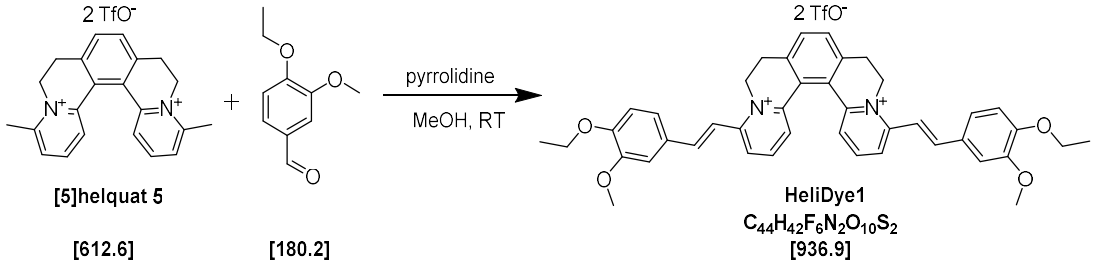


**HeliDye1** was synthesized by stirring mixture containing [5]helquat **5** (50 mg, 0.082 mmol), 4-ethoxy-3-methoxybenzaldehyde (222 mg, 1.232 mmol, 15 equiv.), pyrrolidine (101 µL, 87.5 mg, 1.230 mmol, 15 equiv.) and dry MeOH (5 mL) at RT until complete consumption of **5** was detected by TLC analysis (2.5 h). By following the purification procedure described in the general procedure, **HeliDye1** was obtained as an orange solid. Yield: 64 mg, 0.068 mmol, 83%.

**Analytical data:** m.p. 263-265 °C.

$^1$H NMR (600 MHz, DMSO-$d_6$): 1.38 (t, $J$ = 7.0 Hz, 6H), 3.23 (ddd, $J$ = 4.5, 14.0, 17.1, 2H), 3.36 (ddd, $J$ = 2.0, 3.5, 17.1, 2H), 3.90 (s, 6H), 4.12 (q, $J$ = 7.0 Hz, 4H), 4.50 (dt, $J$ = 3.5, 13.6, 13.6 Hz, 2H), 5.40 (bdd, $J$ = 2.0, 4.5, 13.4 Hz, 2H), 7.11 (d, $J$ = 8.0 Hz, 2H), 7.45 (dd, $J$ = 2.1, 8.5 Hz, 2H), 7.55 (d, $J$ = 2.1

Hz, 2H), 7.68 (d, *J* = 15.8 Hz, 2H), 7.79 (s, 2H), 7.85 (d, *J* = 15.8 Hz, 2H), 7.98 (dd, *J* = 1.3, 8.0 Hz, 2H), 8.15 (t, *J* = 7.9 Hz, 2H), 8.34 (dd, *J* = 1.3, 7.8 Hz, 2H).

$^{13}$C NMR (151 MHz, DMSO-$d_6$): 14.6, 26.9, 49.1, 55.8, 63.9, 110.8, 112.5, 115.7, 123.7, 124.7, 127.1, 127.7, 127.7, 131.0, 139.9, 142.0, 143.8, 146.2, 149.2, 150.7, 153.8.

IR (KBr) *v* (cm$^{-1}$): 551 w, 637 m, 813 s, 822 s, 962 m, 1029 s, 1141 s, 1171 s, 1230 w, 1259 w, 1425 w, 1475 w, 1490 w, 1513 m, 1563 w, 1597 m, 1610 w, 1622 w, 2841 w, 2928 w, 2983 w, 3075 w.

MS (ESI) *m/z* (%): 185.1 (23), 227.1 (91), 251.1 (17), 319.2 [(M - 2TfO)$^{2+}$] (100), 319.7 (45), 320.2 (10), 413.3 (5), 637.3 (5), 787.3 [(M - TfO)$^{+}$] (3). HRMS (ESI) *m/z*: [(M - 2TfO)$^{2+}$] [($C_{42}H_{42}O_4N_2$)$^{2+}$] calcd: 319.15668, found: 319.15659.

## *[5]helquat dye 6a:*

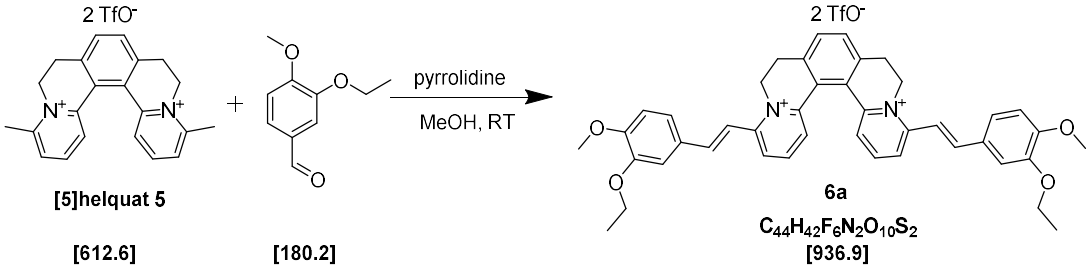


[5]Helquat dye **6a** was synthesized by stirring mixture containing [5]helquat **5** (50 mg, 0.082 mmol), 3-ethoxy-4-methoxybenzaldehyde (222 mg, 1.232 mmol, 15 equiv.), pyrrolidine (101 µL, 87.5 mg, 1.230 mmol, 15 equiv.) and dry MeOH (5 mL) at RT until complete consumption of **5** was detected by TLC analysis (2.5 h). By following the purification procedure described in the general procedure, [5]helquat dye **6a** was obtained as a yellow solid. Yield: 65 mg, 0.069 mmol, 84%.

**Analytical data:** m.p. 268-270 °C.

$^{1}$H NMR (400 MHz, DMSO-$d_6$): 1.40 (t, *J* = 7.0 Hz, 6H), 3.23 (ddd, *J* = 4.5, 14.0, 17.1, 2H), 3.36 (ddd, *J* = 2.0, 3.5, 17.1, 2H), 3.86 (s, 6H), 4.12 (q, *J* = 7.0 Hz, 4H), 4.50 (dt, *J* = 3.5, 13.6, 13.6 Hz, 2H), 5.40 (bdd, *J* = 2.0, 4.5, 13.4 Hz, 2H), 7.12 (d, *J* = 8.4 Hz, 2H), 7.45 (dd, *J* = 2.0, 8.4 Hz, 2H), 7.55 (d, *J* = 2.1 Hz, 2H), 7.68 (d, *J* = 15.8 Hz, 2H), 7.79 (s, 2H), 7.85 (d, *J* = 15.8 Hz, 2H), 7.98 (dd, *J* = 1.3, 8.0 Hz, 2H), 8.15 (t, *J* = 8.1 Hz, 2H), 8.34 (dd, *J* = 3.9, 6.9 Hz, 2H).

$^{13}$C NMR (101 MHz, DMSO-$d_6$): 14.7, 26.9, 49.2, 55.7, 64.1, 111.7, 111.8, 115.7, 123.7, 124.7, 127.1, 127.7, 127.8, 131.0, 140.0, 142.0, 143.8, 146.5, 148.3, 151.6, 153.9.

IR (KBr) *v* (cm$^{-1}$): 517 w, 551 w, 574 m, 639 m, 966 w, 1031 m, 1261 s, 1437 w, 1473 w, 1490 w, 1513 w, 1562 w, 1596 m, 1610 w, 1623 m, 2853 w, 2929 w, 2979 w, 3076 w.

MS (ESI) *m/z* (%): 305.1 (10), 319.2 [(M - 2TfO)$^{2+}$] (100), 319.7 (46), 320.2 (11), 637.3 (4), 787.3 [(M - TfO)$^{+}$] (15), 788.3 (10). HRMS (ESI) *m/z*: [(M - 2TfO)$^{2+}$] [($C_{42}H_{42}O_4N_2$)$^{2+}$] calcd: 319.15668, found: 319.15674.

## *[5]helquat dye 6b:*

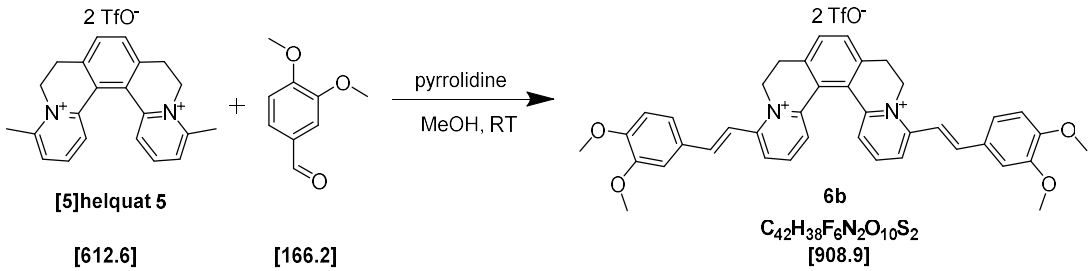

[5]Helquat dye **6b** was synthesized by stirring mixture containing [5]helquat **5** (50 mg, 0.082 mmol), 3,4-dimethoxybenzaldehyde (204 mg, 1.228 mmol, 15 equiv.), pyrrolidine (101 µL, 87.5 mg, 1.230 mmol, 15 equiv.) and dry MeOH (5 mL) at RT until complete consumption of **5** was detected by TLC analysis (2.5 h). By following the purification procedure described in the general procedure, [5]helquat dye **6b** was obtained as a yellow solid. Yield: 61 mg, 0.067 mmol, 82%.

**Analytical data:** m.p. 264-266 °C.

$^{1}$H NMR (400 MHz, DMSO-$d_6$): 3.23 (ddd, $J$ = 4.5, 14.0, 17.1, 2H), 3.36 (ddd, $J$ = 2.0, 3.5, 17.1, 2H), 3.86 (s, 6H), 3.90 (s, 6H), 4.50 (dt, $J$ = 3.5, 13.6, 13.6 Hz, 2H), 5.40 (bdd, $J$ = 2.0, 4.5, 13.4 Hz, 2H), 7.12 (d, $J$ = 8.5 Hz, 2H), 7.46 (dd, $J$ = 1.9, 8.5 Hz, 2H), 7.56 (d, $J$ = 1.9 Hz, 2H), 7.70 (d, $J$ = 15.8 Hz, 2H), 7.79 (s, 2H), 7.86 (d, $J$ = 15.8 Hz, 2H), 7.99 (td, $J$ = 0.3, 8.1 Hz, 2H), 8.15 (t, $J$ = 8.1 Hz, 2H), 8.34 (dd, $J$ = 1.3, 8.1 Hz, 2H).

$^{13}$C NMR (101 MHz, DMSO-$d_6$): 26.9, 49.2, 55.7, 55.9, 110.7, 111.7, 115.8, 123.7, 124.7, 127.1, 127.1, 127.8, 131.1, 140.0, 142.0, 143.8, 146.5, 149.1, 151.5, 153.9.

IR (KBr) $v$ (cm$^{-1}$): 518 w, 559 w, 574 m, 639 s, 966 w, 1031 s, 1143 br, 1262 br, 1424 m, 1473 m, 1491 m, 1514 w, 1563 m, 1597 m, 1611 w, 1623 w, 2840 w, 2939 w, 2979 w, 3005 w, 3076 w.

MS (ESI) *m/z* (%): 231.2 (22), 305.2 [(M – 2TfO)$^{+2}$] (100), 305.8 (58), 306.3, 461.4 (29), 462.4 (12), 609.5 (19), 611.5 (21), 612.5 (9), 723.6 (21), 759.5 [(M - TfO)$^{+}$] (74), 760.6 (35). HRMS (ESI) *m/z*: [(M - 2TfO)$^{2+}$] [($C_{40}H_{38}O_4N_2$)$^{2+}$] calcd: 305.14103, found: 305.14104.

## *4.2. General procedure for the synthesis of helquat dyes 7a, 7b and 7c:*

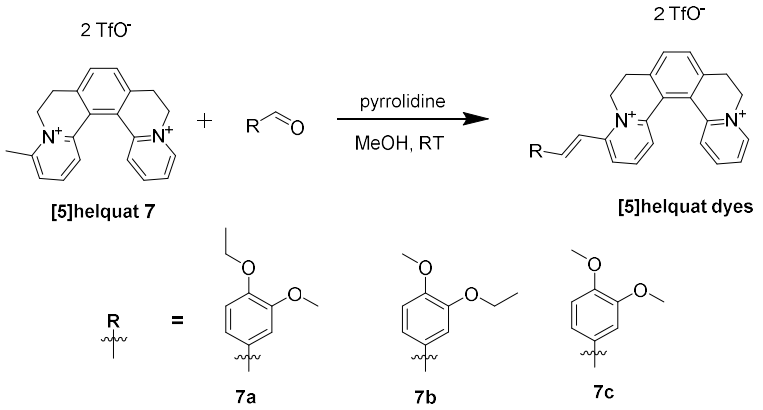


[5]Helquat **7** (0.082 mmol) and respective aldehyde (1.230 mmol, 15 equiv.) were placed into an oven dried Schlenk flask equipped with a rubber septum and a stirring bar. Content of the Schlenk flask was placed under argon atmosphere. Dry MeOH (5 mL) and pyrrolidine (1.230 mmol) were added and the resulting mixture was stirred at RT. The flask was protected from ambient light using Alufoil cover. A color change was observed immediately after addition of pyrrolidine. Progress of the reaction was monitored by TLC analysis with the first TLC typically after 30 minutes (mobile phase: Stoddart's magic mixture, see *Materials Section*). After complete consumption of starting helquat was detected by TLC analysis**,** $Et_2O$ (40 mL) was added to the reaction mixture to precipitate crude product, which was separated from supernatant after sonication and centrifugation. Isolated crude solid was further purified using re-precipitation from its acetonitrile solution (6 mL) by addition of $Et_2O$ (36 mL). This dissolution/precipitation procedure was repeated two times. Each time, solid and liquids were sonicated together to get a free-flowing suspension followed by centrifugation to settle down the solid. After final separation of supernatants, the solid pellet was re-suspended in $Et_2O$ (8-10 mL) and transferred into a pre-weighed vial for storage. After separation of $Et_2O$, the solid product was dried under high vacuum to remove the residual solvents.

## *[5]helquat dye 7a:*

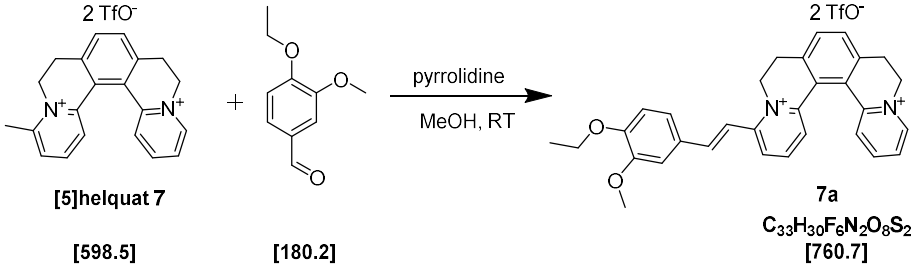


[5]Helquat dye **7a** was synthesized by stirring mixture containing [5]helquat **7** (50 mg, 0.084 mmol), 4-ethoxy-3-methoxybenzaldehyde (227 mg, 1.260 mmol, 15 equiv.), pyrrolidine (103 µL, 89.6 mg, 1.260 mmol, 15 equiv.) and dry MeOH (5 mL) at RT until complete consumption of **7** was detected by TLC analysis (1 h). By following the purification procedure described in the general procedure, [5]helquat dye **7a** was obtained as a yellow solid. Yield: 61 mg, 0.080 mmol, 95%.

**Analytical data:** m.p. 231-233 °C.

$^{1}$H NMR (400 MHz, DMSO-$d_6$): 1.37 (t, $J$ = 7.0 Hz, 3H), 3.23 (ddd, $J$ = 4.5, 14.0, 17.1, 2H), 3.36 (ddd, $J$ = 2.0, 3.5, 17.1, 2H), 3.90 (s, 3H), 4.12 (q, $J$ = 7.0 Hz, 2H), 4.45 (dt, $J$ = 3.5, 13.6, 13.6 Hz, 1H), 4.83 (dt, $J$ = 3.5, 13.6, 13.6 Hz, 1H), 5.04 (bdd, $J$ = 2.0, 4.5, 13.4 Hz, 1H), 5.40 (bdd, $J$ = 2.0, 4.5, 13.4 Hz, 1H), 7.10 (d, $J$ = 8.4 Hz, 1H), 7.45 (dd, $J$ = 1.9, 8.4 Hz, 1H), 7.55 (d, $J$ = 1.9 Hz, 1H), 7.69 (d, $J$ = 15.8 Hz, 1H), 7.77 (d, $J$ = 7.8 Hz, 1H), 7.80 (d, $J$ = 7.9 Hz, 1H), 7.87 (d, $J$ = 15.8 Hz, 1H), 8.01-8.06 (m, 2H), 8.17 (t, $J$ = 8.2 Hz, 1H), 8.20 (d, $J$ = 8.2 Hz, 1H), 8.28 (t, $J$ = 7.9 Hz, 1H), 8.36 (d, $J$ = 8.2 Hz, 1H), 9.19 (d, $J$ = 6.1 Hz, 1H).

$^{13}$C NMR (101 MHz, DMSO-$d_6$): 14.6, 26.9, 49.2, 54.4, 55.8, 63.9, 110.8, 112.5, 115.7, 119.1, 122.3, 123.7, 124.9, 126.1, 126.3, 127.1, 127.6, 127.7, 129.6, 131.5, 131.6, 140.1, 142.2, 143.9, 144.1, 145.8, 146.1, 146.6, 149.2, 150.7, 154.0.

IR (KBr) $\nu$ (cm$^{-1}$): 518 m, 551 w, 573 m, 638 m, 972 m,1031 s, 1156 m, 1261 s, 1425 w, 1478 w, 1490 w, 1512 w, 1564 w, 1596 w, 1613 m, 1625 m, 2836 w, 2939 w, 2986 w, 3078 w.

MS (ESI) *m/z* (%): 217.1 (9), 231.1 [(M - 2TfO)$^{2+}$] (100), 231.6 (35), 232.1 (5), 461.2 (8), 611.2 [(M - TfO)$^{+}$] (100), 612.2 (35). HRMS (ESI) *m/z*: [(M - 2TfO)$^{2+}$] [($C_{31}H_{30}O_2N_2$)$^{2+}$] calcd: 231.11482, found: 231.11487.

## *[5]helquat dye 7b:*

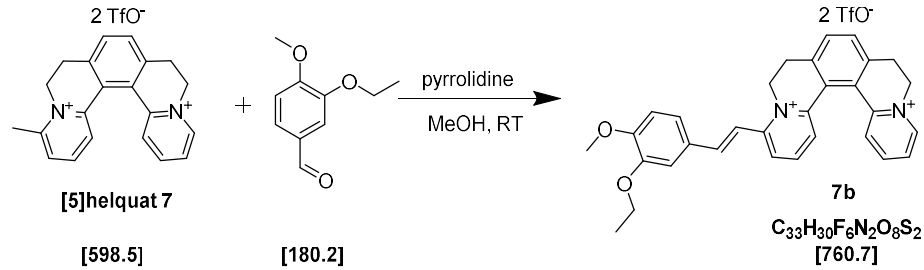


[5]Helquat dye **7b** was synthesized by stirring mixture containing [5]helquat **7** (50 mg, 0.084 mmol), 3-ethoxy-4-methoxybenzaldehyde (227 mg, 1.258 mmol, 15 equiv.), pyrrolidine (103 µL, 89.6 mg, 1.260 mmol, 15 equiv.) and dry MeOH (5 mL) at RT until complete consumption of **7** was detected by TLC analysis (1 h). By following the purification procedure described in the general procedure, [5]helquat dye **7b** was obtained as a yellow solid. Yield: 53 mg, 0.070 mmol, 83%.

**Analytical data:** m.p. 260-262 °C.

$^1$H NMR (400 MHz, DMSO-$d_6$): 1.40 (t, $J$ = 7.0 Hz, 3H), 3.23 (ddd, $J$ = 4.5, 14.0, 17.1 Hz, 2H), 3.36 (ddd, $J$ = 2.0, 3.5, 17.1 Hz, 2H), 3.86 (s, 3H), 4.12 (q, $J$ = 7.0 Hz, 2H), 4.45 (dt, $J$ = 3.5, 13.6, 13.6 Hz, 1H), 4.83 (dt, $J$ = 3.5, 13.6, 13.6 Hz, 1H), 5.04 (bdd, $J$ = 2.0, 4.5, 13.4 Hz, 1H), 5.40 (bdd, $J$ = 2.0, 4.5, 13.4 Hz, 1H), 7.12 (d, $J$ = 8.5 Hz, 1H), 7.45 (dd, $J$ = 2.0, 8.5 Hz, 1H), 7.55 (d, $J$ = 2.0 Hz, 1H), 7.68 (d, $J$ = 15.8 Hz, 1H), 7.77 (d, $J$ = 7.8 Hz, 1H), 7.81 (d, $J$ = 7.8 Hz, 1H), 7.86 (d, $J$ = 15.8 Hz, 1H), 8.04 (td, $J$ = 1.5, 6.1 Hz, 1H), 8.05 (dd, $J$ = 0.9, 7.9 Hz, 1H), 8.16 (t, $J$ = 8.1 Hz, 1H), 8.20 (dd, $J$ = 1.3, 8.3 Hz, 1H), 8.27 (dd, $J$ = 1.4, 15.9 Hz, 1H), 8.36 (dd, $J$ = 1.1, 8.3 Hz, 1H), 9.19 (dd, $J$ = 1.0, 6.1 Hz, 1H).

$^{13}$C NMR (101 MHz, DMSO-$d_6$): 14.7, 26.8, 26.9, 49.2, 54.4, 55.7, 64.1, 111.7, 111.8, 115.7, 119.1, 122.3, 123.8, 124.9, 126.1, 126.3, 127.1, 127.6, 127.8, 129.6, 131.5, 140.1, 142.2, 143.9, 144.1, 145.7, 146.1, 146.6, 148.3, 151.6, 154.0.

IR (KBr) $\nu$ (cm$^{-1}$): 518 m, 552 w, 575 m, 640 m, 967 w, 1031 s, 1143 w, 1162 m, 1261 s, 1436 w, 1478 w, 1490 w, 1513 m, 1564 m, 1596 w, 1612 w, 1625 w, 2838 w, 2984 w, 3076 w.

MS (ESI) *m/z* (%): 231.1 [(M - 2TfO)$^{2+}$] (100), 231.6 (35), 232.1 (5), 461.2 (8), 611.2 [(M - TfO)$^+$] (100), 612.2 (35). HRMS (ESI) *m/z*: [(M - 2TfO)$^{2+}$] [($C_{31}H_{30}O_2N_2$)$^{2+}$] calcd: 231.11482, found: 231.11487.

## *[5]helquat dye 7c:*

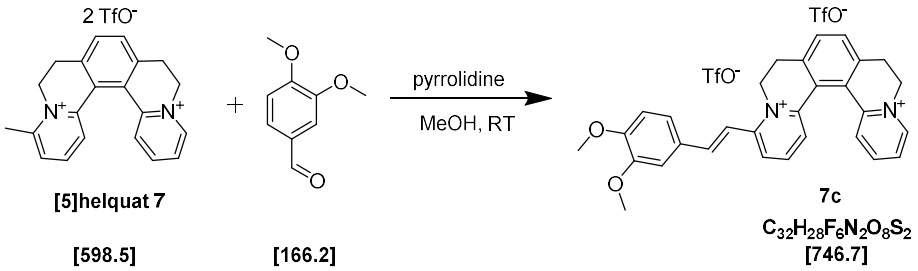


[5]Helquat dye **7c** was synthesized by stirring mixture containing [5]helquat **7** (50 mg, 0.084 mmol), 3,4-dimethoxybenzaldehyde (209 mg, 1.258 mmol, 15 equiv.), pyrrolidine (103 µL, 89.6 mg, 1.260 mmol, 15 equiv.) and dry MeOH (5 mL) at RT until complete consumption of **7** was detected by TLC analysis (1 h). By following the purification procedure described in the general procedure, [5]helquat dye **7c** was obtained as a yellow solid. Yield: 53 mg, 0.071 mmol, 85%.

**Analytical data:** m.p. 272-273 °C.

$^1$H NMR (400 MHz, DMSO-$d_6$): 3.23 (ddd, $J$ = 4.5, 14.0, 17.1 Hz, 2H), 3.36 (ddd, $J$ = 2.0, 3.5, 17.1 Hz, 2H), 3.86 (s, 3H), 3.90 (s, 3H), 4.45 (dt, $J$ = 3.5, 13.6, 13.6 Hz, 1H), 4.83 (dt, $J$ = 3.5, 13.6, 13.6 Hz, 1H), 5.04 (bdd, $J$ = 2.0, 4.5, 13.4 Hz, 1H), 5.40 (bdd, $J$ = 2.0, 4.5, 13.4 Hz, 1H), 7.12 (d, $J$ = 8.5 Hz, 1H), 7.45 (dd, $J$ = 2.0, 8.5 Hz, 1H), 7.55 (d, $J$ = 2.0 Hz, 1H), 7.68 (d, $J$ = 15.8 Hz, 1H), 7.77 (d, $J$ = 7.8 Hz, 1H), 7.81 (d, $J$ = 7.8 Hz, 1H), 7.86 (d, $J$ = 15.8 Hz, 1H), 8.04 (td, $J$ = 1.5, 6.1 Hz, 1H), 8.05 (dd, $J$ = 0.9, 7.9 Hz, 1H), 8.16 (t, $J$ = 8.1 Hz, 1H), 8.20 (dd, $J$ = 1.3, 8.3 Hz, 1H), 8.27 (dd, $J$ = 1.4, 15.9 Hz, 1H), 8.36 (dd, $J$ = 1.1, 8.3 Hz, 1H), 9.19 (dd, $J$ = 1.0, 6.1 Hz, 1H).

$^{13}$C NMR (101 MHz, DMSO-$d_6$): 26.8, 26.9, 49.2, 54.4, 55.7, 55.9, 110.7, 111.7, 115.8, 119.1, 122.3, 123.8, 124.9, 126.1, 126.3, 127.6, 127.8, 129.6, 131.5, 131.6, 140.1, 143.9, 144.1, 141.2, 145.8, 146.1, 146.6, 149.1, 151.5, 154.0.

IR (KBr) $\nu$ (cm$^{-1}$): 519 w, 551 w, 574 w, 640 m, 967 w, 1032 s, 1162 m, 1262 s, 1425 w, 1478 w, 1490 w, 1513 m, 1564 m, 1596 m, 1625 w, 2837 w, 3007 w, 3074 w.

MS (ESI) *m/z* (%): 202.1 (5), 216.1 (14), 224.1 [(M - 2TfO)$^{2+}$] (100), 224.6 (31), 225.1 (7), 447.2 (25), 448.2 (12), 479.2 (7), 597.2 [(M - TfO)$^+$] (62), 598.2 (22). HRMS (ESI) *m/z*: [(M - 2TfO)$^{2+}$] [($C_{30}H_{28}O_2N_2$)$^{2+}$] calcd: 224.10699, found: 224.10700.

## *4.3. General procedure for the* synthesis of pyridinium dyes 8a-c and 9a-c

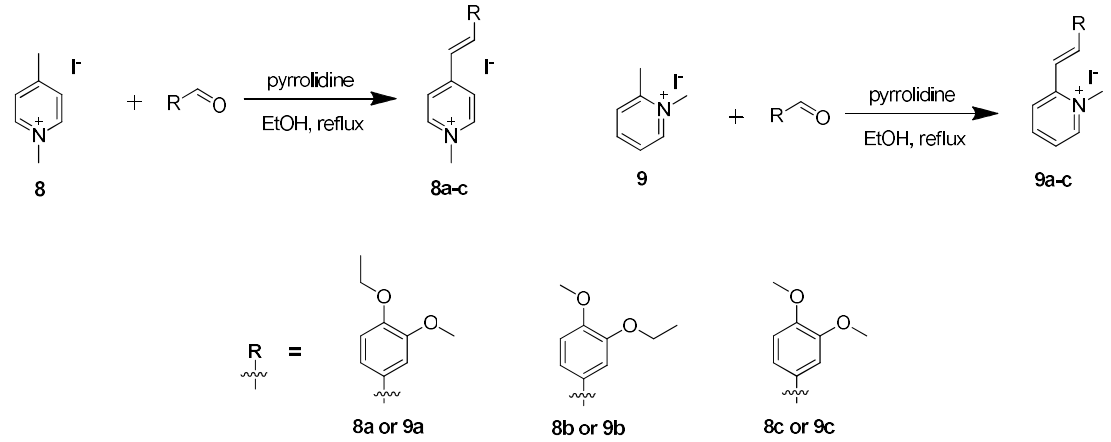


Pyridinium dyes **8a-c** and **9a-c** were synthesized and purified by following this general procedure. Pyridinium dye precursor **8** or **9** (30 mg, 0.128 mmol) and respective aldehyde (0.638 mmol, 5.0 equiv.) were placed into an oven dried Schlenk flask equipped with a rubber septum and a stirring bar. Content of the Schlenk flask was placed under argon atmosphere. Dry EtOH (3 mL) and pyrrolidine (16 µL, 13.7 mg, 0.192 mmol, 1.5 equiv.) were added and the resulting mixture was refluxed under argon. The flask was protected from ambient light using Alufoil cover. A color change was observed immediately after addition of pyrrolidine. Progress of the reaction was monitored by TLC analysis with the first TLC typically after 30 minutes (mobile phase: Stoddart's magic mixture, see *Materials Section*). After complete consumption of starting pyridinium dye precursor was detected by TLC analysis, $Et_2O$ (24 mL) was added to the reaction mixture to precipitate crude product. Crude solid product was separated from supernatant after sonication and centrifugation. Isolated crude solid was further purified using re-precipitation from its acetonitrile solution (6 mL) by addition of $Et_2O$ (36 mL). This dissolution/precipitation procedure was repeated two times. Each time, solid and liquids were sonicated together to get a free-flowing suspension followed by centrifugation to settle down the solid. Finally, solid was washed by sonication with MeOH (1 mL) and after final separation of supernatant, the solid pellet was re-suspended in $Et_2O$ (8-10 mL) and transferred into a pre-weighed vial for storage. After separation of $Et_2O$, the solid product was dried under high vacuum to remove the residual solvents.

### *Pyridinium dye 8a:*

***CAS number: 1106570-90-4***

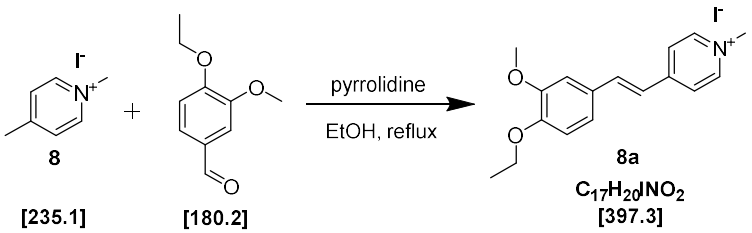


Pyridinium dye **8a** was synthesized by refluxing mixture containing pyridinium dye precursor **8** (30 mg, 0.128 mmol), 4-ethoxy-3-methoxybenzaldehyde (115 mg, 0.638 mmol, 5 equiv.), pyrrolidine (16 µL, 13.7 mg, 0.192 mmol, 1.5 equiv.) and dry EtOH (3 mL) until complete consumption of **8** was detected by TLC analysis (2 h). By following the purification procedure described in the general procedure, pyridinium dye **8a** was obtained as a yellow solid. Yield: 50 mg, 0.126 mmol, 98%.

**Analytical data:** m.p. 268-271 °C.

$^{1}$H NMR (400 MHz, DMSO-$d_6$): 1.35 (t, $J$ = 7.0 Hz, 3H), 3.85 (s, 3H), 4.09 (q, $J$ = 7.0 Hz, 2H), 4.23 (s, 3H), 7.05 (d, $J$ = 8.4 Hz, 1H), 7.28 (d, $J$ = 2.0, 8.4 Hz, 1H), 7.39 (d, $J$ = 2.0 Hz, 1H), 7.42 (d, $J$ = 16.4 Hz, 1H), 7.96 (d, $J$ = 16.3 Hz, 1H), 8.15 (d, $J$ = 7.0 Hz, 2H), 8.80 (d, $J$ = 6.5 Hz, 2H).

$^{13}$C NMR (101 MHz, DMSO-$d_6$): 14.6, 46.7, 55.6, 63.8, 110.0, 112.5, 120.7, 122.9, 123.1, 127.8, 141.0, 144.9, 149.1, 150.4, 152.9.

IR (KBr) $v$ (cm$^{-1}$): 738 w, 778 w, 922 w, 1036 m, 1141 m, 1168 w, 1268 m, 1457 sh, 1426 m, 1474 m, 1519 s, 1579 sh, 1594 s, 1616 s, 1645 m, 2833 w, 2910 w, 3002 w, 3028 w.

MS (ESI) *m/z* (%): 270.2 [(M - I)$^+$] (100), 271.2 (13). HRMS (ESI) m/z: [(M - I$^-$)$^+$] [($C_{17}H_{20}O_2N$)$^+$] calcd: 270.14886, found: 270.14889.

## *Pyridinium dye 8b:*

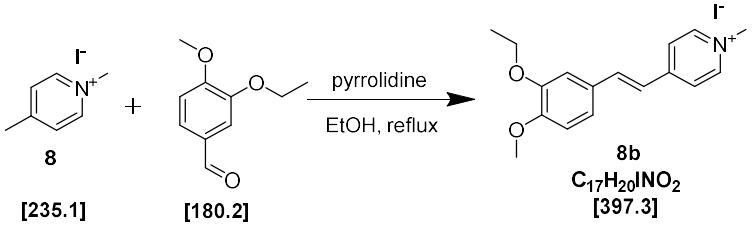


Pyridinium dye **8b** was synthesized by refluxing mixture containing pyridinium dye precursor **8** (30 mg, 0.128 mmol), 3-ethoxy-4-methoxybenzaldehyde (115 mg, 0.638 mmol, 5 equiv.), pyrrolidine (16 µL, 13.7 mg, 0.192 mmol, 1.5 equiv.) and dry EtOH (3 mL) until complete consumption of **8** was detected by TLC analysis (2 h). By following the purification procedure described in the general procedure, pyridinium dye **8b** was obtained as a yellow solid. Yield: 30 mg, 0.076 mmol, 59%.

**Analytical data:** m.p. 263-265 °C.

$^{1}$H NMR (400 MHz, DMSO-$d_6$): 1.37 (t, $J$ = 7.0 Hz, 3H), 3.83 (s, 3H), 4.10 (q, $J$ = 7.0 Hz, 2H), 4.22 (s, 3H), 7.07 (d, $J$ = 8.4 Hz, 1H), 7.28 (dd, $J$ = 2.0, 8.4 Hz, 1H), 7.37 (d, $J$ = 2.0 Hz, 1H), 7.41 (d, $J$ = 16.3 Hz, 1H), 7.94 (d, $J$ = 16.3 Hz, 1H), 8.13 (d, $J$ = 6.8 Hz, 2H), 8.79 (d, $J$ = 6.8 Hz, 2H).

$^{13}$C NMR (101 MHz, DMSO-$d_6$): 14.7, 46.7, 55.6, 63.9, 111.0, 111.8, 120.8, 122.9, 123.1, 128.0, 141.0, 144.9, 148.3, 151.2, 152.9.

IR (KBr) $v$ (cm$^{-1}$): 732 m, 774 w, 924 m, 1043 m, 1140 s, 1265 s, 1432 m, 1469 m, 1517 s, 1580 m, 1594 s, 1616 s, 1643 m, 2838 w, 2929 w, 2977 w, 3028 w, 3076 w.

MS (ESI) *m/z* (%): 270.1 [(M - I)$^+$] (100), 271.2 (22). HRMS (ESI) *m/z*: [(M - I)$^+$] [($C_{17}H_{20}O_2N$)$^{+2}$] calcd: 270.14886, found: 270.14891.

## *Pyridinium dye 8c:*

***CAS number: 97989-24-7*** **(ref.** [2]**)**

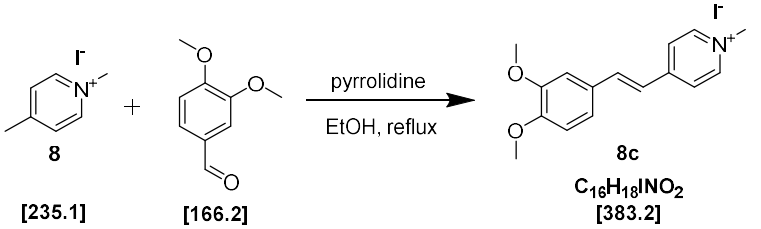


Pyridinium dye **8c** was synthesized by refluxing mixture containing pyridinium dye precursor **8** (30 mg, 0.128 mmol), 3,4-dimethoxybenzaldehyde (106 mg, 0.638 mmol, 5 equiv.), pyrrolidine (16 µL, 13.7 mg, 0.192 mmol, 1.5 equiv.) and dry EtOH (3 mL) until complete consumption of **8** was detected by TLC analysis (2h). By following the purification procedure described in the general procedure, pyridinium dye **8c** was obtained as a yellow solid. Yield: 27 mg, 0.070 mmol, 55%.

**Analytical data:** m.p. 265-267 °C.

$^1$H NMR (400 MHz, DMSO-$d_6$): 3.83 (s, 3H), 3.85 (s, 3H), 4.23 (s, 3H), 7.07 (d, $J$ = 8.4 Hz, 1H), 7.29 (dd, $J$ = 2.0, 8.4 Hz, 1H), 7.40 (d, $J$ = 2.0 Hz, 1H), 7.45 (d, $J$ = 16.2 Hz, 1H), 7.96 (d, $J$ = 16.2 Hz, 1H), 8.15 (d, $J$ = 6.5 Hz, 2H), 8.81 (d, $J$ = 6.5 Hz, 2H).

$^{13}$C NMR (101 MHz, DMSO-$d_6$): 46.8, 55.6, 55.7, 109.9, 111.7, 120.8, 122.9, 123.1, 128.0, 141.0, 145.0, 149.1, 151.1, 152.9.

IR (KBr) $\nu$ (cm$^{-1}$): 740 w, 766 w, 981 w, 1020 m, 1142 m, 1163 m, 1186 m, 1209 m, 1238 m, 1271 s, 1423 m, 1446 w, 1487 m, 1517 s, 1595 s, 1615 s, 1644 m, 2831 w, 2911 w, 2988 w, 3005 w, 3030 w, 3075 w.

MS (ESI) *m/z* (%): 256.2 [(M - I$^-$)$^+$] (100), 257.2 (20). HRMS (ESI) *m/z*: [(M - I$^-$)$^+$] [($C_{16}H_{18}O_2N$)$^+$] calcd: 256.13321, found: 256.13323.

## *1,2-Dimethylpyridin-1-ium iodide 9:*

***CAS number: 872-73-1* (ref. 3)**

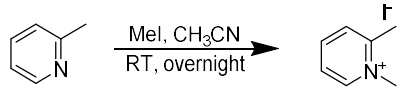


**9**
$C_7H_{10}IN$
[93.1] [235.1]

This compound was prepared by following literature procedure[3]. A reaction mixture containing 2-methylpyridine (4.7 g, 50 mmol) and iodomethane (14.2 g, 100 mmol, 2.0 equiv.) and acetonitrile (50 mL) was stirred at RT, under argon. The reaction progress was monitored by TLC (mobile phase methanol, starting material $R_f$ = 0.80, product $R_f$ = 0.20). After completion of reaction, the hygroscopic, white precipitate was filtered under argon and washed two times with acetonitrile (2 x 5 mL) and two times with $Et_2O$ (2 x 20 mL) and vacuum dried **9** as a white solid. Yield: 9.9 g, 42.0 mmol, 84%.

**Analytical data:** m.p. 237-239 °C.

$^1$H NMR (400 MHz, DMSO-$d_6$): 2.79 (s, 3H), 4.24 (s, 3H), 7.94 (ddd, $J$ = 1.5, 6.3, 7.9 Hz, 1H), 8.05 (dd, $J$ = 1.5, 7.9 Hz, 1H), 8.47 (td, $J$ = 1.5, 7.9 Hz, 1H), 8.98 (d, $J$ = 6.2 Hz, 1H).

## *Pyridinium dye 9a:*

***CAS number: 1106574-87-1***

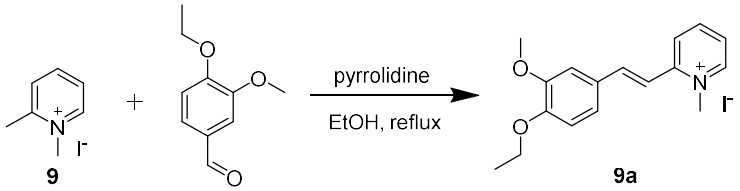


**9** [235.1] + [180.2]

**9a**
$C_{17}H_{20}INO_2$
[397.3]

Pyridinium dye **9a** was synthesized by refluxing mixture containing pyridinium dye precursor **9** (30 mg, 0.128 mmol), 4-ethoxy-3-methoxybenzaldehyde (115 mg, 0.638 mmol, 5 equiv.), pyrrolidine (16 µL, 13.7 mg, 0.192 mmol, 1.5 equiv.) and dry EtOH (3 mL) until complete consumption of **9** was detected by TLC analysis (2.5 h). By following the purification procedure described in the general procedure, pyridinium dye **9a** was obtained as a yellow solid. Yield: 40 mg, 0.101 mmol, 79%.

**Analytical data:** m.p. 235-237 °C.

$^1$H NMR (400 MHz, DMSO-$d_6$): 1.36 (t, $J$ = 7.0 Hz, 3H), 3.87 (s, 3H), 4.10 (q, $J$ = 7.0 Hz, 2H), 4.37 (s, 3H), 7.07 (d, $J$ = 8.4 Hz, 1H), 7.38 (dd, $J$ = 2.0, 8.4 Hz, 1H), 7.45 (d, $J$ = 15.9 Hz, 1H), 7.49 (d, $J$ = 2.0 Hz, 1H), 7.85 (td, $J$ = 2.2, 6.5 Hz, 1H), 7.91 (d, $J$ = 15.9 Hz, 1H), 8.43-8.50 (m, 2H), 8.86 (dt, $J$ = 0.9, 6.2 Hz, 1H).

$^{13}$C NMR (101 MHz, DMSO-$d_6$): 14.6, 46.0, 55.8, 63.9, 110.7, 112.4, 114.7, 123.7, 124.4, 124.4, 127.6, 143.4, 143.9, 145.8, 149.1, 150.7, 152.8.

IR (KBr) $v$ (cm$^{-1}$): 738 w, 921 m, 1032 m, 1145 s, 1185 s, 1233 m, 1267 s, 1427 m, 1442 w, 1459 m, 1484 w, 1516 s, 1565 s, 1577 s, 1539 m, 1613 s, 1631 m, 2832 w, 2937 w, 2971 w, 3003 w, 3033 w.

MS (ESI) *m/z* (%): 270.2 [(M - I$^-$)$^+$] (100), 271.2 (19), 450.2 (5). HRMS (ESI) *m/z*: [(M - I$^-$)$^+$] [($C_{17}H_{20}O_2N$)$^+$] calcd: 270.14886, found: 270.14891.

## *Pyridinium dye 9b:*

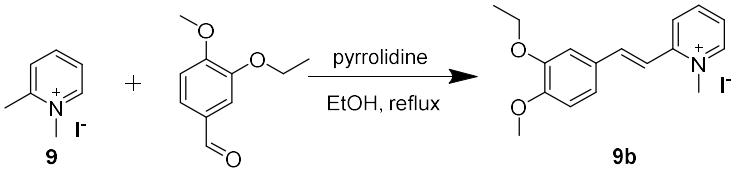


Pyridinium dye **9b** was synthesized by refluxing mixture containing pyridinium dye precursor **9** (30 mg, 0.128 mmol), 3-ethoxy-4-methoxybenzaldehyde (115 mg, 0.638 mmol, 5 equiv.), pyrrolidine (16 µL, 13.7 mg, 0.192 mmol, 1.5 equiv.) and dry EtOH (3 mL) until complete consumption of **9** was detected by TLC analysis (2.5 h). By following the purification procedure described in the general procedure, pyridinium dye **9b** was obtained as a yellow solid. Yield: 22 mg, 0.055 mmol, 43%.

**Analytical data:** m.p. 233-235 °C.

$^1$H NMR (400 MHz, DMSO-$d_6$): 1.38 (t, $J$ = 7.0 Hz, 3H), 3.84 (s, 3H), 4.11 (q, $J$ = 7.0 Hz, 2H), 4.36 (s, 3H), 7.09 (d, $J$ = 8.4 Hz, 1H), 7.39 (dd, $J$ = 2.0, 8.4 Hz, 1H), 7.44 (d, $J$ = 15.9 Hz, 1H), 7.48 (d, $J$ = 2.0 Hz, 1H), 7.85 (td, $J$ = 2.8, 6.2 Hz, 1H), 7.90 (d, $J$ = 15.9 Hz, 1H), 8.41-8.51 (m, 2H), 8.86 (dt, $J$ = 0.9, 6.2 Hz, 1H).

$^{13}$C NMR (101 MHz, DMSO-$d_6$): 14.7, 46.0, 55.7, 64.0, 111.7, 111.8, 114.7, 123.7, 124.4, 124.4, 127.7, 143.4, 143.9, 145.8, 148.3, 151.6, 152.8.

IR (KBr) $v$ (cm$^{-1}$): 740 w, 773 m, 938 w, 974 m, 1022 m, 1148 m, 1171 m, 1181 m, 1238 m, 1268 s, 1440 m, 1461 m, 1514 s, 1566 s, 1577 m, 1592 m, 1616 m, 1631 m, 2838 w, 2931 w, 2980 m, 3001 w, 3034 w, 3070 w.

MS (ESI) *m/z* (%): 270.2 [(M - I$^-$)$^+$] (100), 271.2 (22), 539.3 (5), 667.2 (3). HRMS (ESI) *m/z*: [(M - I$^-$)$^+$] ($C_{17}H_{20}O_2N$) calcd: 270.14886, found: 270.14891.

## *Pyridinium dye 9c:*

***CAS number: 198140-94-2***

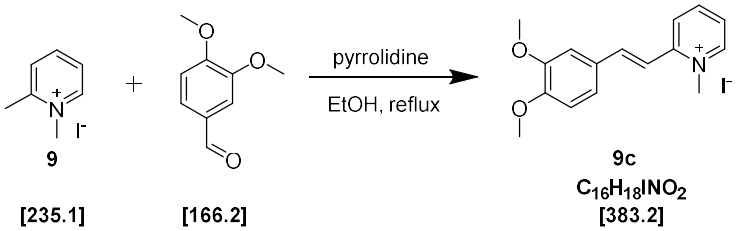

Pyridinium dye **9c** was synthesized by refluxing mixture containing pyridinium dye precursor **9** (30 mg, 0.128 mmol), 3,4-dimethoxybenzaldehyde (106 mg, 0.638 mmol, 5 equiv.), pyrrolidine (16 µL, 13.7 mg, 0.192 mmol, 1.5 equiv.) and dry EtOH (3 mL) until complete consumption of **9** was detected by TLC analysis (2.5 h). By following the purification procedure described in the general procedure, pyridinium dye **9c** was obtained as a yellow solid. Yield: 26 mg, 0.068 mmol, 53%.

**Analytical data:** m.p. 235-237 °C.

$^1$H NMR (400 MHz, DMSO-$d_6$): 3.84 (s, 3H), 3.87 (s, 3H), 4.36 (s, 3H), 7.09 (d, $J$ = 8.4 Hz, 1H), 7.40 (dd, $J$ = 2.0, 8.4 Hz, 1H), 7.46 (d, $J$ = 15.9 Hz, 1H), 7.49 (d, $J$ = 2.0 Hz, 1H), 7.85 (td, $J$ = 2.5, 6.4 Hz, 1H), 7.91 (d, $J$ = 15.9 Hz, 1H), 8.40-8.53 (m, 2H), 8.86 (dt, $J$ = 0.9, 6.2 Hz, 1H).

$^{13}$C NMR (101 MHz, DMSO-$d_6$): 46.04, 55.70, 55.86, 110.60, 111.68, 114.80, 123.71, 124.42, 124.44, 127.74, 143.38, 143.93, 145.82, 149.06, 151.43, 152.77.

IR (KBr) $v$ (cm$^{-1}$): 741 w, 773 m, 961 m, 1012 m, 1141 m, 1178 m, 1237 m, 1267 s, 1331 m, 1425 m, 1449 m, 1458 m, 1515 s, 1567 s, 1593 m, 1614 m, 1630 w, 2838 w, 2938 w, 2963 m, 3001 w, 3034 w, 3070 w.

MS (ESI) *m/z* (%): 256.2 [(M - I$^-$)$^+$] (100), 257.2 (22). HRMS (ESI) *m/z*: [(M - I$^-$)$^+$] ($C_{16}H_{18}O_2N$) calcd: 256.13321, found: 256.13323.

## *4.4. Synthesis of (rac)-HeliDye3, (P)-HeliDye3 and (M)-HeliDye3*

### *Synthesis of (rac)-HeliDye3:*

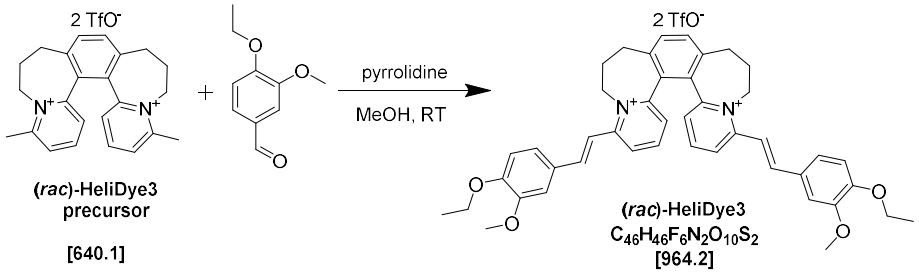


(*rac*)-**HeliDye3** precursor[4] (20 mg, 0.031 mmol), 4-ethoxy-3-methoxybenzaldehyde (83.8 mg, 0.465 mmol, 15.0 equiv.), and pyrrolidine (38 µL, 33.0 mg, 0.464 mmol, 15.0 equiv.) in dry MeOH (1.0 mL) were mixed together under argon atmosphere and the resulting reaction mixture was stirred at RT. The flask was protected from ambient light using Alufoil cover. A color change was observed immediately after addition of pyrrolidine. Progress of the reaction was monitored by TLC analysis (mobile phase: Stoddart's magic mixture, see *Materials Section*). After complete consumption of dye precursor was detected by TLC analysis, $Et_2O$ (8 mL) was added to the reaction mixture to precipitate crude product. Crude solid product was separated from supernatant after sonication and centrifugation. Isolated crude solid was further purified using re-precipitation from its MeOH solution (2 mL) by addition of $Et_2O$ (16 mL). This dissolution/precipitation procedure was repeated two times. Each time, solid and liquids were sonicated together to get a free-flowing suspension followed by centrifugation to settle down the solid. After final separation of supernatants, the solid pellet was re-suspended in $Et_2O$ (8-10 mL) and transferred into a pre-weighed vial for storage. After separation of $Et_2O$, the solid product was dried under high vacuum to remove the residual solvents. Yield: 26.2 mg, 0.027 mmol, 87.6%.

**Analytical data:** m.p. 280-282 °C.

$^1$H-NMR (DMSO-$d_6$, 400 MHz): $\delta$ 1.37 (t, $J$ = 6.9 Hz, 6H), 2.24-2.45 (m, 4H), 2.66-2.77 (m, 2H), 3.03 (dd, $J$ = 6.1, 13.5 Hz, 1H), 3.05 (dd, $J$ = 6.1, 13.5 Hz, 1H), 3.89 (s, 6H), 4.12 (q, $J$ = 7.0 Hz, 4H), 4.32-4.41 (m, 2H), 5.17-5.22 (m, 2H), 7.10 (d, $J$ = 8.4 Hz, 2H), 7.39 (dd, $J$ = 1.3, 7.8 Hz, 2H), 7.48 (dd, $J$ =

2.0, 8.5 Hz, 2H), 7.54 (d, *J* = 15.7 Hz, 2H), 7.57 (d, *J* = 1.0 Hz, 2H), 7.77 (s, 2H), 7.90 (d, *J* = 15.7 Hz, 2H), 8.12 (t, *J* = 8.1 Hz, 2H), 8.41 (dd, *J* = 1.3, 8.6 Hz, 2H).
$^{13}$C-NMR (DMSO-$d_6$, 101 MHz): $\delta$ 14.6, 28.2, 30.5, 52.5, 55.9, 63.9, 111.2, 112.5, 115.0, 123.8, 125.3, 127.6, 128.7, 131.1, 132.5, 138.5, 142.8, 144.8, 149.1, 150.9, 151.5, 154.1.
IR: *v* (cm$^{-}$) 763, 836, 1031, 1160, 1226, 1259, 1272, 1478, 1490, 1511, 1565, 1580, 1595, 1612, 1624.
MS (ESI) *m/z* (%): 333.1 (100), 333.6 (73), 334.1 (20), 503.2 (5), 815.3 (17), 816.3 (10). HRMS *m/z*: calc. for $[(M - 2CF_3SO_3^-)^{2+}]$ $[(C_{44}H_{46}O_4N_2)^{2+}]$ 333.1723, found 333.1726.

## *Synthesis of (P)-HeliDye3:*

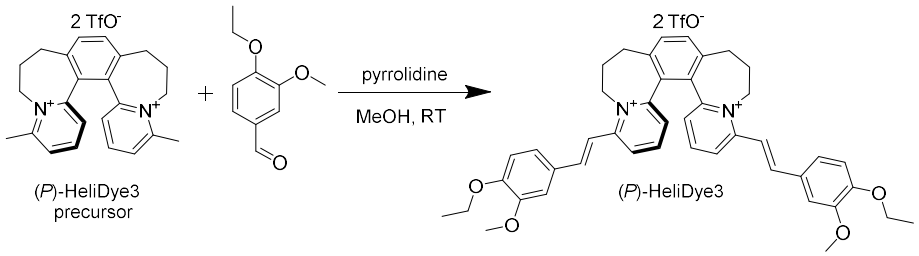


(*P*)-**HeliDye3** precursor [4] (20 mg, 0.031 mmol), 4-ethoxy-3-methoxybenzaldehyde (83.8 mg, 0.465 mmol, 15.0 equiv.), and pyrrolidine (38 µL, 33.0 mg, 0.464 mmol, 15.0 equiv.) in dry MeOH (1.0 mL) were mixed together under argon atmosphere and the resulting reaction mixture was stirred at RT. The flask was protected from ambient light using Alufoil cover. A color change was observed immediately after addition of pyrrolidine. Progress of the reaction was monitored by TLC analysis (mobile phase: Stoddart's magic mixture, see *Materials Section*). After complete consumption of dye precursor was detected by TLC analysis, $Et_2O$ (8 mL) was added to the reaction mixture to precipitate crude product. Crude solid product was separated from supernatant after sonication and centrifugation. Isolated crude solid was further purified using re-precipitation from its MeOH solution (2 mL) by addition of $Et_2O$ (16 mL). This dissolution/precipitation procedure was repeated two times. Each time, solid and liquids were sonicated together to get a free-flowing suspension followed by centrifugation to settle down the solid. After final separation of supernatants, the solid pellet was re-suspended in $Et_2O$ (8-10 mL) and transferred into a pre-weighed vial for storage. After separation of $Et_2O$, the solid product was dried under high vacuum to remove the residual solvents. Yield: 25.0 mg, 0.026 mmol, 83.6%.

**Analytical data:** m.p. 280-282 °C.
$^1$H-NMR (DMSO-$d_6$, 400 MHz): $\delta$ 1.37 (t, *J* = 6.9 Hz, 6H), 2.24-2.45 (m, 4H), 2.66-2.77 (m, 2H), 3.03 (dd, *J* = 6.1, 13.5 Hz, 1H), 3.05 (dd, *J* = 6.1, 13.5 Hz, 1H), 3.89 (s, 6H), 4.12 (q, *J* = 7.0 Hz, 4H), 4.32-4.41 (m, 2H), 5.17-5.22 (m, 2H), 7.10 (d, *J* = 8.4 Hz, 2H), 7.39 (dd, *J* = 1.3, 7.8 Hz, 2H), 7.48 (dd, *J* = 2.0, 8.5 Hz, 2H), 7.54 (d, *J* = 15.7 Hz, 2H), 7.57 (d, *J* = 1.0 Hz, 2H), 7.77 (s, 2H), 7.90 (d, *J* = 15.7 Hz, 2H), 8.12 (t, *J* = 8.1 Hz, 2H), 8.41 (dd, *J* = 1.3, 8.6 Hz, 2H).

## *Synthesis of (M)-HeliDye3:*

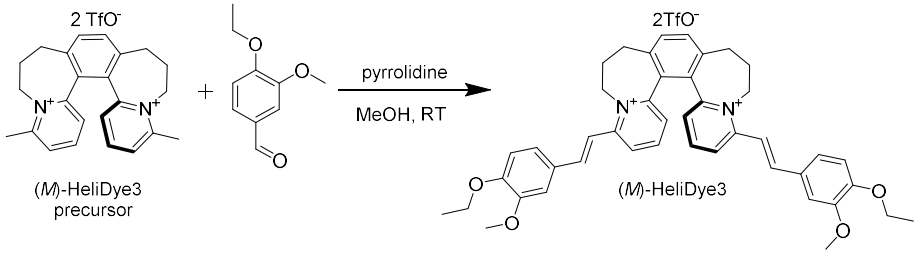

(*M*)-**HeliDye3** precursor [4] (20 mg, 0.031 mmol), 4-ethoxy-3-methoxybenzaldehyde (83.8 mg, 0.465 mmol, 15.0 equiv.), and pyrrolidine (38 µL, 33.0 mg, 0.464 mmol, 15.0 equiv.) in dry MeOH (1.0 mL) were mixed together under argon atmosphere and the resulting reaction mixture was stirred at RT. The flask was protected from ambient light using Alufoil cover. A color change was observed immediately after addition of pyrrolidine. Progress of the reaction was monitored by TLC analysis (mobile phase: Stoddart's magic mixture, see *Materials Section*). After complete consumption of dye precursor was detected by TLC analysis, $Et_2O$ (8 mL) was added to the reaction mixture to precipitate crude product. Crude solid product was separated from supernatant after sonication and centrifugation. Isolated crude solid was further purified using re-precipitation from its MeOH solution (2 mL) by addition of $Et_2O$ (16 mL). This dissolution/precipitation procedure was repeated two times. Each time, solid and liquids were sonicated together to get a free-flowing suspension followed by centrifugation to settle down the solid. After final separation of supernatants, the solid pellet was re-suspended in $Et_2O$ (8-10 mL) and transferred into a pre-weighed vial for storage. After separation of $Et_2O$, the solid product was dried under high vacuum to remove the residual solvents. Yield: 22.0 mg, 0.023 mmol, 73.5%.

**Analytical data:** m.p. 280-282 °C.
$^1$H-NMR (DMSO-$d_6$, 400 MHz): $\delta$ 1.37 (t, $J$ = 6.9 Hz, 6H), 2.24-2.45 (m, 4H), 2.66-2.77 (m, 2H), 3.03 (dd, $J$ = 6.1, 13.5 Hz, 1H), 3.05 (dd, $J$ = 6.1, 13.5 Hz, 1H), 3.89 (s, 6H), 4.12 (q, $J$ = 7.0 Hz, 4H), 4.32-4.41 (m, 2H), 5.17-5.22 (m, 2H), 7.10 (d, $J$ = 8.4 Hz, 2H), 7.39 (dd, $J$ = 1.3, 7.8 Hz, 2H), 7.48 (dd, $J$ = 2.0, 8.5 Hz, 2H), 7.54 (d, $J$ = 15.7 Hz, 2H), 7.57 (d, $J$ = 1.0 Hz, 2H), 7.77 (s, 2H), 7.90 (d, $J$ = 15.7 Hz, 2H), 8.12 (t, $J$ = 8.1 Hz, 2H), 8.41 (dd, $J$ = 1.3, 8.6 Hz, 2H).

## 5. Capillary electrophoresis (CE) of (*rac*)-HeliDye3, (*P*)-HeliDye3 and (*M*)-HeliDye3

Chiral analysis of (*rac*)-**HeliDye3**, (*P*)-**HeliDye3** and (*M*)-**HeliDye3** was carried out by capillary electrophoresis (CE) with sulphated cyclodextrin-based chiral selector. Specifically, the Beckman-Coulter MDQ apparatus with a photodiode array (PDA) modul was used. Analytes were detected by UV absorption at 200 nm. Capillaries were Polymicro fused silica TSP050375 (Polymicro Technologies, Phoenix, AZ, USA) of 50/370 μm id/od. The capillaries were coated with hydroxypropylcellulose (HPC)[5,6] and used for experiments in 29.5/39.5 cm effective/total length. A background electrolyte consisted of 22 mM sodium + 35 mM phosphate buffer, pH 2.4, with 1.5 % wt. of highly sulfated γ-cyclodextrin (Sciex Separations, cat. no. A50924). **HeliDye3** samples (*racemate*, (*P*)- and (*M*)-enantiomers) were dissolved in DMSO and injected as approx. 0.5 mM solution into the capillary by pressure of 1.4 kPa for 5 s. Separation voltage was –11.4 kV (i.e. cathode at the injection capillary end), capillary temperature was 22°C and generated current was 36 μA.

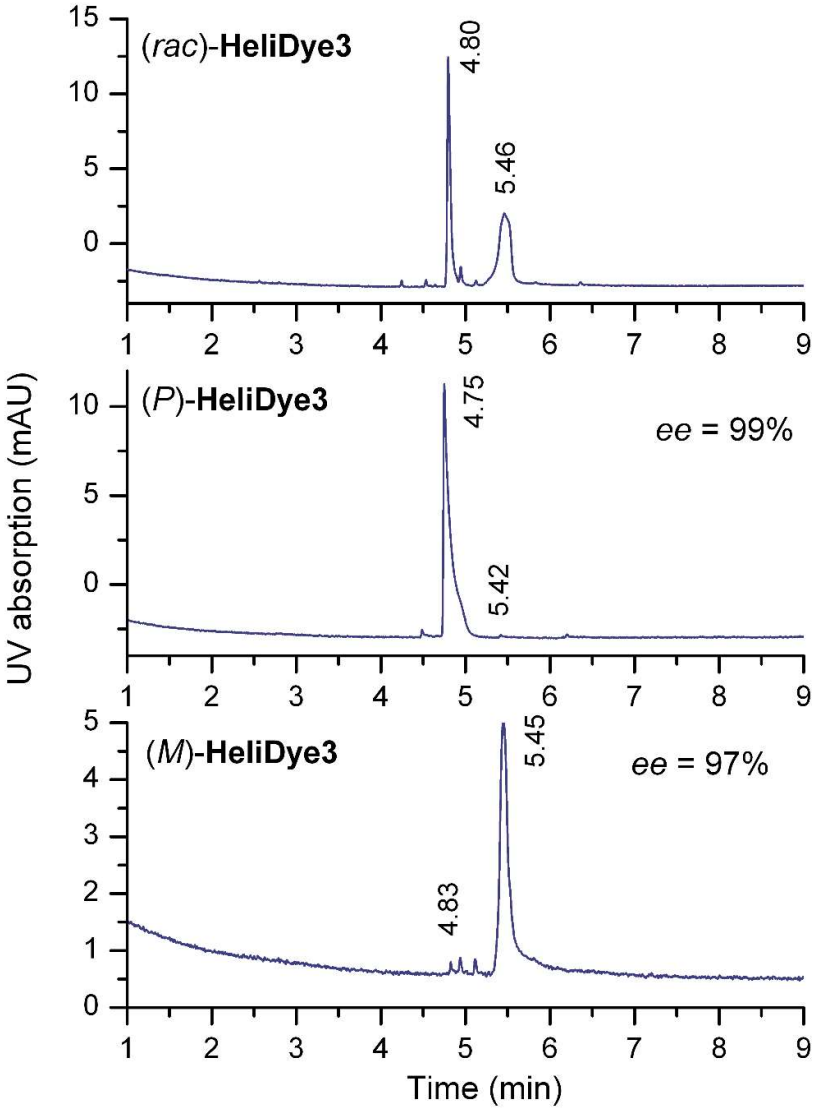


***Fig. S1*** *Chiral analysis of (rac)-**HeliDye3**, (P)-**HeliDye3** and (M)-**HeliDye3**, by capillary electrophoresis with sulfated γ-cyclodextrin as chiral selector.*

## 6. $^{1}H$ and $^{13}C$ NMR spectra scans

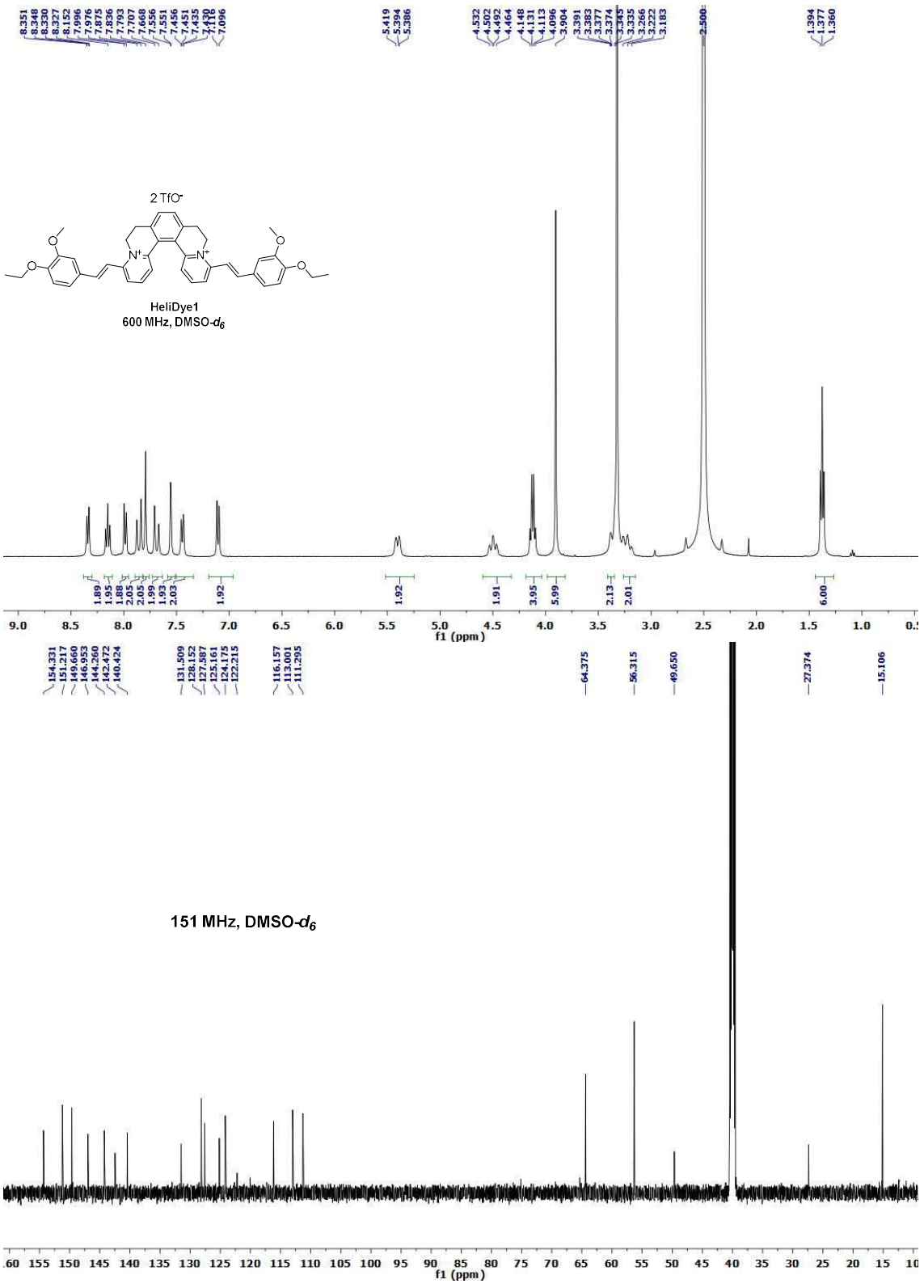

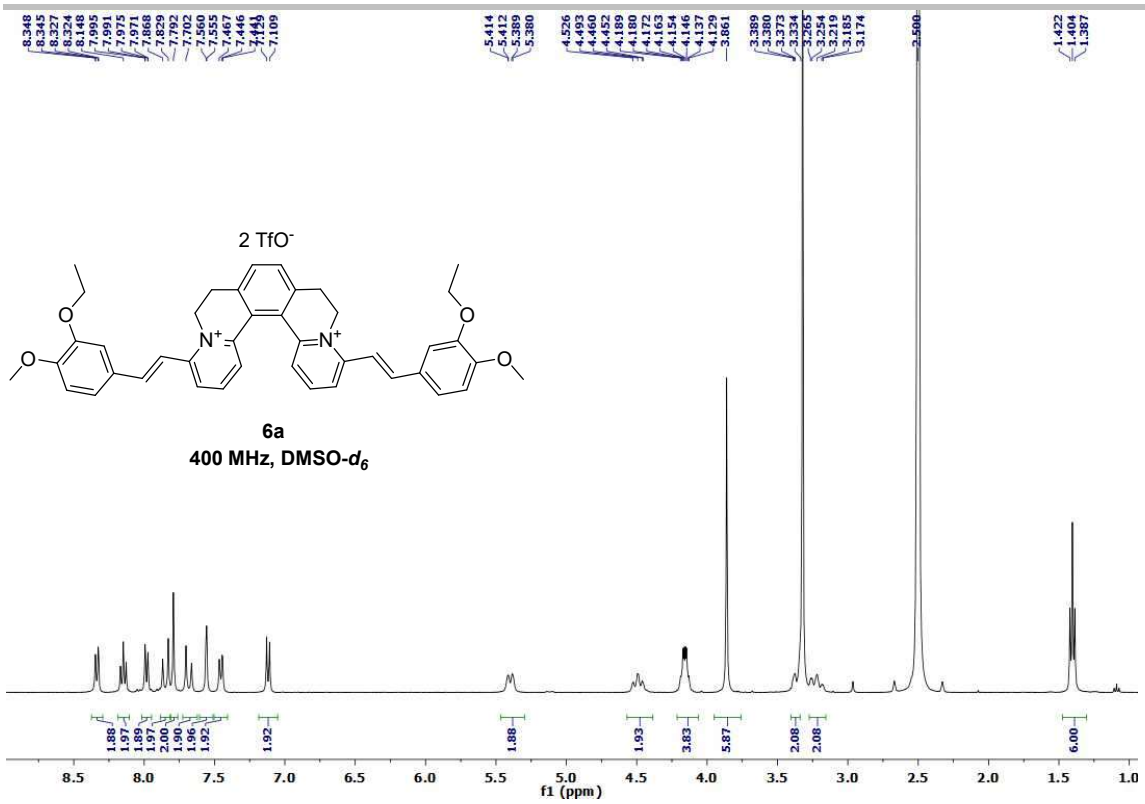
2 TfO⁻
6a
400 MHz, DMSO-$d_6$
f1 (ppm)

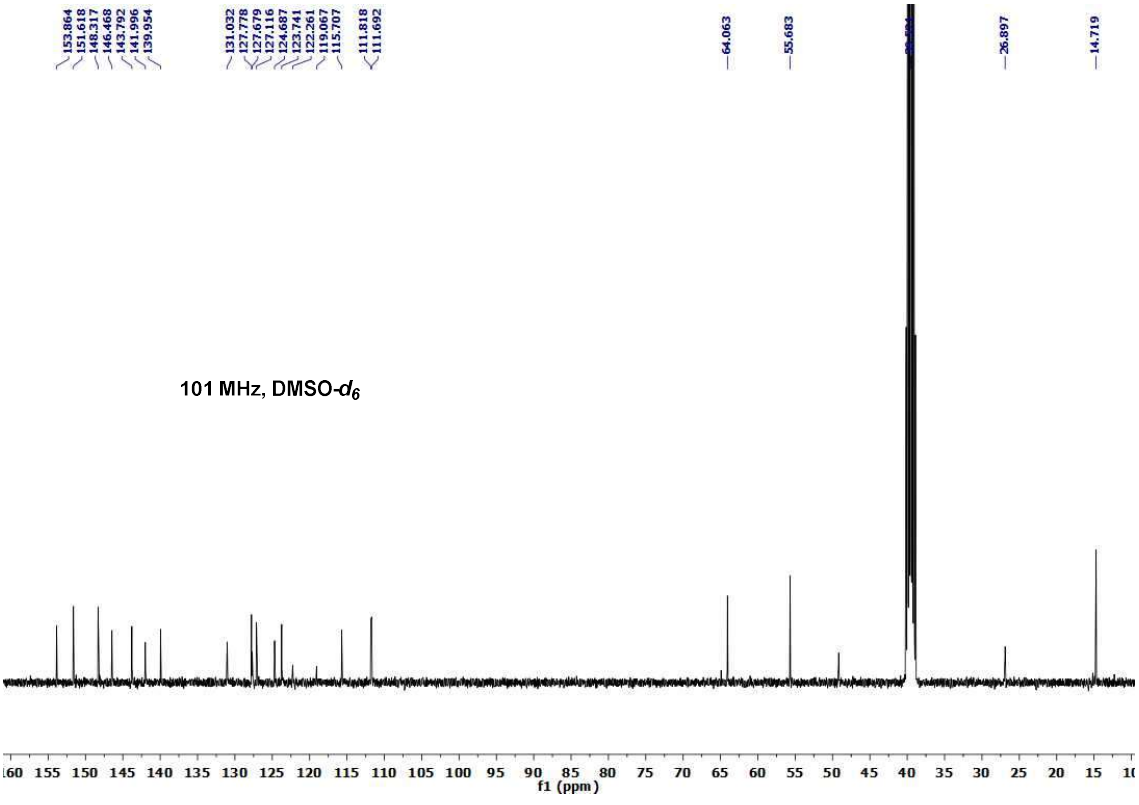
101 MHz, DMSO-$d_6$
f1 (ppm)

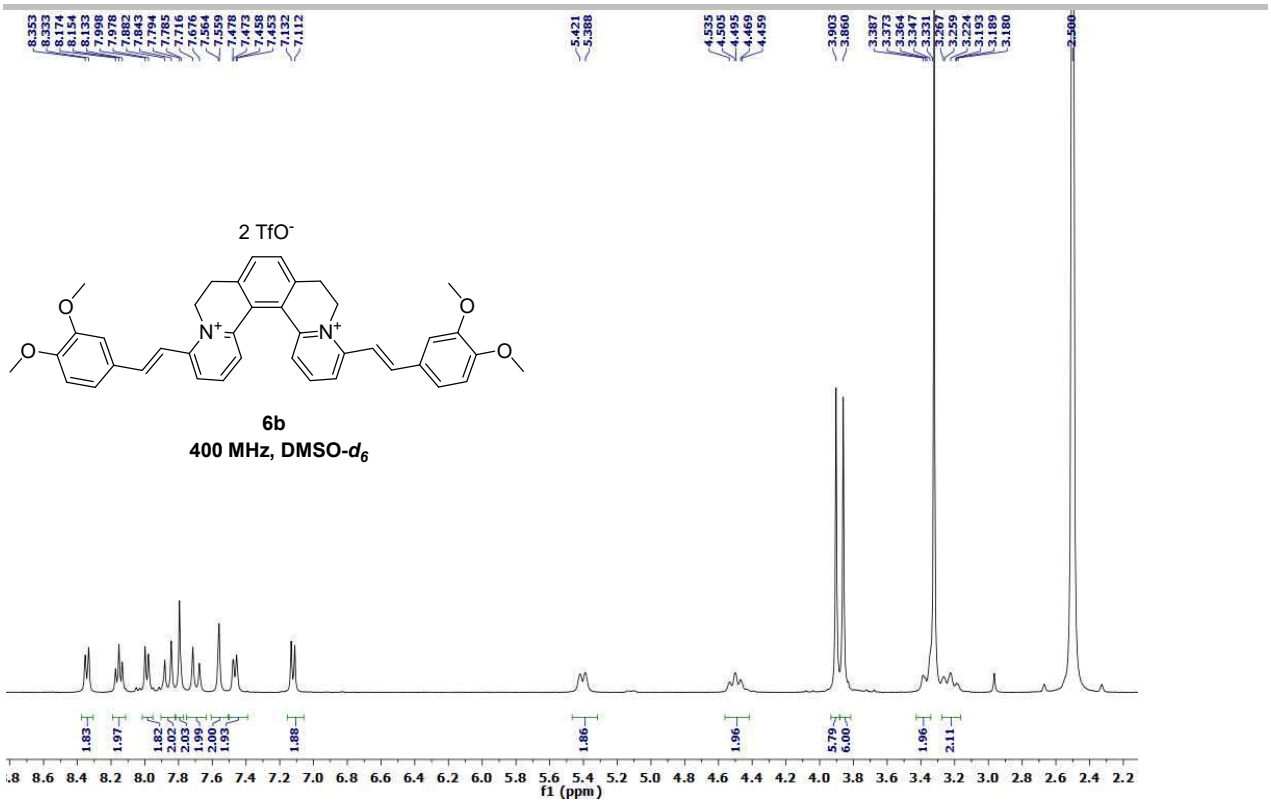


**6b**
**400 MHz, DMSO-*d*$_6$**

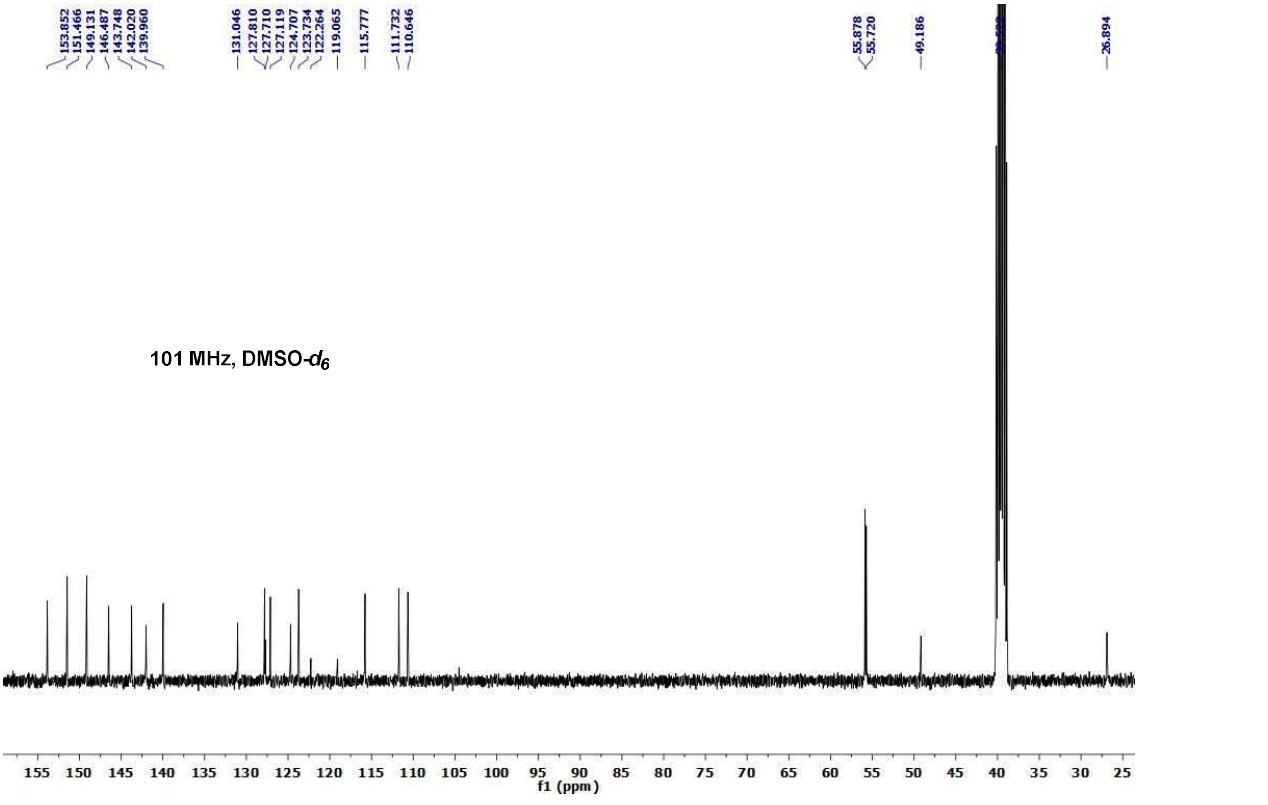


**101 MHz, DMSO-*d*$_6$**

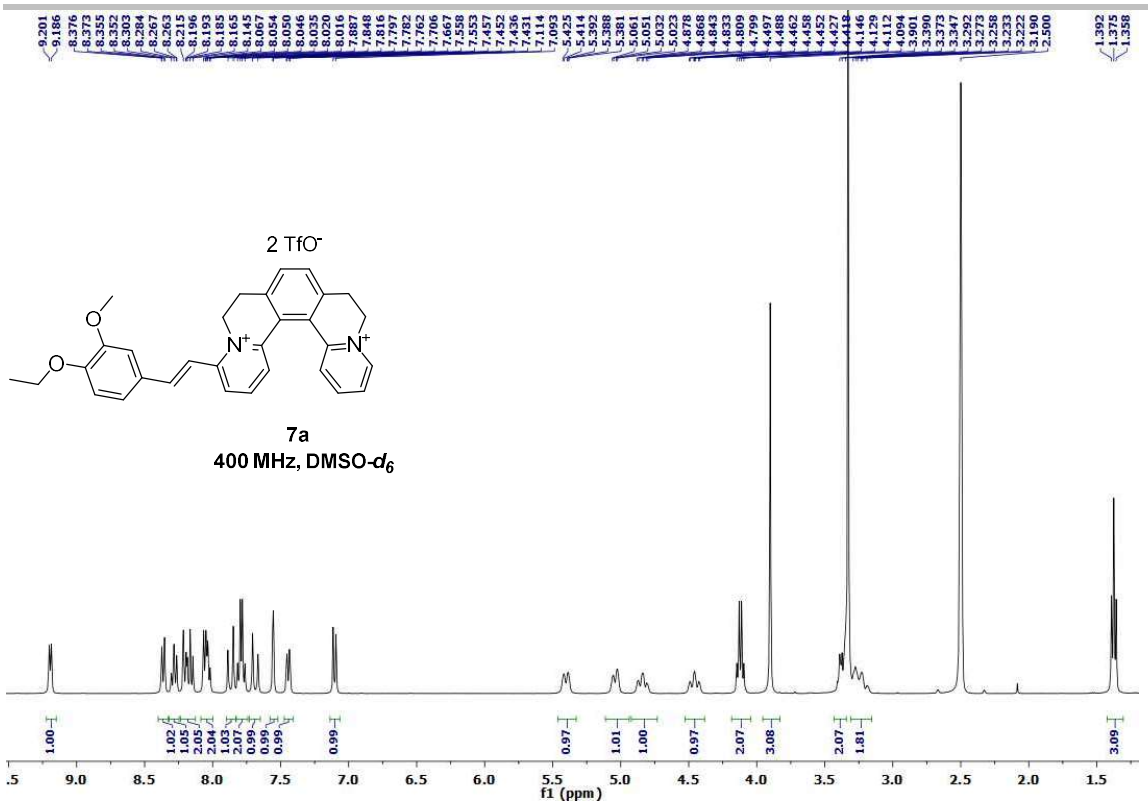
2 TfO-
7a
400 MHz, DMSO-d6
f1 (ppm)

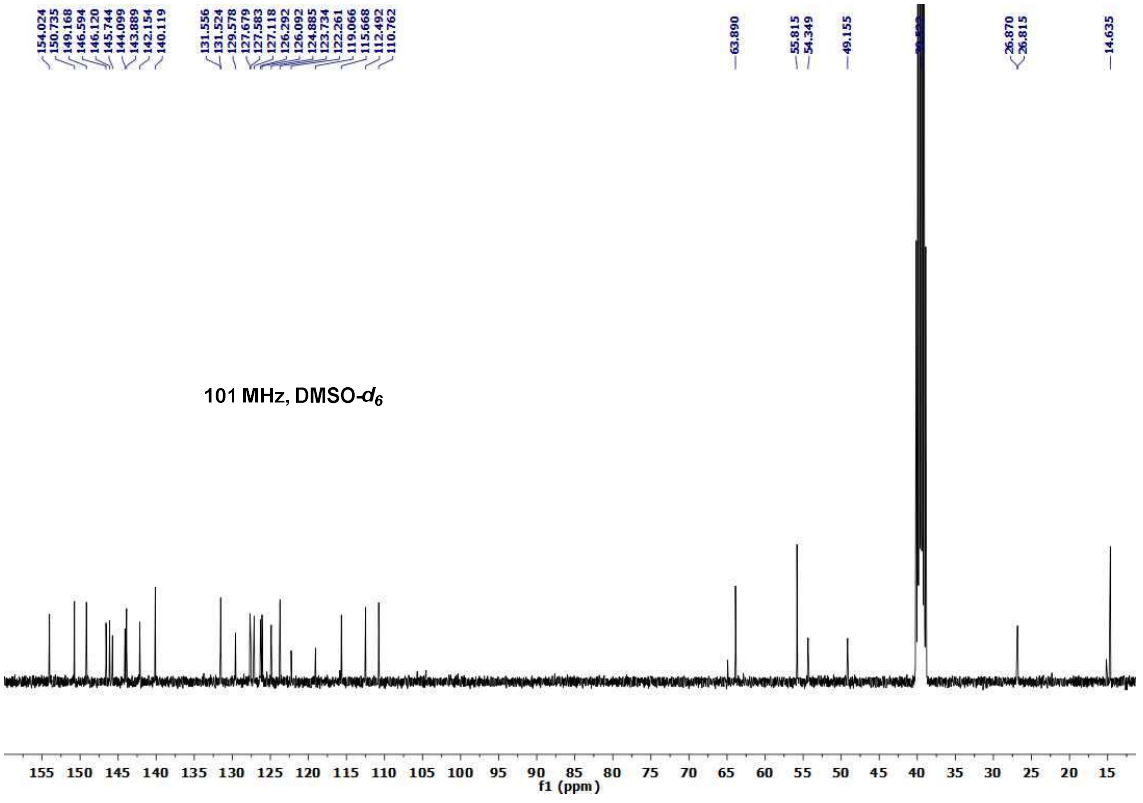
101 MHz, DMSO-d6
f1 (ppm)

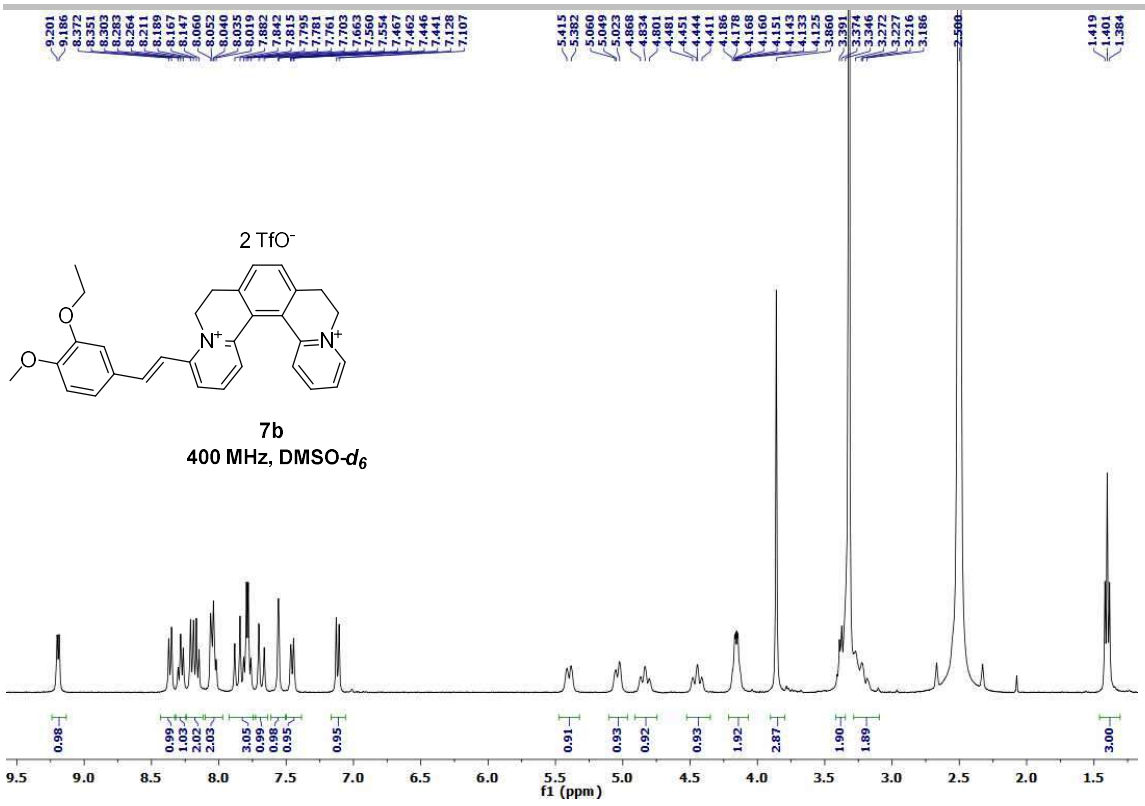
2 TfO⁻
7b
400 MHz, DMSO-$d_6$
f1 (ppm)

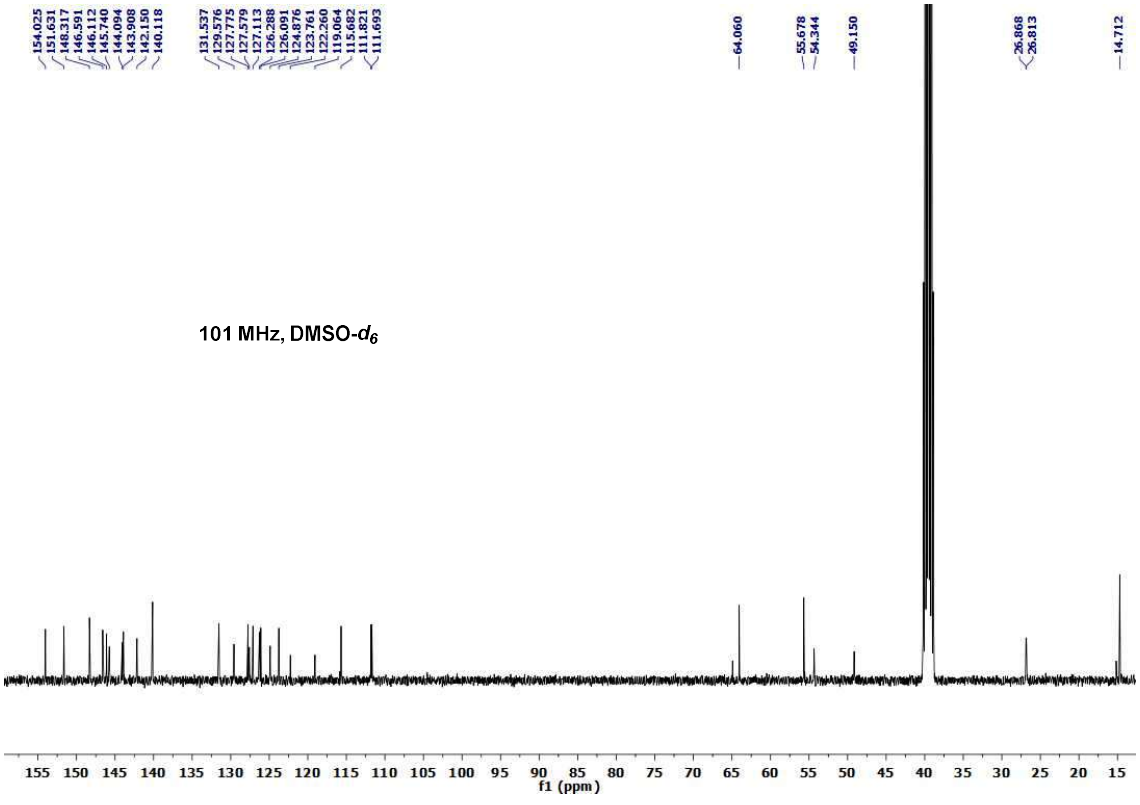
101 MHz, DMSO-$d_6$
f1 (ppm)

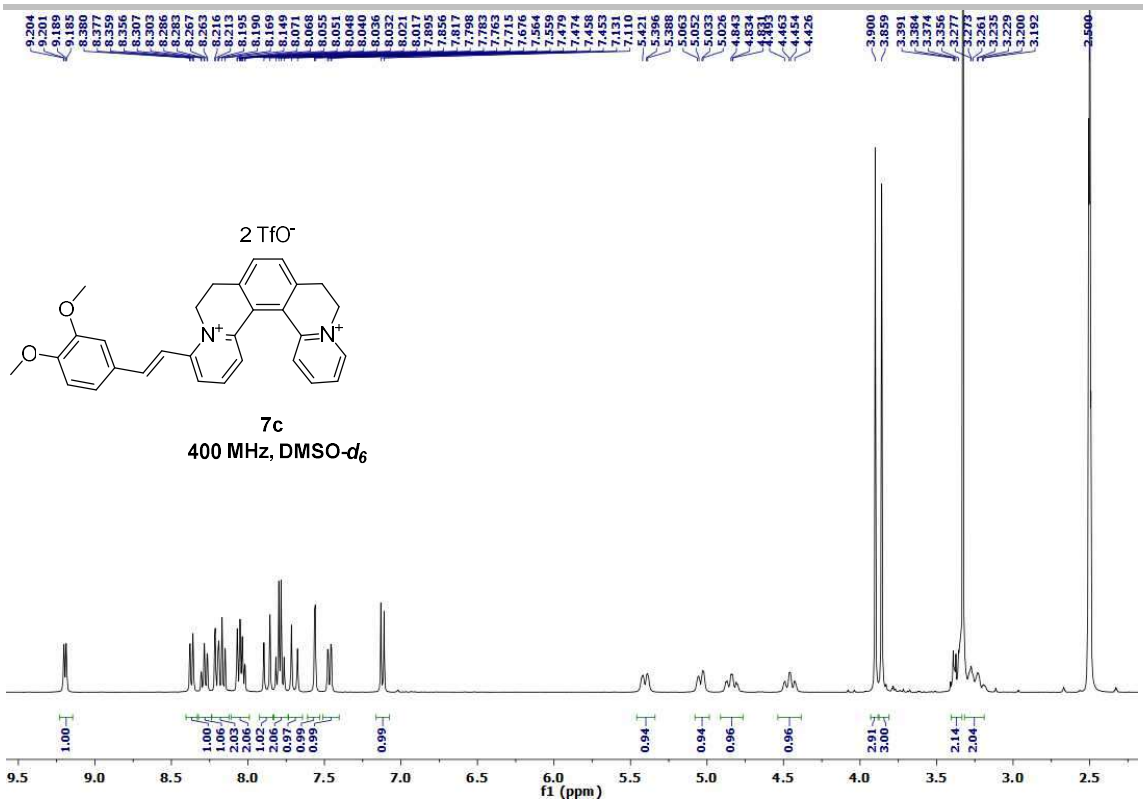
2 TfO-
7c
400 MHz, DMSO-d6

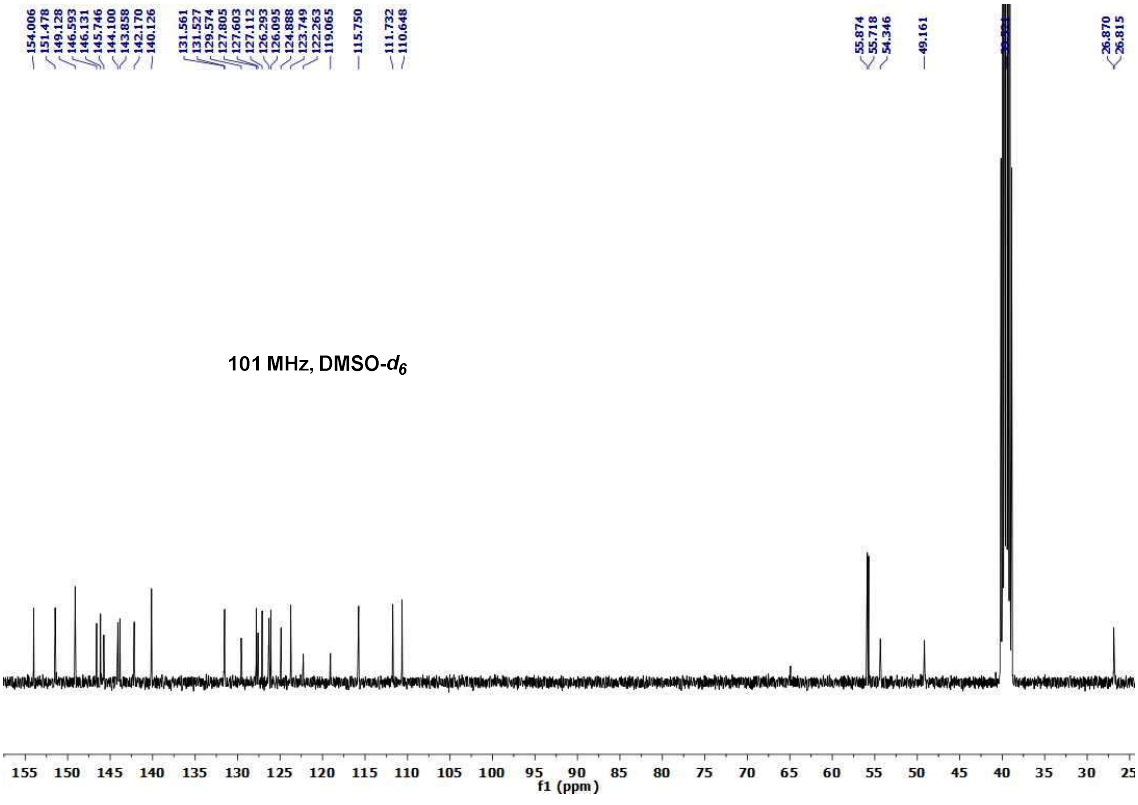
101 MHz, DMSO-d6

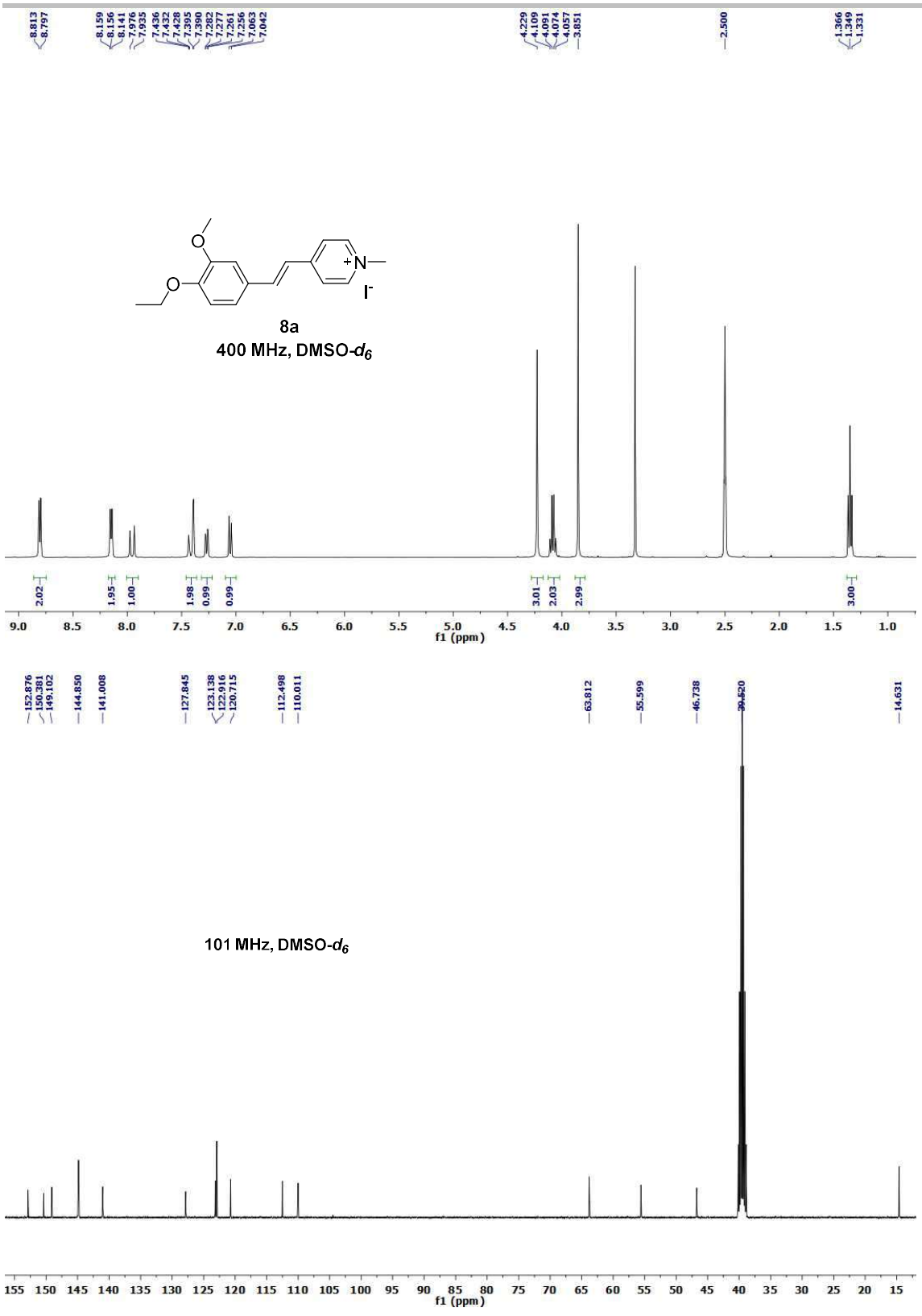
8.813
8.797
8.159
8.156
8.141
7.976
7.935
7.436
7.432
7.428
7.395
7.390
7.282
7.277
7.261
7.256
7.063
7.042
4.229
4.109
4.091
4.074
4.057
3.851
2.500
1.366
1.349
1.331
8a
400 MHz, DMSO-d6
2.02
1.95
1.00
1.98
0.99
0.99
3.01
2.03
2.99
3.00
f1 (ppm)
152.876
150.381
149.102
144.850
141.008
127.845
123.138
122.916
120.715
112.498
110.011
63.812
55.599
46.738
39.620
14.631
101 MHz, DMSO-d6
f1 (ppm)

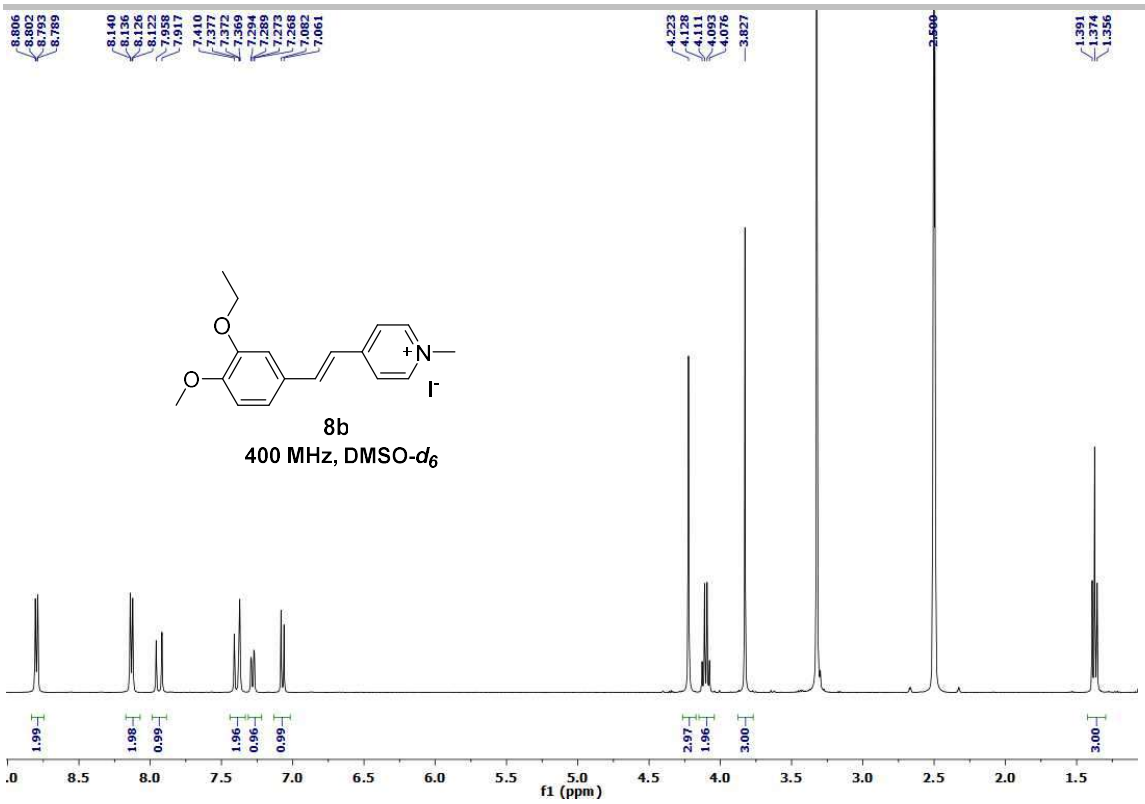
8.806
8.802
8.793
8.789
8.140
8.136
8.126
8.122
7.958
7.917
7.410
7.377
7.372
7.369
7.294
7.289
7.273
7.268
7.082
7.061
4.223
4.128
4.111
4.093
4.076
3.827
2.500
1.391
1.374
1.356
O
O
+N
I-
8b
400 MHz, DMSO-d6
1.99
1.98
0.99
1.96
0.96
0.99
2.97
1.96
3.00
3.00
f1 (ppm)

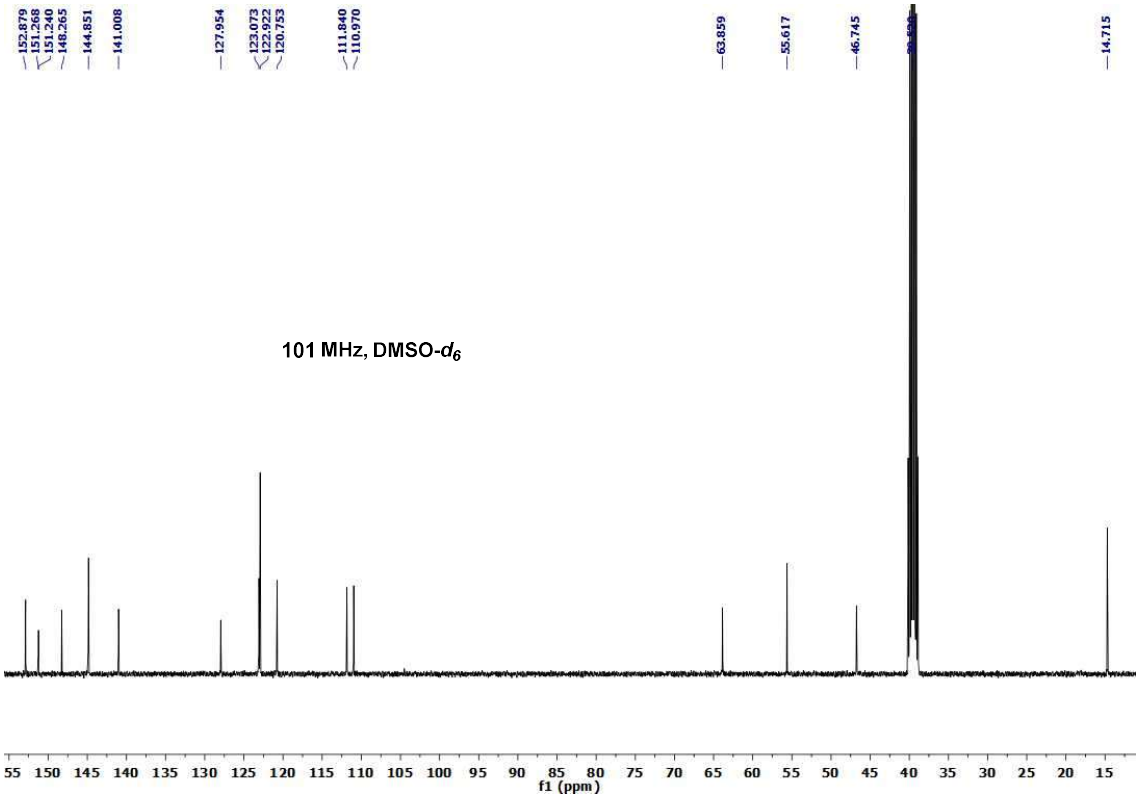
152.879
151.268
151.240
148.265
144.851
141.008
127.954
123.073
122.922
120.753
111.840
110.970
63.859
55.617
46.745
14.715
101 MHz, DMSO-d6
f1 (ppm)

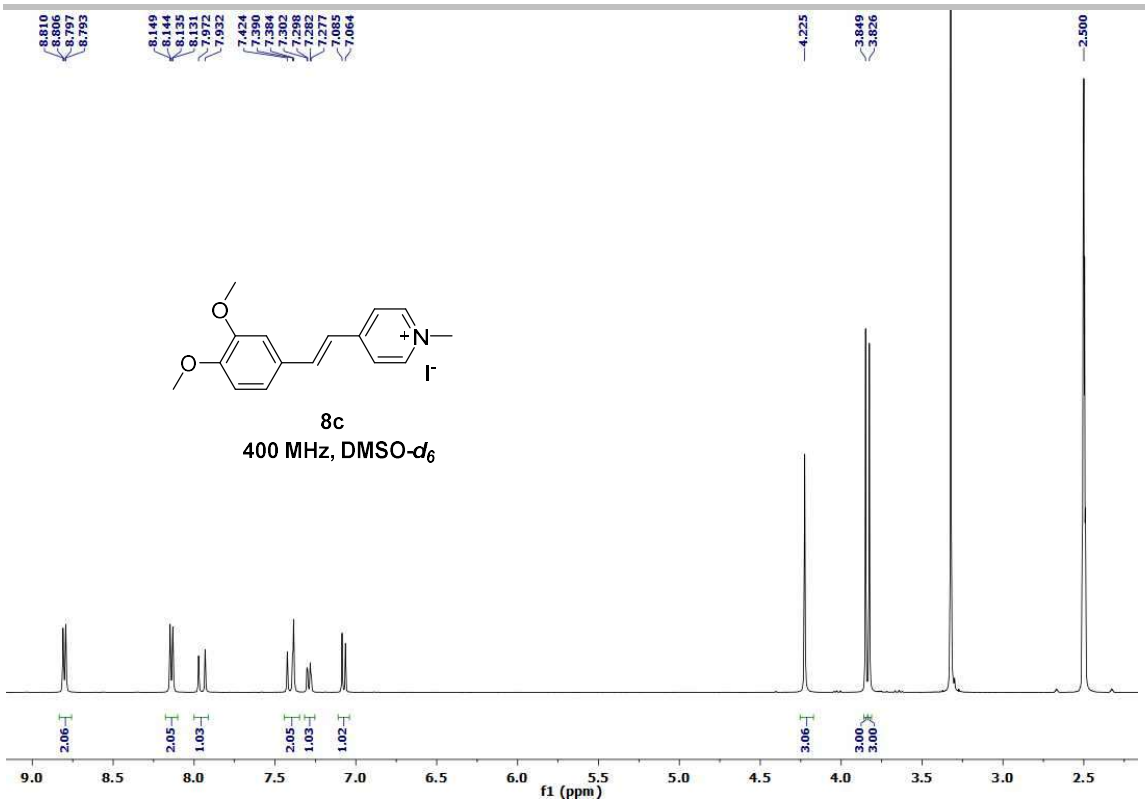


8c
400 MHz, DMSO-$d_6$

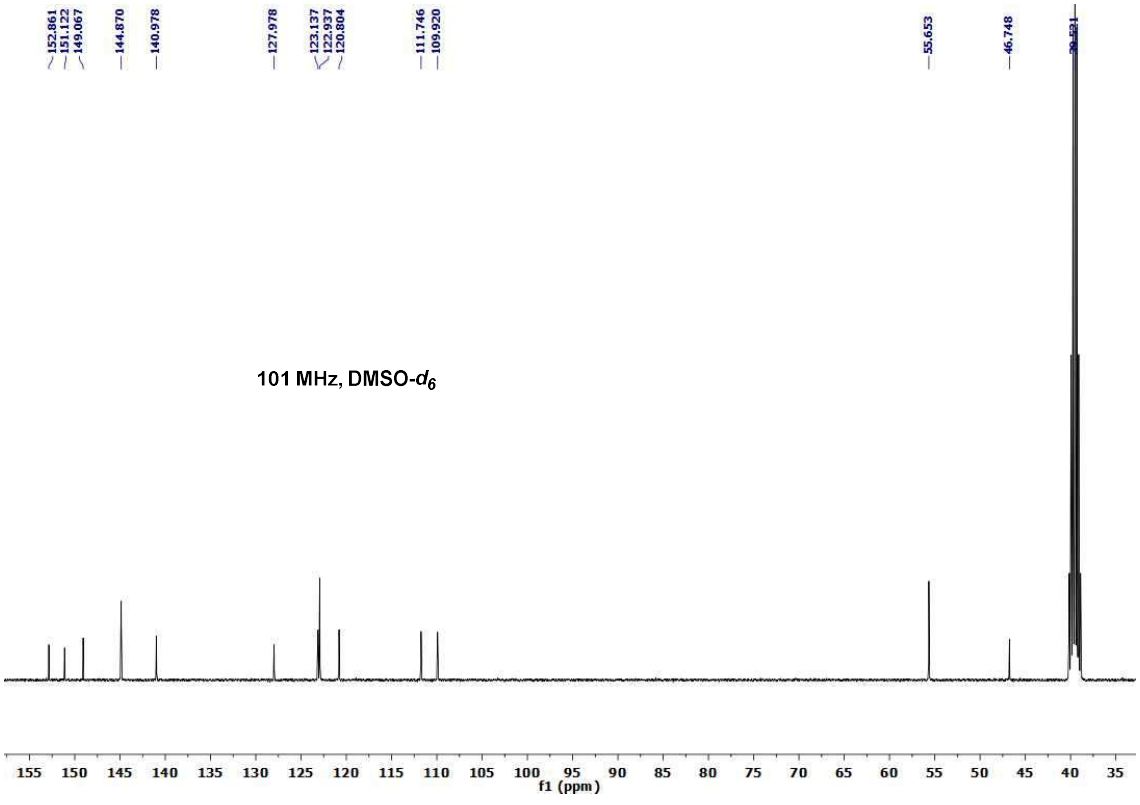


101 MHz, DMSO-$d_6$

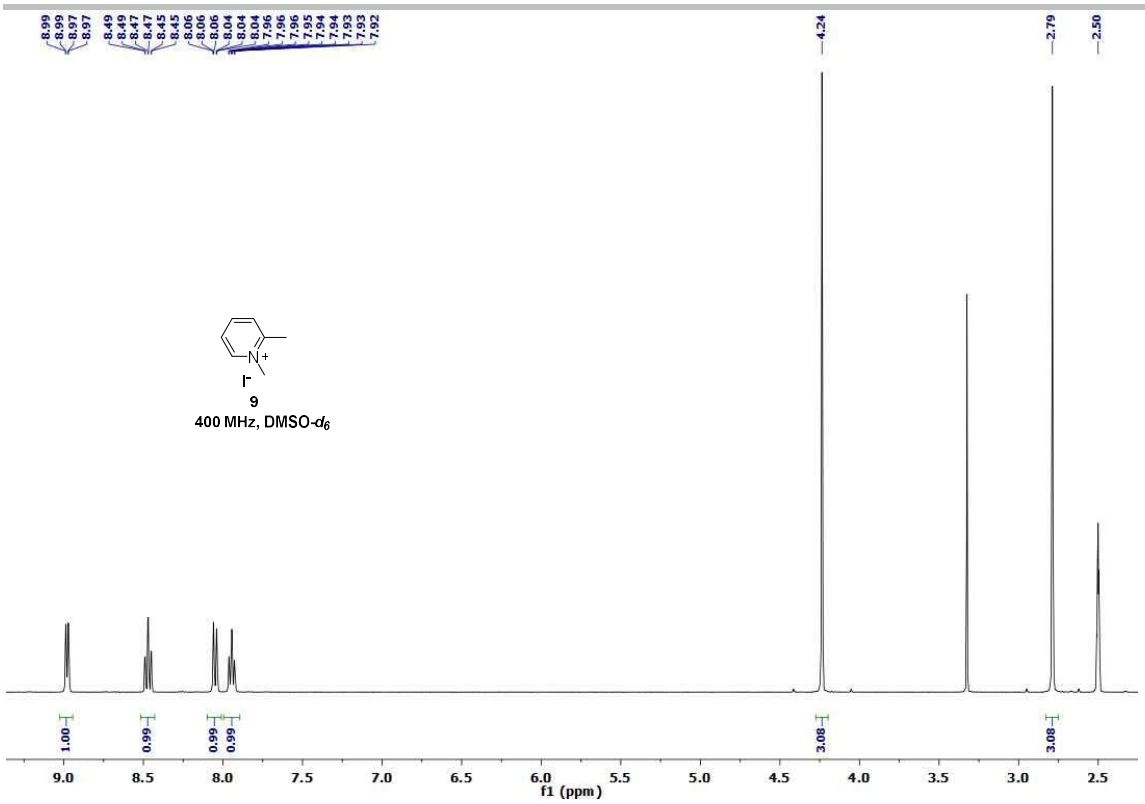
8.99
8.99
8.97
8.97
8.49
8.49
8.47
8.47
8.45
8.45
8.06
8.06
8.06
8.04
8.04
7.96
7.96
7.95
7.94
7.94
7.93
7.93
7.92
4.24
2.79
2.50
I⁻
9
400 MHz, DMSO-$d_6$
1.00
0.99
0.99
0.99
3.08
3.08
9.0
8.5
8.0
7.5
7.0
6.5
6.0
5.5
5.0
4.5
4.0
3.5
3.0
2.5
f1 (ppm)

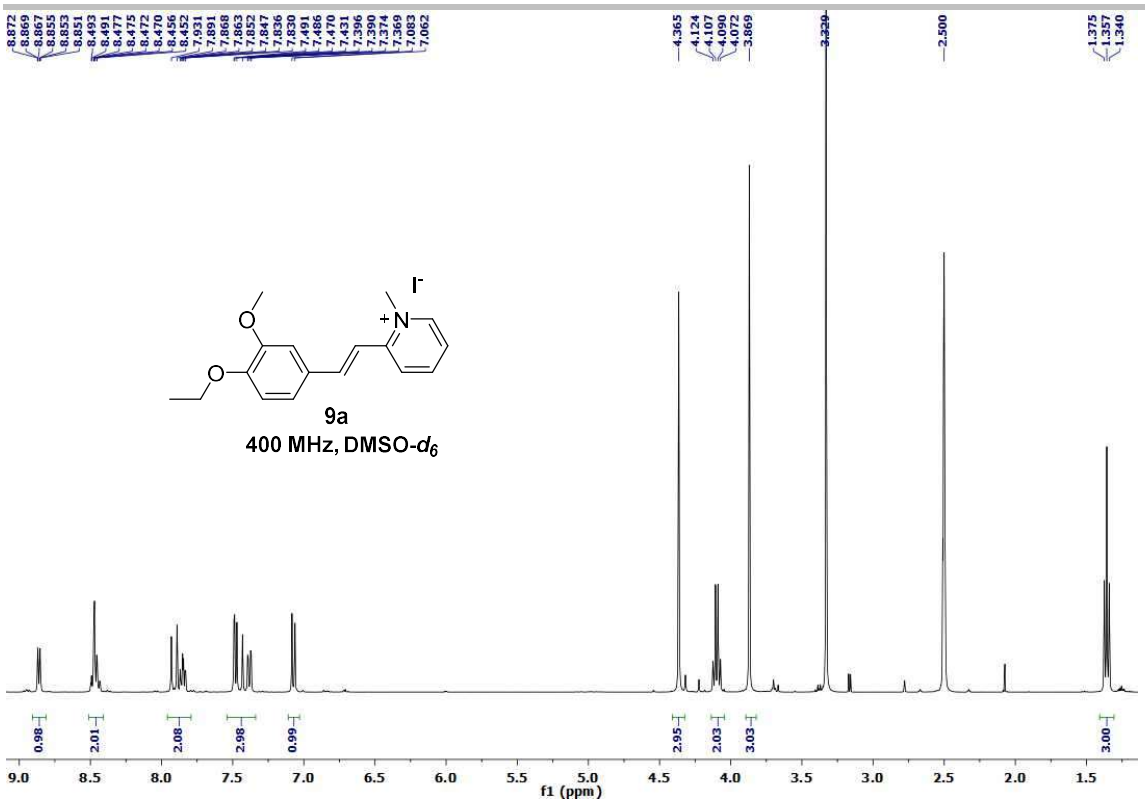
8.872
8.869
8.867
8.855
8.853
8.851
8.493
8.491
8.477
8.475
8.472
8.470
8.456
8.452
7.891
7.868
7.863
7.852
7.847
7.836
7.830
7.491
7.486
7.470
7.431
7.396
7.390
7.374
7.369
7.083
7.062
4.365
4.124
4.107
4.090
4.072
3.869
3.329
2.500
1.375
1.357
1.340
I-
+N
O
O
9a
400 MHz, DMSO-d6
0.98
2.01
2.08
2.98
0.99
2.95
2.03
3.03
3.00
f1 (ppm)

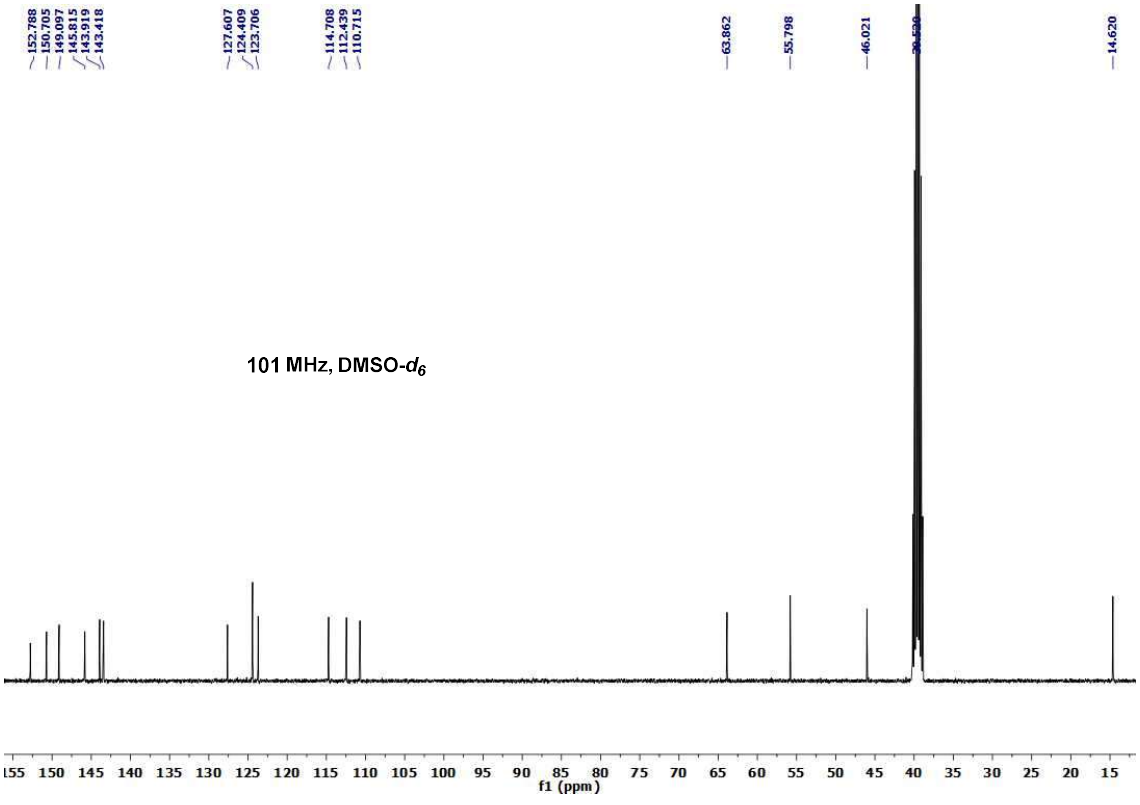
152.788
150.705
149.097
145.815
143.919
143.418
127.607
124.409
123.706
114.708
112.439
110.715
63.862
55.798
46.021
39.520
14.620
101 MHz, DMSO-d6
f1 (ppm)

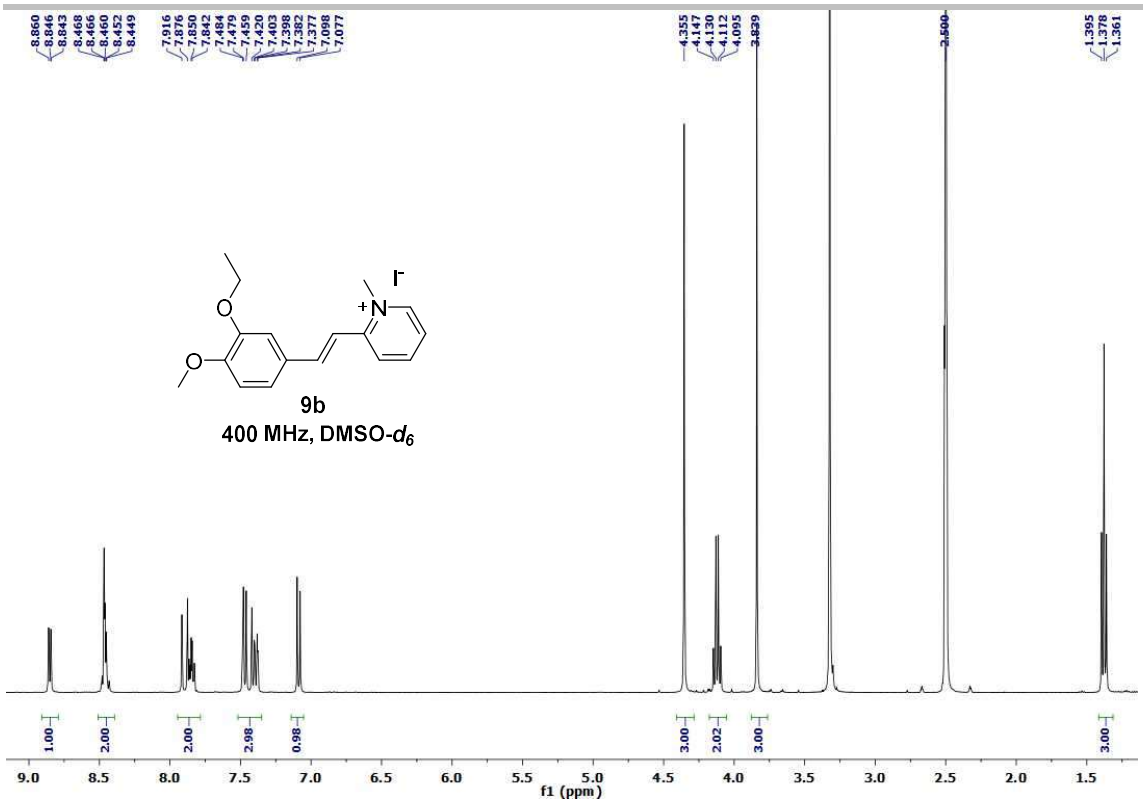


9b
400 MHz, DMSO-$d_6$

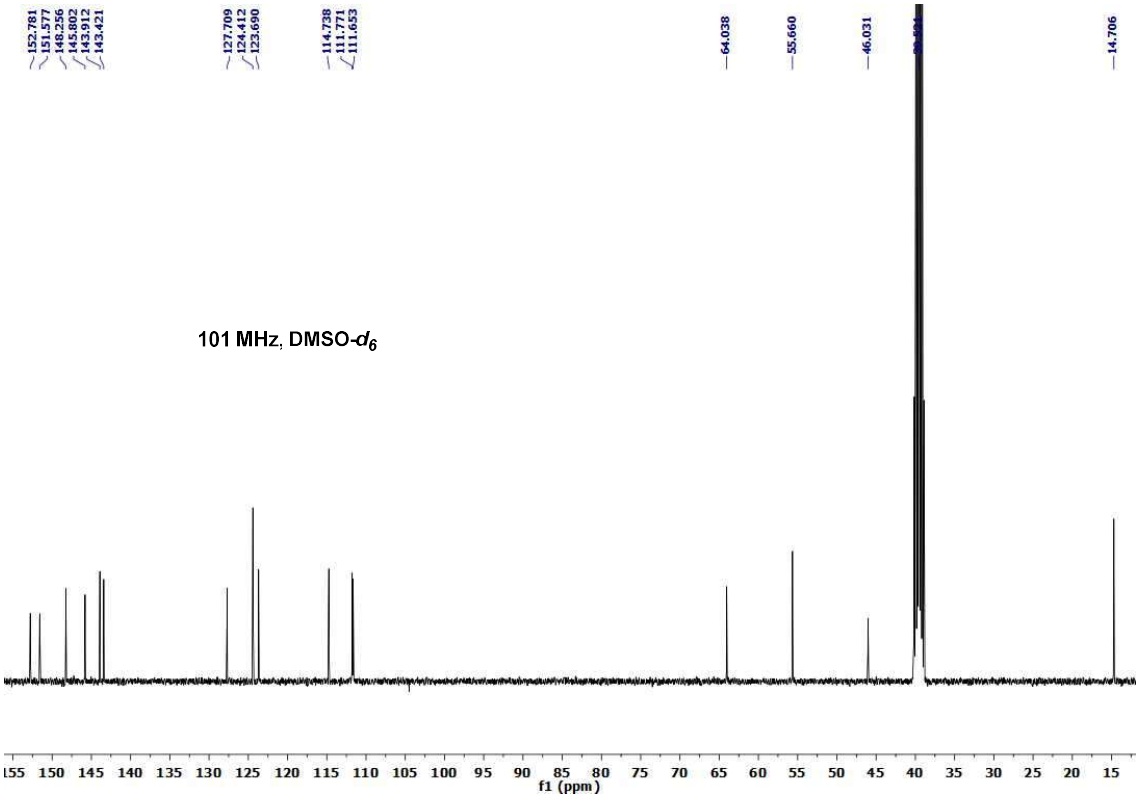


101 MHz, DMSO-$d_6$

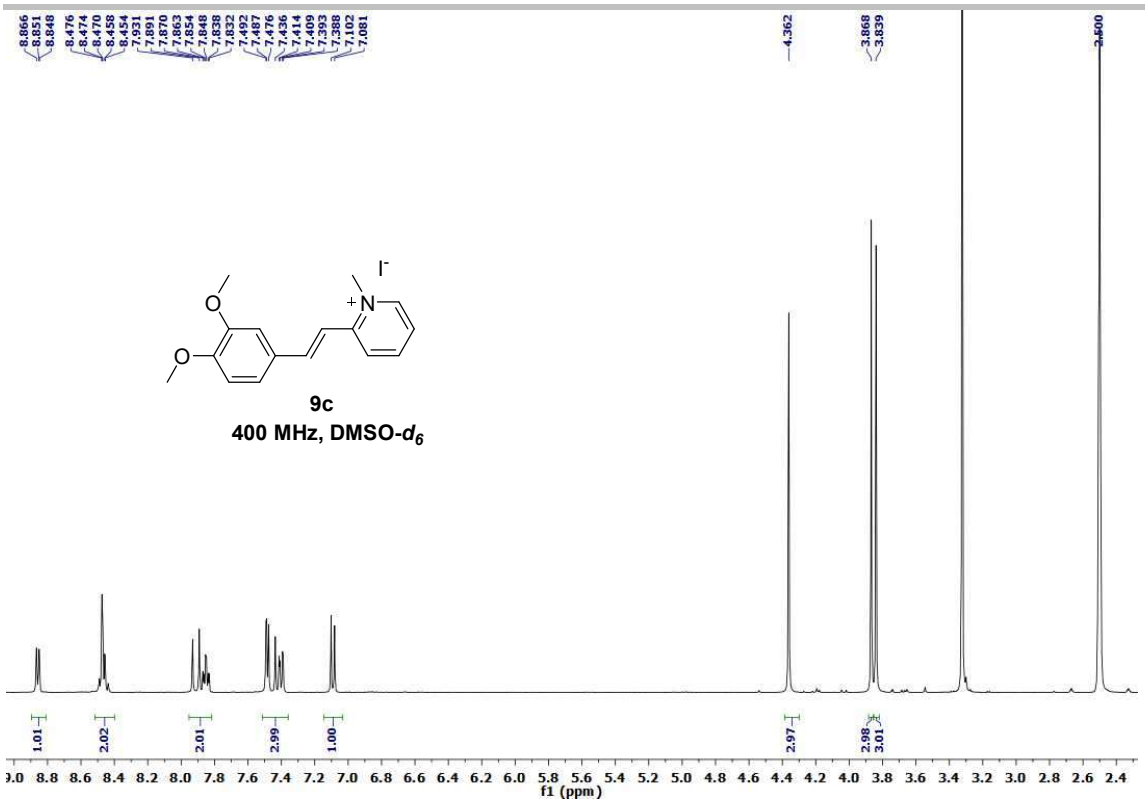
8.866
8.851
8.848
8.476
8.474
8.470
8.458
8.454
7.931
7.891
7.870
7.863
7.854
7.848
7.838
7.832
7.492
7.487
7.476
7.436
7.414
7.409
7.393
7.388
7.102
7.081
4.362
3.868
3.839
3.600
I-
O
O
+N
9c
400 MHz, DMSO-d6
1.01
2.02
2.01
2.99
1.00
2.97
2.98
3.01
f1 (ppm)

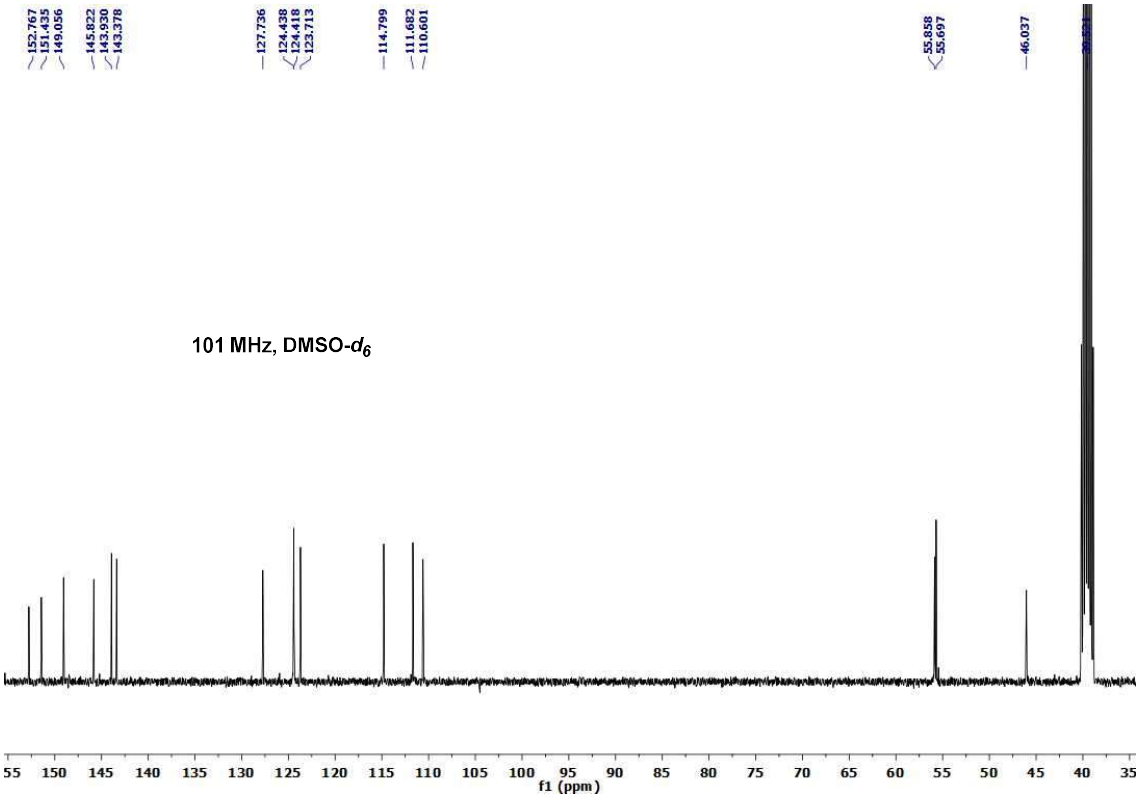
152.767
151.435
149.056
145.822
143.930
143.378
127.736
124.438
124.418
123.713
114.799
111.682
110.601
55.858
55.697
46.037
101 MHz, DMSO-d6
f1 (ppm)

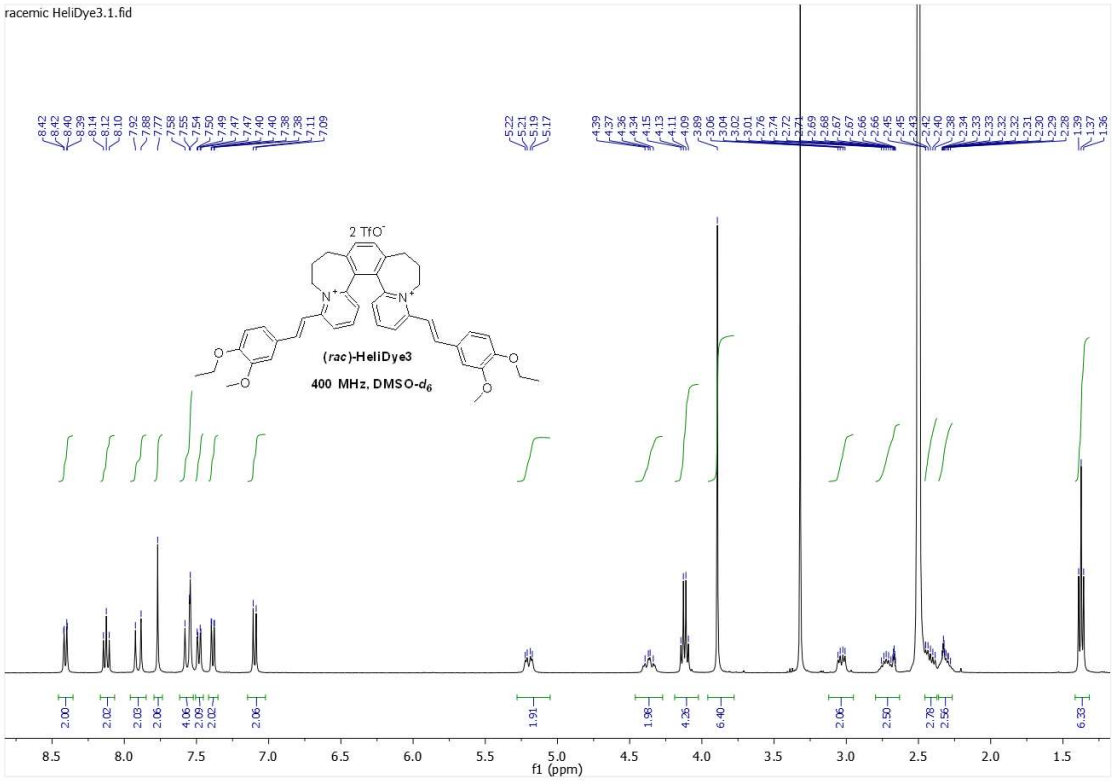
racemic HeliDye3.1.fid
2 TfO⁻
(rac)-HeliDye3
400 MHz, DMSO-d6
f1 (ppm)

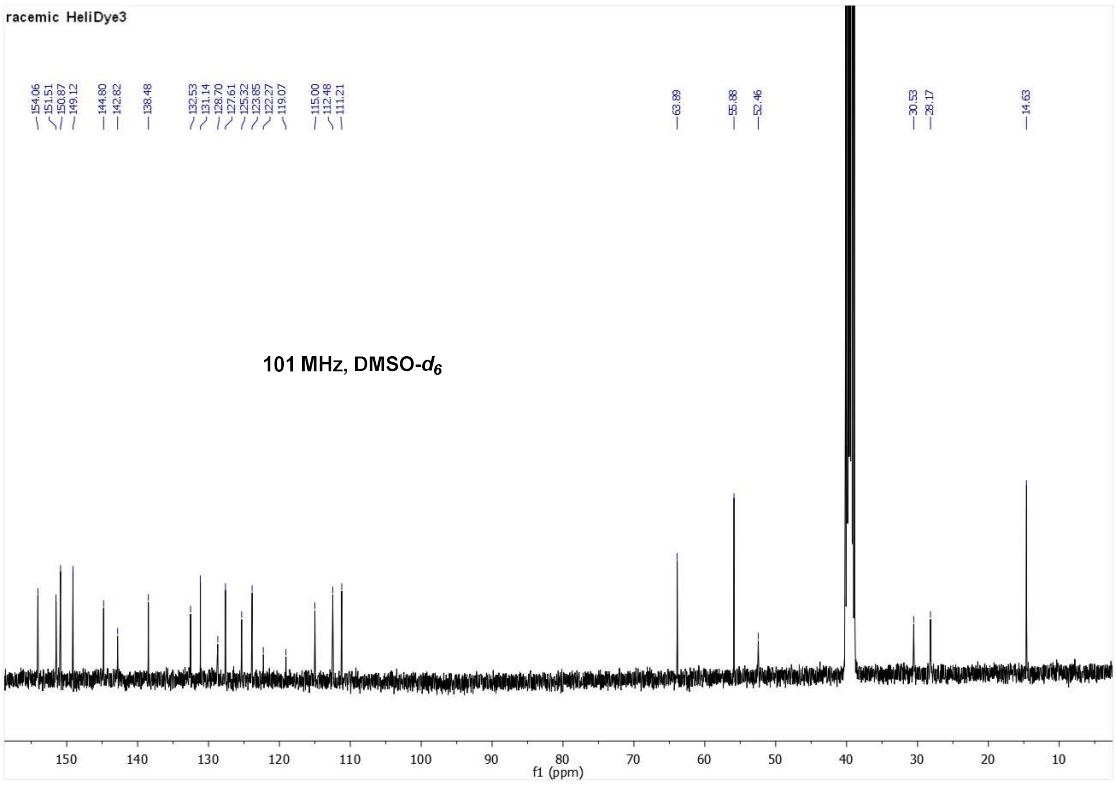
racemic HeliDye3
101 MHz, DMSO-d6
f1 (ppm)

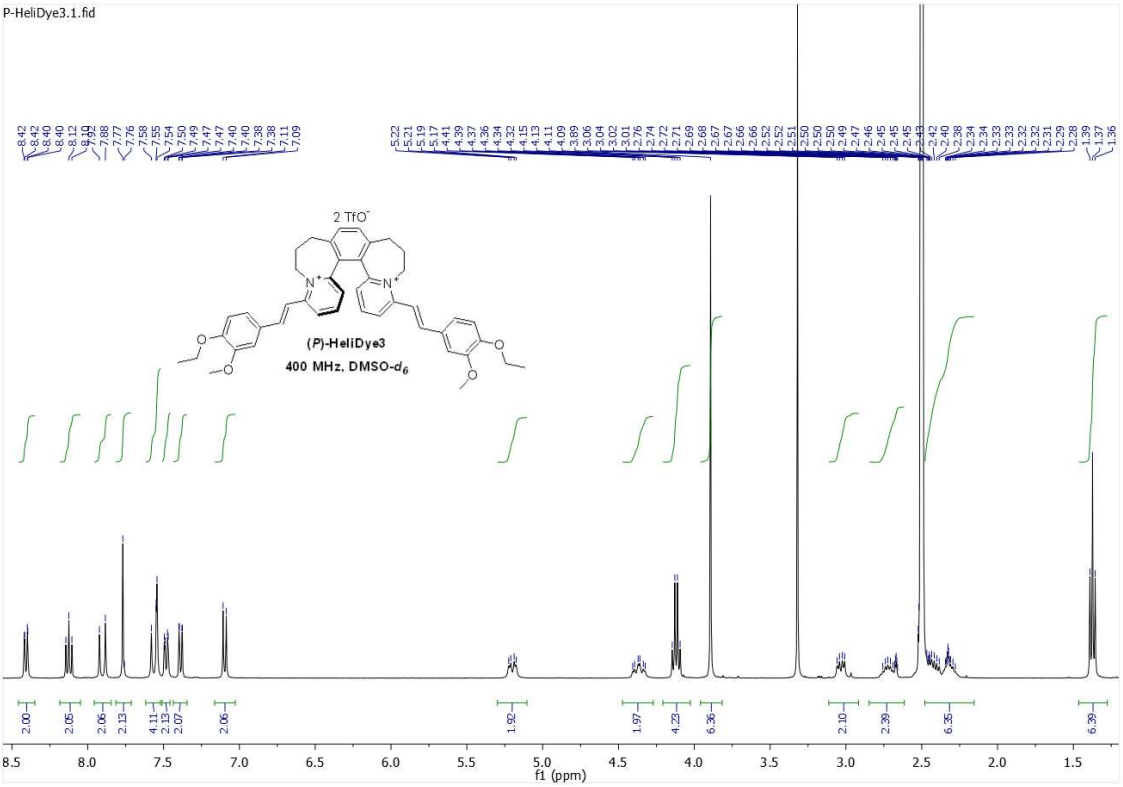
P-HeliDye3.1.fid
2 TfO⁻
(P)-HeliDye3
400 MHz, DMSO-d6
f1 (ppm)

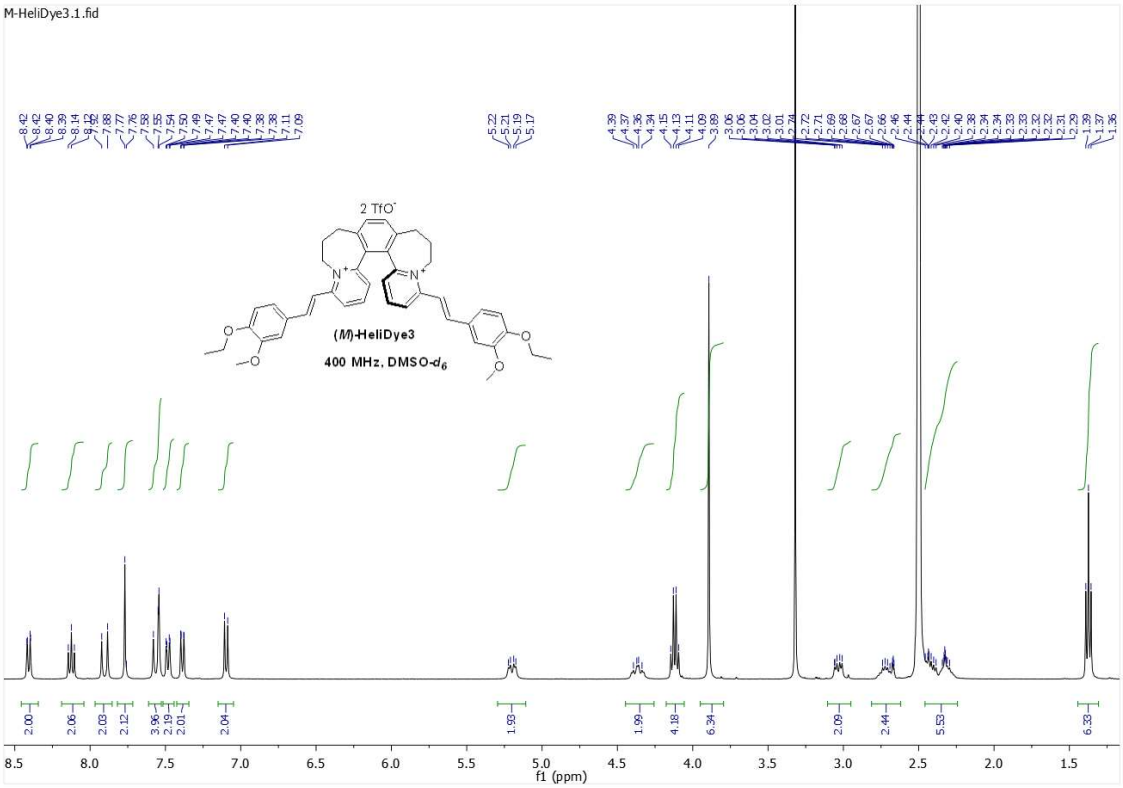
M-HeliDye3.1.fid
2 TfO⁻
(M)-HeliDye3
400 MHz, DMSO-d6
f1 (ppm)

## 7. X-ray crystallography

Crystallographic data were collected on Nonius Kappa CCD diffractometer equipped with Bruker APEX-II CCD detector using monochromatized MoKα radiation (λ = 0.71073 Å) at a temperature of 150(2) K. The structures were solved by direct methods (SHELXS)[7] and refined by full matrix least squares based on $F^2$ (SHELXL97)[7]. The hydrogen atoms on carbons were fixed into idealized positions (riding model) and assigned temperature factors either $H_{iso}$(H) = 1.2 Ueq(pivot atom) or 1.5 for methyl moiety.

**HeliDye1**
**CCDC 1412114**

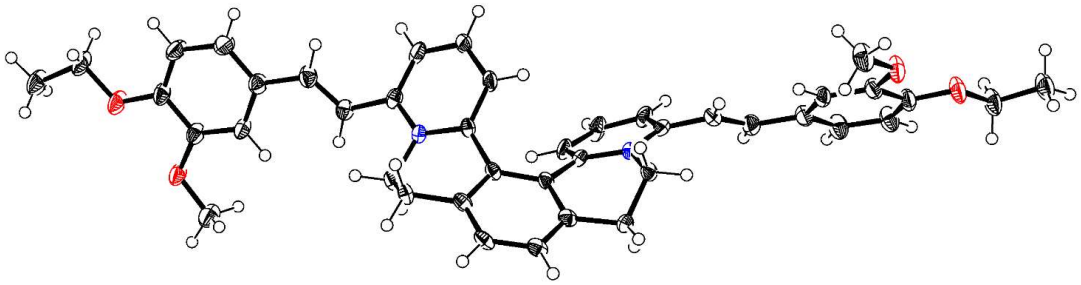

The displacement ellipsoids in this illustration were set to 50% probability level.

Dibromide salt of **HeliDye1** was obtained by anion exchange from the corresponding bistriflate salt. **HeliDye1** (10 mg, 0.0107 mmol) and tetra-*n*-butylammonium bromide (14 mg, 0.0434 mmol, 4 equiv.) were mixed in acetonitrile (3 mL) and the solution was stirred at RT overnight. The resulting precipitate was purified by repetitive washing with acetone (1 mL). Sonication, centrifugation and supernatant removal led to the solid product, which was then dried under high vacuum (8.3 mg, 0.0104 mmols, 97%).

Dibromide salt of **HeliDye1** (2 mg) was dissolved in MeOH (0.2 mL). Single crystals suitable for X-ray analysis were grown *via* slow diffusion of *i*-$Pr_2O$ into the methanolic solution at RT (22-25°C) in the dark within 8-10 days.

CCDC 1412114. Crystal data: $C_{42}H_{42}N_2O_4$•2Br, $M_r$ = 798.60, Monoclinic, *C*2/*c* (No 15), *a* = 45.657 (4) Å, *b* = 12.2162 (12) Å, *c* = 7.4051 (6) Å, *β* = 93.046 (3)°, *V* = 4124.4 (7)Å$^3$, Z = 4, $D_x$ = 1.286 Mg m$^{-3}$, yellow plate of dimensions 0.38 × 0.18 × 0.06 mm, numerical absorption correction ($\mu$ = 2.01 mm$^{-1}$) $T_{min}$ = 0.515, $T_{max}$ = 0.896, a total of 13287 measured reflections ($\theta_{max}$= 26˚), from which 4050 were unique ($R_{int}$ = 0.039) and 2859 observed according to the $I > 2\sigma(I)$ criterion. The refinement converged ($\Delta/\sigma_{max}$= 0.001) to *R* = 0.048 for observed reflections and $wR(F^2)$ = 0.116, GOF = 1.01 for 228 parameters and all 4050 reflections. The final difference Fourier map displayed no peaks of chemical significance, ($\Delta\rho_{max}$ = 0.74, $\Delta\rho_{min}$ = -0.34 e.Å$^{-3}$).
PLATON/ SQUEEZE procedure was used to correct the diffraction data for the presence of the disordered methanol solvent.

## 8. Initial screening for dsDNA binding fluorescence light-up probes

In the initial screening for dsDNA binding fluorescence light-up probes, each member of a dye candidate library was tested for its fluorescence in presence and absence of ds26 DNA. All test dyes were used as 1 mM stock solutions in DMSO. 1 mM stock solution of ds26 DNA was prepared by dissolving lyophilized solid in nuclease free water, by following protocol supplied by the producer (See Materials, Section 2). All dyes were tested in a black transparent bottom 384-well plate (Nunc® MaxiSorp™) with one row filled with ds26 DNA and the respective dyes. The neighboring row was filled with the respective dyes only (*i.e.* without dsDNA).

a) Wells containing ds26 DNA: In each well 1 mM stock solution of ds26 DNA (0.75 µL) and 1 mM DMSO stock solution of the test dye (1.5 µL) were mixed with 147.75 µL of BPES buffer, to achieve 5 µM final dsDNA concentration and 10 µM final concentration of the test compound.

b) Wells without ds26 DNA (blank experiment): In each well 1 mM DMSO stock solution of the test dye (1.5 µL) was mixed with 148.5 µL of BPES buffer.

A fluorescence image of the well plate was recorded using ChemiDoc UV-transilluminator (BIO-RAD) imaging device using $\lambda_{excitation}$ = 302 nm.

### 8.1 Structure-activity relationship:

To determine influence of different moieties of **HeliDye1** on its dsDNA specificity, **HeliDye1** was compared with structurally related compounds using five different oligonucleotides: ds$(A_4T_4)_2$, ds$(C_4G_4)_2$, ss$(C_2AGT_2CGCGTAGTA_2C_3)$ [ssDNA], ds$(CA_2UCG_2AUCGA_2U_2CGAUC_2GAU_2G)$ [dsRNA] and total RNA isolated from HeLa S3 cells (Fig. S2 and S3). Oligonucleotides were mixed with dyes in PBS buffer in wells of 96-well plate to reach final concentrations 5 µM for oligonucleotide and 10 µM for the dye. Light up was observed using ChemiDoc UV-transilluminator (BIO-RAD) imaging device using $\lambda_{excitation}$ = 302 nm.

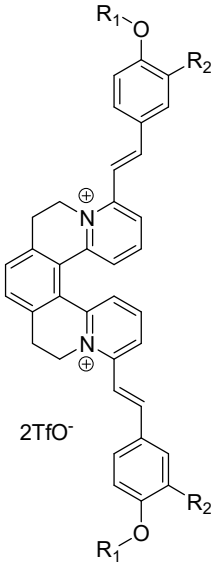


| | $R_1$ | $R_2$ |
|---|---|---|
| **HeliDye1** | Et | OMe |
| | Et | H |
| | Bu | OMe |
| | Heptyl | OMe |

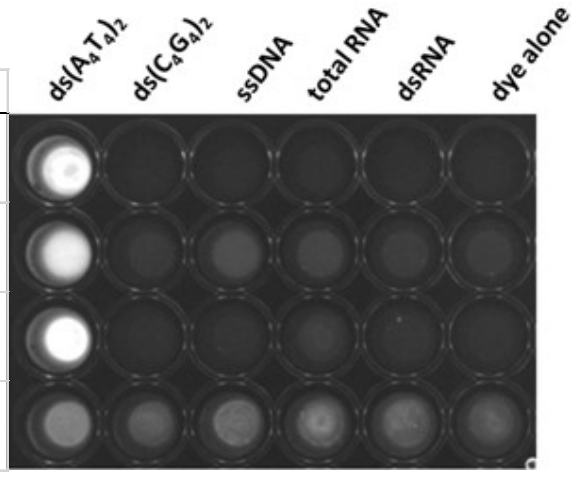


***Fig. S2*** *Comparison of AT selectivity of* ***HeliDye1*** *and its derivatives with modifications in alkoxyl groups.*

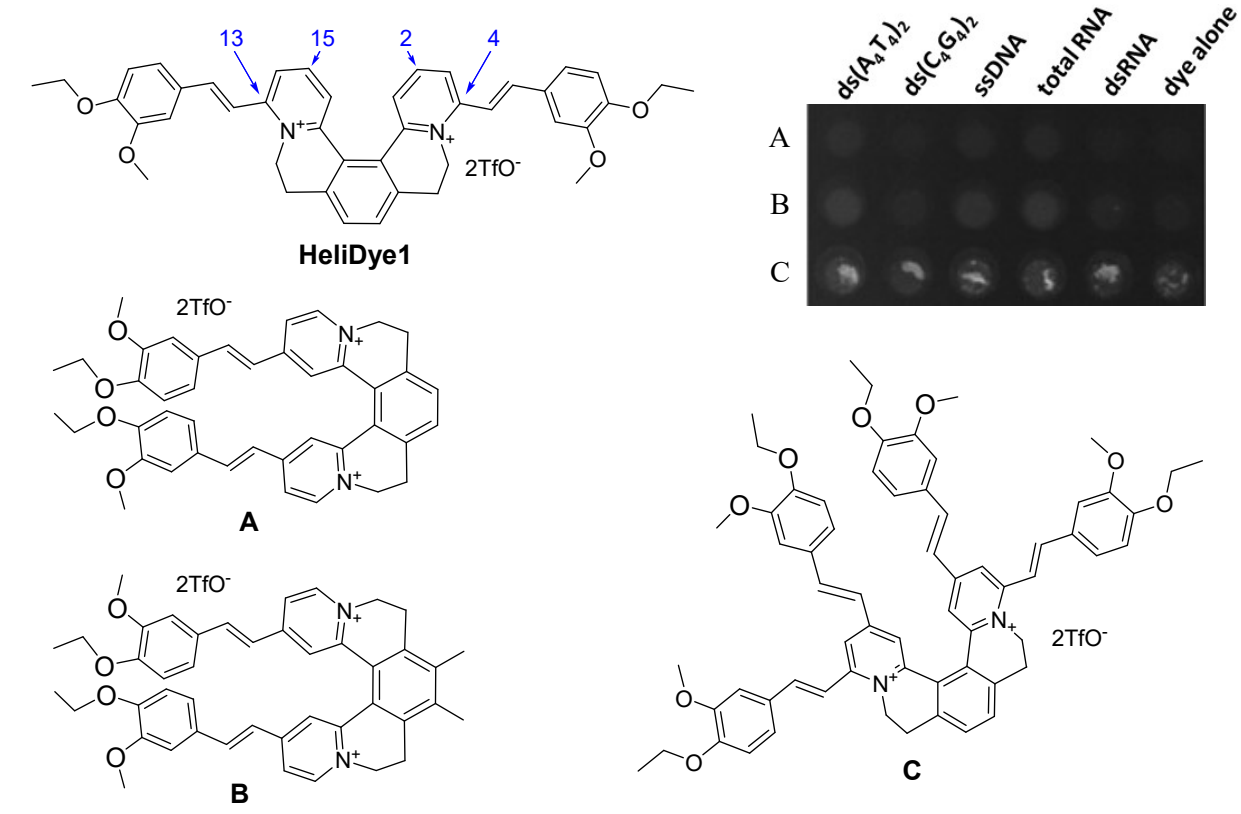


***Fig. S3*** *Comparison of AT selectivity of* ***HeliDye1*** *and its derivatives with modifications in position of styryl moieties.*

## 9. Characterization of HeliDye1

UV-vis absorption and fluorescence spectra of **HeliDye1** (10 µM) in presence and absence of various oligonucleotides (5 µM) were measured using standard UV-vis spectrometer Varian Cary 5000 series and fluorescence spectrometer Fluoromax-4, respectively.

### 9.1. UV-vis absorption and fluorescence spectroscopy:

All UV-vis and fluorescence spectra were measured in semi-micro quartz fluorescence cuvettes (Hellma Analytics) of path length 1 cm. The individual samples were prepared with or without oligonucleotide using 1 mM **HeliDye1** stock solution and 1 mM oligonucleotide stock solution as follows:

1. with oligonucleotide: Mixing of 1mM oligonucleotide stock solution (5 µL) + BPES buffer (985 µL) + **HeliDye1** 1mM stock solution (10 µL) in a 1.5 mL Eppendorf tube.

2. without oligonucleotide: Mixing of 1 mM **HeliDye1** stock solution (10 µL) + BPES buffer (990 µL) in a 1.5 mL Eppendorf tube.

UV-vis absorption spectra of each sample was measured in 300–750 nm range with reference to the corresponding blank solution. For **HeliDye1** in absence of oligonucleotide, BPES buffer containing 1% DMSO was used as a reference. For each sample of **HeliDye1** with each oligonucleotide, respective oligonucleotide solution (5 µM) in BPES buffer (containing 1% DMSO) was used as a reference solution.

After measurements of absorption spectra of each solution, fluorescence spectra of each sample was recorded at $\lambda_{excitation}$ = 460 nm. UV-vis and fluorescence spectra for **HeliDye1** with and without respective oligonucleotide were plotted. See Fig. 2C in the manuscript for UV-vis and fluorescence spectra with and without ds26 DNA and Fig. S4 for UV-vis and fluorescence spectra with and without other dsDNA oligonucleotide sequences. The UV-vis absorption maxima were shifted more for dsDNAs with higher number of AT-pairs in the oligonucleotide sequences. The spectral properties of **HeliDye1** in presence of different oligonucleotides are summarized in Table S1.

***Table S1*** *Spectral properties of* ***HeliDye1*** *in presence and absence of different Oligonucleotides ($c_{HeliDye1}$ = 10 μM; $c_{dsDNA}$ = 5 μM).*

| dsDNA | $\lambda_{abs}$ (nm) | $\lambda_{em}$ (nm) | $\epsilon$ (l.mol$^{-1}$cm$^{-1}$) |
|---|---|---|---|
| **ds26** | 438 | 590 | 19500 |
| **ds(GCA$_3$T$_3$GC)$_2$** | 435 | 590 | 20600 |
| **ds(A$_4$T$_4$)$_2$** | 458 | 590 | 20500 |
| **-** | 417 | - | 23000 |

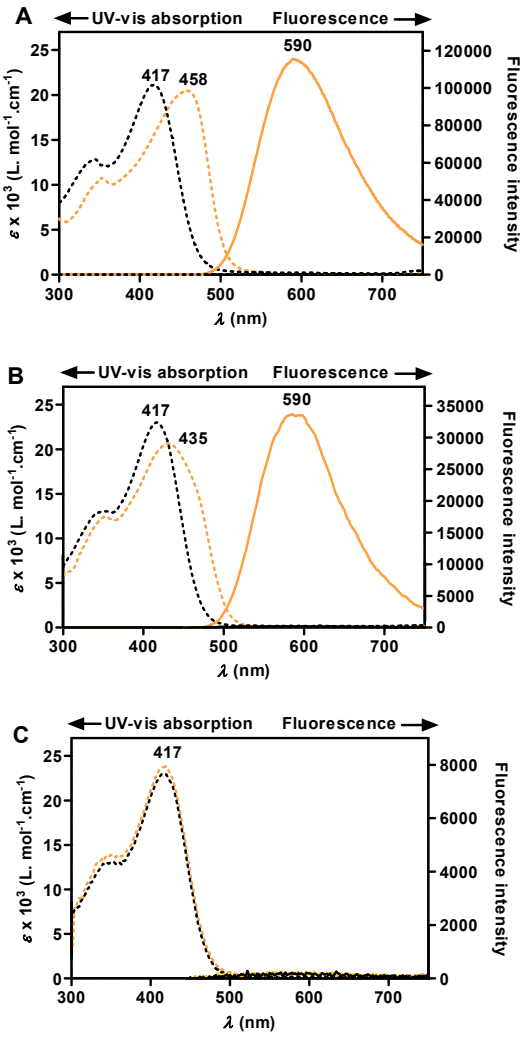


***Fig. S4*** *UV-vis absorption and emission spectra of* ***HeliDye1*** *in presence (orange) and absence (black) of: A) ds(A$_4$T$_4$)$_2$; B) ds(GCA$_3$T$_3$GC)$_2$ and C) ds(C$_4$G$_4$)$_2$.*

## 9.2. Selectivity profile of HeliDye1:

Light-up properties of **HeliDye1** were studied with various dsDNAs, ssDNAs and RNA to determine the selectivity profile. All tested nucleic acids were dissolved in nuclease free water at 1 mM concentration and **HeliDye1** was dissolved in pure DMSO at 1 mM concentration.

In a 96 well plate, each well, 1 mM stock solution of respective nucleic acid (0.75 µL) and 1 mM DMSO stock solution of **HeliDye1** (1.5 µL) were mixed with 147.75 µL of BPES buffer, to achieve 5 µM final respective nucleic acid concentrations and 10 µM final concentration of **HeliDye1**. Fluorescence spectra of **HeliDye1** in presence of each analyte were measured 5 minutes after mixing ($\lambda_{excitation}$ = 460 nm). No fluorescence light-up was observed in presence of dsDNA sequences lacking AT pairs, ssDNAs and total RNA isolated from HeLa S3 cells using regular RNA isolation and purification kit and protocol[8].

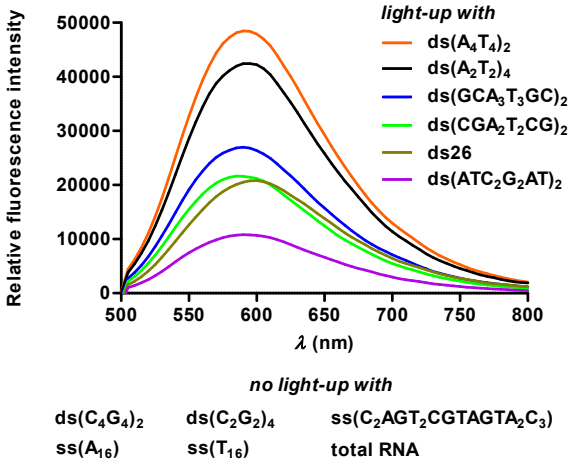


***Fig. S5*** *Fluorescence light-up of* ***HeliDye1*** *with dsDNA sequences containing AT pairs. Light-up occurs only for AT containing dsDNA and is absent in case of ssDNA sequences or RNA.*

## 9.3. Variable temperature NMR of HeliDye1:

Variable temperature $^1$H NMR spectra of **HeliDye1** in $CD_3CN$ (Fig. S6, black line) to determine the activation barrier of dye racemization were measured in 10-80 °C temperature range in 10 °C steps at 500 MHz Bruker Avance II NMR spectrometer. Rate constant values *k* at each temperature were determined by lineshape analysis of $^1$H NMR spectra (Fig. S6, red line) of **HeliDye1** at each temperature, using Dynamic NMR Lineshape Fitting module implemented in TopSpin 3.1 software. The values of $\Delta H$, $\Delta S$ and $\Delta G$ were determined from the slope of the graph (Fig. S7) between $(1/T)$ *Vs.* ln $(k/T)$ using linear form of the Eyring-Polanyi equation.

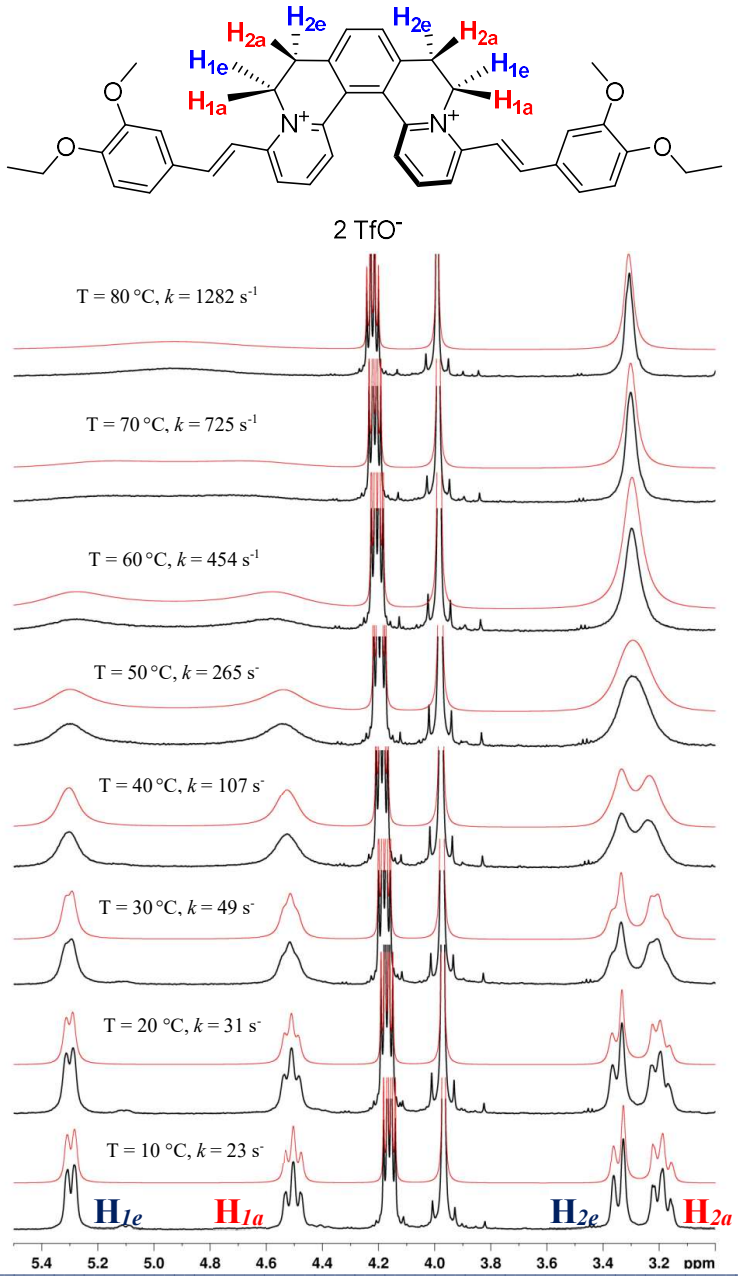


***Fig. S6*** *Variable temperature $^1$H NMR spectra of **HeliDye1** in $CD_3CN$ (black line) and simulated $^1$H NMR spectra (red line) at each temperature.*

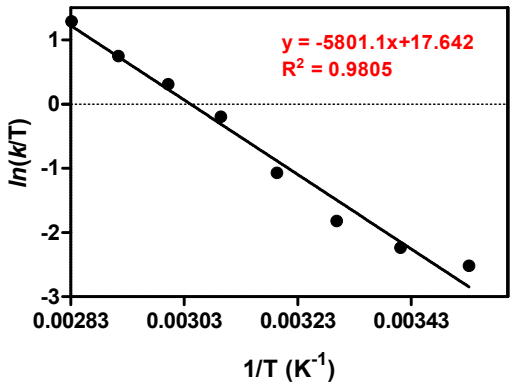


***Fig. S7*** *Plot of 1/T (K$^{-1}$) vs. ln (k/T).*

$-\Delta H/R$ = -5801.1 (where $R$ = gas constant = 8.314 J mol$^{-1}$ K$^{-1}$)
$\Delta H$ = 48.23 kJ mol$^{-1}$
$\Delta S = 17.642 \times R - ln(k_B/h) \times R$ (where $k_B$ = 1.380658 x 10$^{-23}$ J K$^{-1}$ and $h$ = 6.6260755 x 10$^{-34}$ J s)
$\Delta S$ = -50.88 J k$^{-1}$mol$^{-1}$
$\Delta G = \Delta H - T \times \Delta S$
$\Delta G$ = 63.15 kJ mol$^{-1}$ (at 20 °C)

## 10. $K_D$ values of interaction of HeliDye1 and various dsDNA sequences

The dissociation constants ($K_D$) of interaction of **HeliDye1** with various example DNA duplexes were determined by fluorescence titration method (Fig. 4A, B in the manuscript and Table S2). Each oligonucleotide (1 µM) was titrated with increasing concentrations of **HeliDye1** from 0 to 200 µM in BPES buffer. The dissociation curves were best fitted using 1:1 binding with Hill slope model (nonlinear regression least square method) from GraphPad Prism 5[9]. The dissociation constants for each of the dsDNA sequence are summarized in Table S2. An inverse relationship was found between number of AT pairs and $K_D$.

***Table S2:*** *$K_D$ values for interaction of* ***HeliDye1*** *with various DNA duplexes ($c_{dsDNA}$ = 1 µM).*

| | *Sequence (5' - 3')* | *$K_D$ (µM)* | *Number of AT pairs* |
|---|---|---|---|
| | ***Part A: self-complementary dsDNA sequences*** | | |
| 1 | ds(AAAATTTTAAAATTTT) | 2.9 ± 0.04 | 8 |
| 2 | ds(AATTAATTAATTAATT) | 3.5 ± 0.20 | 8 |
| 3 | ds(GCAAATTTGCGCAAATTTGC) | 5.0 ± 0.20 | 6 |
| 4 | ds(CGAATTCGCGAATTCG) | 5.7 ± 0.20 | 4 |
| 5 | ds(CGCGAATTCGCGCGCGAATTCGCG) | 6.0 ± 0.10 | 4 |
| 6 | ds(ATCCGGATATCCGGAT) | 15.1± 0.10 | 4 |
| | ***Part B: hairpin-forming dsDNA sequences*** | | |
| 7 | ds(CAATCGGATCGAATTCGATCCGATTG) | 5.9 ± 0.20 | 7 |
| 8 | ds(GGCAAAAACGCGGTCCGCGTTTTTGCC) | 9.7 ± 0.10 | 5 |
| 9 | ds(GGCAAAACCGCGGTCCGCGGTTTTGCC) | 11.2 ± 0.03 | 4 |
| 10 | ds(GGCAAAGCCGCGGTCCGCGGCTTTGCC) | 16.1 ± 0.20 | 3 |
| 11 | ds(GGCAACGCCGCGGTCCGCGGCGTTGCC) | 26.5 ± 0.30 | 2 |
| 12 | ds(GGCAGCGCCGCGGTCCGCGGCGCTGCC) | 48.2 ± 0.50 | 1 |

## 11. AT selectivity of HeliDye1 compared to commercial probes

Selectivity profile of **HeliDye1** was compared to three representative commercial dsDNA binding probes; propidium iodide (PI) and Hoechst 33258 and DAPI. Five different oligonucleotides were dissolved in nuclease free water to give 1 mM stock solutions: ds($A_4T_4$)$_2$, ds($C_4G_4$)$_2$, ss($C_2AGT_2CGCGTAGTA_2C_3$) [ssDNA], ds($CA_2UCG_2AUCGA_2U_2CGAUC_2GAU_2G$) [dsRNA] and total RNA isolated from HeLa S3 cells. All four test dyes (**HeliDye1**, DAPI, PI and Hoechst 33258) were dissolved in DMSO to give 1 mM stock solutions. A 96-well plate was prepared as follows: Each oligonucleotide was filled in its own well at 5 µM final concentration in PBS buffer, followed by addition of a dye into each well (10 µM final concentration). Last well was filled with dye alone. The well plate picture was recorded using ChemiDoc UV-transilluminator (BIO-RAD) imaging device using $\lambda_{excitation}$ = 302 nm. The selectivity of **HeliDye1** towards AT containing DNA duplex in comparison to commercial dyes was shown by fluorescence measurements of each dye separately under its optimal exposure time (Fig. S8) and by quantitative fluorescence measurements of each dye (excited

at its appropriate wavelengths, according to producer[10]) in presence of each analyte (appropriate necleic acid; Fig. 5 in the manuscript), using Tecan infinite M1000 microplate reader. For better comparison within the Fig. S8, the intensities of empty wells were equalised as following. The average intensity of pixels in emty wells was calculated as the average of modes (it is important to use the mode since it is not affected by several intensive pixels caused by dast or noise of detector) of both empty wells for each dye separately. The calculated average intensities differed due to different exposition times, different location of the plate in the instrument, and even different location of the compounds within the plate (we observed it experimentaly). Then a background was subtracted from each subfigure separately such a way that after the subtraction the everage intensities of pixels in emty wells were the same for all four subfigures. The pixel intensities in the empty wells were not set to zero intentionally, so the intensities of emty wells can be compared with the other wells. Note that only in the case of **HeliDye1** the other wells are comparable to the empty wells.

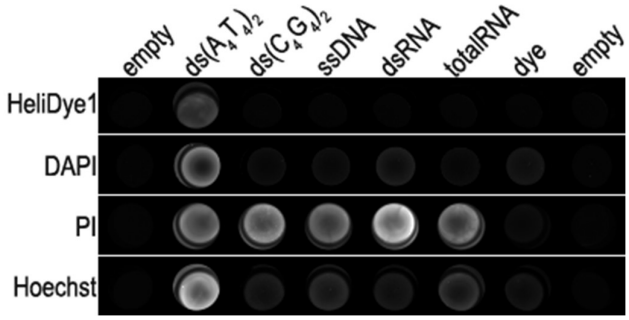


***Fig. S8*** *Sequence selectivity of* ***HeliDye1*** *as compared to commercial probes propidium iodide (**PI**), **Hoechst 33258** and **DAPI**. Note that a monitor is necessary to provide complete information of the figure and the printed version is not suitable.*

General protocol for post-staining, used in case of GelRed™ was followed[11]. Different nucleic acid sequences were loaded (100 pmol) in each well of 16% nondenaturing polyacrylamide gel in TBE (pH 7.5) and run using a standard protocol[12]. After running the gels, staining of nucleic acid bands was performed with 1 μM solution of **HeliDye1** or GelRed™ staining solution for 15 minutes (10000x solution from supplier was diluted to a final 4x concentration). The gels were visualized with Typhoon FLA 9500 fluorescence scanner, GE Healthcare, USA equipped with 473 nm blue LD laser and LBP filter (Fig. S9).

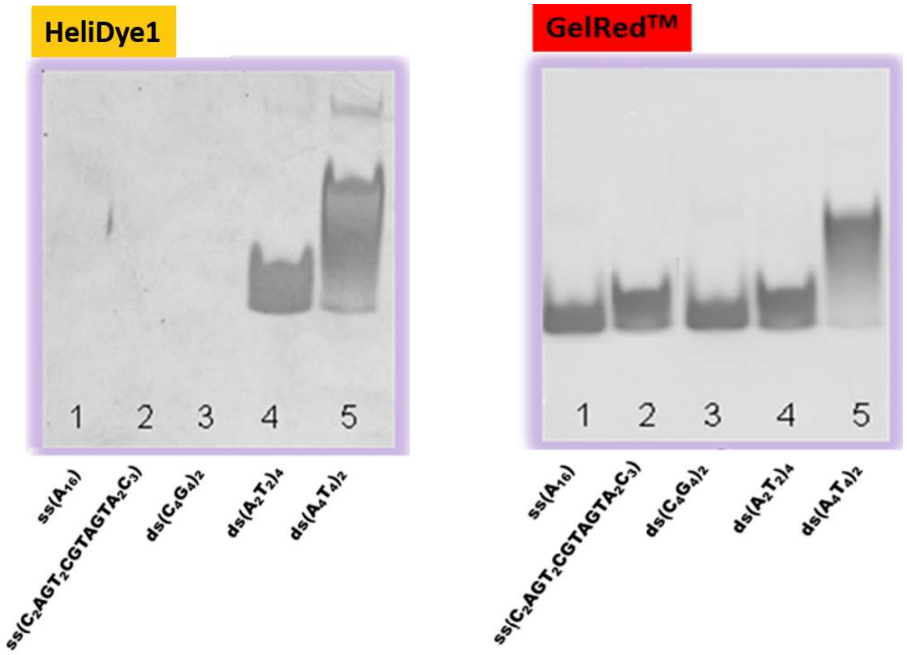


***Fig. S9*** *Staining in nondenaturing polyacrylamide gel electrophoresis shows selectivity of* ***HeliDye1*** *(1 μM, left panel) for AT-containing DNA duplexes as compared to non-selective staining with commercial probe GelRed™ (right panel).*

## 12. Hydrodynamic study (viscosimetry)

Viscosity measurements were performed using Rolling Ball Viscometer Lovis 2000 M/ME series, from Anton Parr GmbH. Following solutions with five different ratios of **HeliDye1** : dsDNA solutions were prepared (Table S3), while keeping the concentration of dsDNA constant at 100 μM bp. Base pair molarity of the ctDNA stock solution was determined as follows. Concentration value of the DNA stock solution (in ng/μL) was determined by *NanoDrop*™ 1000 spectrophotometer and using this information in combination with DNA calculator at molbiotools webpage[13], the base pair molarity of the DNA stock solution was determined.

***Table S3*** *Solutions of different* ***HeliDye1****: dsDNA ratios used for viscosity measurement.*

| | $c_{dye}$ (μM) | $c_{dsDNA}$ (μM) | Ratio (dye/dsDNA) |
|---|---|---|---|
| 1. | 0 | 100 | 0 |
| 2. | 25 | 100 | 0.25 |
| 3. | 50 | 100 | 0.5 |
| 4. | 100 | 100 | 1 |
| 5. | 200 | 100 | 2 |

Viscosity of each solution was measured four times, and a graph presenting $(n/n_o)^{1/3}$ *vs.* **HeliDye1**:dsDNA ratio was plotted in Fig. 8 in the manuscript; $n$ stands for the average viscosity of the solution and $n_o$ stands for viscosity of the solution for which **HeliDye1**:dsDNA ratio = 0).
Analogues experiments were performed for propidium iodide (**PI**) and **DAPI.**

## 13. Electronic circular dichroism (ECD) spectroscopy

### 13.1. Experimental ECD spectra:

ECD spectra were measured on a Jasco-815 spectropolarimeter at room temperature in spectral region from 220 nm to 700 nm in 1 mm quartz cell (scanning speed of 5 nm/min, response time of 32 s, data pitch 0.1 nm and 2 spectra accumulations). After baseline subtraction, the final data were plotted using differential absorbance (Fig. 9 in the manuscript and Fig. S10).

1 mM DMSO Stock solutions of **HeliDye1** or the respective **HeliDye3** (*racemate*, *(P-)* or *(M)*-enantiomers), were used. 1 mM stock solution of ds26 DNA was prepared by dissolving lyophilized solid in nuclease free water, by following protocol supplied by the producer (See Materials, Section 2). The experimental mixtures of ds26 DNA with **HeliDye1** or with the respective **HeliDye3** (*racemate*, *(P-)* or *(M)*-enantiomers), were prepared using the stock solutions mentioned above in BPES buffer to get final volume of 200 μL and final concentrations of $c_{ds26}$ = 5 μM and $c_{Dye}$ = 5 μM. ECD spectra of **HeliDye1** and **HeliDye3** (*racemate*, *(P-)* or *(M)*-enantiomers) were measured after mixing with ds26 DNA.

ECD spectra were also measured for a variable concentration of ds26 DNA. Concentration of **HeliDye1** or the respective **HeliDye3** (*racemate*, *(P-*) or *(M)*-enantiomers) was always 10 μM while concentration

of dsDNA was variable from 0 to 400 μM range (See Fig. 9 in the manuscript and Fig. S10). The sample preparation for these experiments was similar to the described above.

Ather DNA sequenses tested for interaction with **HeliDye1** are shown in Fig. S10. The sample preparation for these experiments was similar to the one described above.

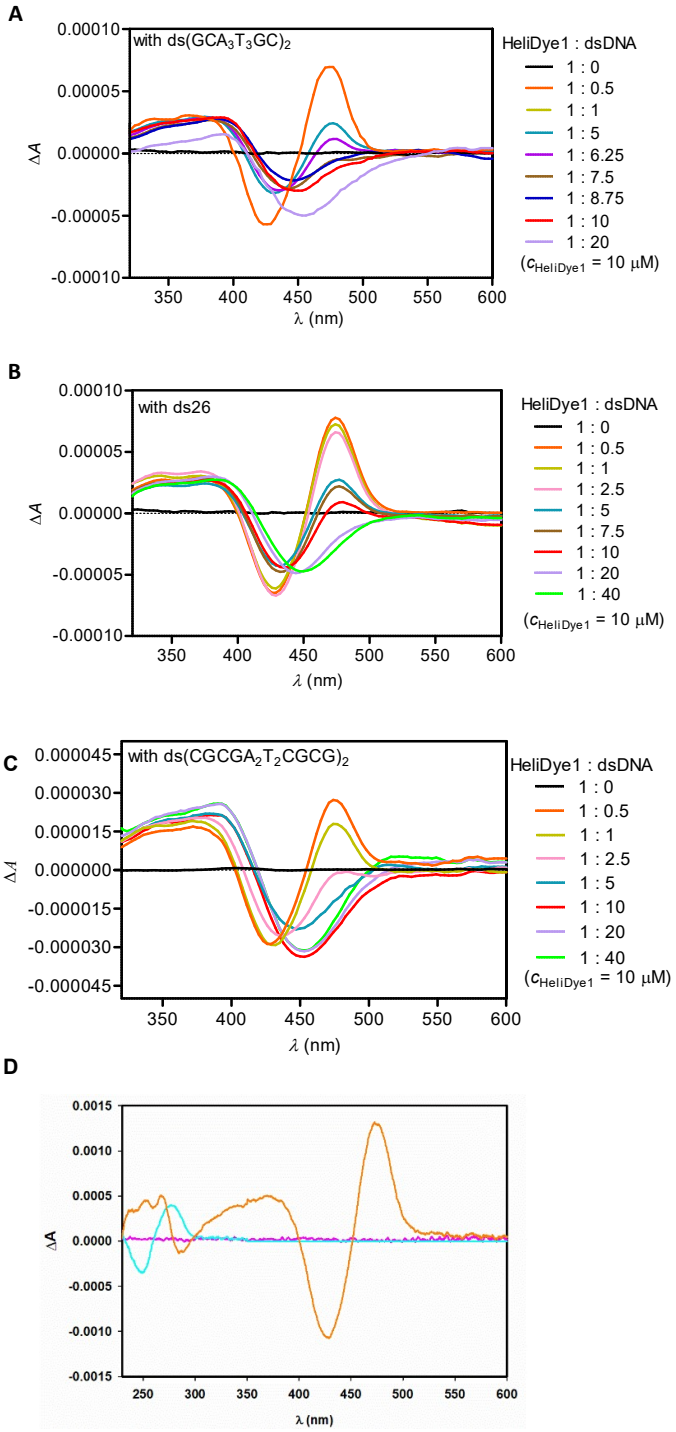


***Fig. S10*** *(A, B, C) ECD spectra in the course of titration of* ***HeliDye1*** *(constant at 10 μM) with dsDNA (0 to 400 μM) in BPES buffer for three different dsDNA. (D) ECD spectra of* ***HeliDye1****-dsDNA complex (orange line), neat* ***HeliDye1*** *solution (pink line), and neat dsDNA solution (cyan line) depicting also UV spectral region.*

## 13.2. Simulated ECD spectra:

All DFT calculations were performed in Gaussian 16, Revision A.03 program[14–16]. Starting geometry of **HeliDye1** from the single crystal X-ray structure analysis (SI section 7) was further optimized using B3LYP functional[17] with 6-31+G* basis set using D3 version of Grimme's empirical dispersion (EmpiricalDispersion = GD3 keyword)[18] in water as a solvent (PCM model[18], $\varepsilon_r$ = 78.3553, scrf=(solvent=water) keyword). Optimized structure was confirmed to be the minimum by harmonic frequency calculation at the same level of theory (Fig. S11).

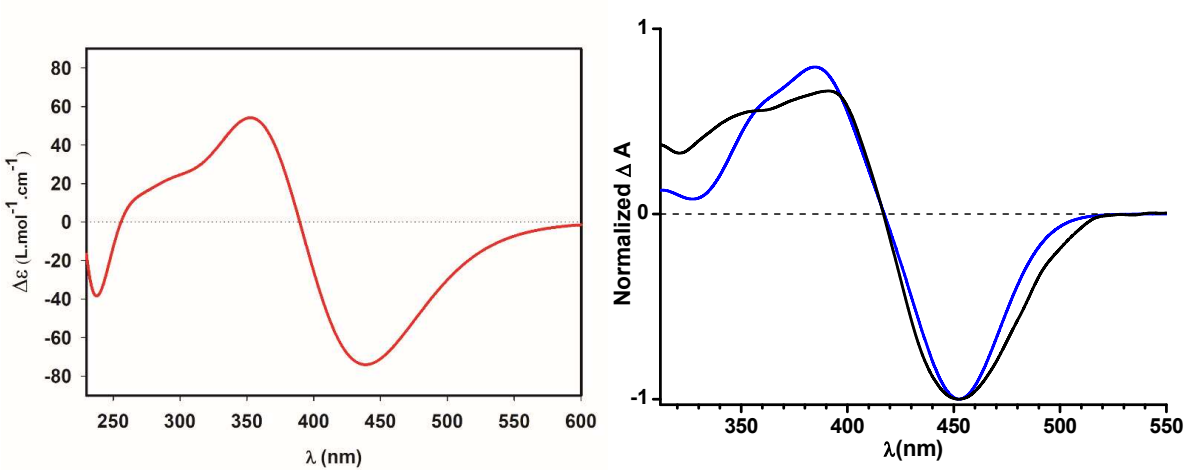


***Fig. S11*** *Simulated ECD spectra of free P-enantiomer of* ***HeliDye1*** *(left spectrum) is similar to the experimental spectrum of the monomer of* ***HeliDye1*** *inside of dsDNA (right spectrum black line). Simulated spectrum of the monomer inside of dsDNA is also shown (right spectrum blue line). Experimental spectrum was obtained as an average of three spectra upon a FFT smoothing and normalisation.*

**Calculation of ECD spectrum of single molecule of *(P)*-HeliDye1 in water**

Geometry from the previous procedure for the dication of **HeliDye1** was directly used for TD-DFT excited state calculation. Polarizable continuum model (PCM)[19] was used for the description of solvent in all the calculations (water, $\varepsilon_r$ = 78.3553, scrf=(solvent=water) keyword). For the spectrum, 150 excited states were calculated (td=(nstate=150,singlets) keyword). BMK functional[20] was used with 6-31+G* basis set[21]. The simulated ECD spectrum was generated by broadening the calculated transition intensities by Gaussian curve with standard deviation $\sigma$ = 0.3 eV. Due to a low racemisation barrier of **HeliDye1**, experimental spectra canot be measured, so no scaling of the wavelengths and intensities was employed[21].

**Calculation of ECD spectrum of *(P)*-HeliDye1 dimer and monomer in dsDNA**

Firstly a QM/MM approach was tried, however, no conformation converged within a few months of calculations. Thus we simplified the problem to the optimisation of the **HeliDye1** dimer inside the frozen dsDNA at QM/MM level (oniom). The **HeliDye1** dimer was optimised without any constrains by M062X/6-31+G* inside the frozen dsDNA described by the Amber force field. The MM charges were embedded into DFT calculations (oniom=embedcharge). Implicit solvent model of water (PCM) was used firstly with a solvent-accessible-surface type of solute-solvent boundary (during the frequency calculation and optimisation; surface=sas) and then with solvent-excluding-surface type of solute-solvent boundary (single point and ECD calculation; surface=ses addsph). The reaction field was calculated separately in each subcalculation always using the cavity of the real system (oniompcm=x).

Force constants were calculated at the first point of the optimisation at lower level of theory (M062X/6-31G and amber; freq=noraman oniom(m062x/6-31G:amber)=embedcharge scrf=(solvent=water, read, oniompcm=x) surface=sas).

Then the complex was optimised at higher level of theory (M062X/6-31+G* and amber) with all atoms of dsDNA frozen. (opt=(readfc,readopt) oniom(M062X/6-31+G(d):amber)=embedcharge Integral=(FineGrid) scrf=(solvent=water,read,oniompcm=x) surface=sas).

To improve the solvent model, a single point calculation was performed on the optimised structure with changed type of solute-solvent boundary (oniom(M062X/6-31+G(d):amber)=embedcharge scrf=(solvent=water,read,oniompcm=x) surface=ses addsph).

Finally, the ECD spectrum was calculated with 10 energetically lowest transitions to singlet excited states only. A threshold for printing eigenvector components was increased to 0.01 by iop option. (oniom(td=(nstates=10)/M062X/6-31+g(d):amber)=embedcharge scrf=(solvent=water,read,oniompcm=x) iop(9/40=2).

The calculated stick spectrum was firstly convoluted with a Gaussian function ($\sigma$ = 0.07 eV). Then it was normalized so the negative band has an intensity –1. Then the calculated wavelengts were scaled according to equation $\lambda' = 1.8\lambda - 284.74$, so the negative band at 426 nm matches with the experimental band.

The monomer of **HeliDye1** inside of dsDNA at the same level of theory was calculated as well ($\sigma$ = 0.09 eV, normalized, $\lambda' = 1.6\lambda - 196.25$). The character of the ECD spectrum (Fig. S11 blue line) of *(P)*-**HeliDye1** within this complex was similar to that of the free *(P)*-**HeliDye1** monomer (not inside dsDNA; Fig. S11 left spectrum). In both cases, the positive band in the region around 475 nm was missing.

## 14. Computational methodology

### 14.1. Preparation of starting structures:

For computational modeling we considered (*P)*-enantiomer of the **HeliDye1** compound since only this type of chirality was experimentally observed upon dsDNA-dye interaction. Instead of the ds26 double-stranded DNA tested under experimental conditions, for the sake of simplicity we resorted to the 20-mer model ds20 (sequence: GCAAATTTGCGCAAATTTGC, $K_D$ = 5.0 μM). This choice was dictated by the fact that the structure of the minor groove in both ds26 and ds20 models should be identical. It is important that the sequence of ds20 is enriched with AT base pairs, which is crucial for explanation of the experimentally observed AT-selectivity of **HeliDye1**. The three-dimensional structure of the ds20 model was created in Discovery Studio Visualizer 4.1 by means of Build and Edit Nucleic Acid toolbar (Build Action: Create/Grow at 3'; Nucleic Acid Type: DNA-Duplex; Conformation: B DNA).

Since ECD spectroscopy (bisignate spectra) and 2:1 (**HeliDye1**:DNA) binding stoichiometry provide unambiguous evidence for a **HeliDye1** dimer formation within the DNA minor groove, we aimed at obtaining ds20-dimer associates. The initial attempts to generate starting complexes with the help of various molecular docking algorithms did not yield satisfactory binding poses which can be due to the fact that the rigid docking approach does not take into account the DNA minor groove induced fit accompanying ds20-ligand interaction.

Therefore, the ds20- **HeliDye1** dimer complexes were generated manually. In addition to the ds20 DNA enriched with AT pairs, we constructed a related model, ds20-mut (sequence: GCGGGCCCGCGGAAATTTGC) where some A and T residues were mutated to G and C to cast some light on **HeliDye1** AT-selectivity. Overall, two dimer-ds20 complexes D1 and D2 (Fig. 10 in the manuscript) slightly differing in the stacking patterns between **HeliDye1** monomers within their dimers and dimer positions inside the minor groove, were built. The third complex dimer-ds20-mut (hereafter named as mutD1 complex) involved the GC-rich model of DNA ds20-mut.

All three complexes D1, D2 and mutD1 were subjected to a preliminary force field energy minimizations *in vacuo* to remove steric clashes (number of minimization cycles 4000, the steepest descent algorithm was used for the first 1000 cycles, then switched to the conjugate gradient algorithm for the remaining 3000 cycles; cutoff for electrostatic interactions was set to 10 Å). The minizations were performed within AMBER14 suite of programs (for force field details see the next section).

## 14.2. Molecular dynamics simulations:

The three complexes – AT-rich D1 and D2 and GC-rich mutD1 - described in the previous section served as starting structures for MD simulations. The dsDNA structures were treated with DNA.OL15 force field[22] as implemented in AMBER14 package, whereas the **HeliDye1** dimers were described in terms of GAFF force field[23]. Additional parametrization was needed for the ligands. For this purpose, a monomeric unit of dimers, i.e. *P*-enantiomer of **HeliDye1**, was subjected to DFT optimization (for details, see section 13.2). Electrostatic potential calculation were carried out at the HF/6-31G* computational level. The RESP charges were fitted by the antechamber tool of AMBER14. The atom types and force-field parameters were assigned by the parmcheck program.

Models were further solvated by SPC water molecules[24] and neutralized using tleap program of AMBER 14 by 40 $Na^+$ and 6 $Cl^-$ ions to maintain physiologic 0.15 M $Na^+$ concentration. The rectangular box with overall minimum distance of ~ 12 Å between periodic boundary replicas was used. The hydrogen mass repartitioning was performed by means of ParmEd program, which allowed us to extend the time step in the production run to 4 fs.

Equilibration of the system and unbiased molecular dynamics simulations were carried out using the pmemd.cuda engine designed to run on graphics processing units (GPUs) as implemented in AMBER 14 suite of programs. The equilibration protocol included the following stages: minimization of solute hydrogen with all heavy atoms restrained (with the restraint constant of 1000 kcal.mol$^{-1}$ Å$^{-2}$), water and counter ions minimization with dsDNA and ligand atoms restrained, sequence of minimizations (without SHAKE) of water, counter ions and ligand with the decreasing restraints applied to DNA backbone atoms (1000, 500, 125, 25, 0 kcal mol$^{-1}$ Å$^2$), 10 ps dynamics of solvent and counter ions followed by the heating of the whole system to 285 K.

Long-range electrostatic interactions were calculated using particle-mesh Ewald technique with a 10 Å cutoff for a direct summation. The 300 ns production simulations were carried out at constant temperature of 285 K and constant pressure of 1.0 bar using the Berendsen thermostat and barostat, respectively[25]. Input parameters, structures and MD trajectories are available at http://dx.doi.org/10.17632/vtxgt2y9rc.1.

40 snapshots were taken from the MD simulations of complexes D1 and D2 (20 snapshots each). Each conformation was preoptimised by MM (Amber OL15 force field). For ECD calculation, the conformations were further optimised by QM/MM (for details, see section 13.2).

## 15. AT duplex DNA selectivity of enantiomericaly stable analogues of HeliDye1, (*rac*)-HeliDye3, (*P*)-HeliDye3 and (*M*)-HeliDye3.

Selectivity profile of **HeliDye1** was compared to enantiomericaly stable analogues (*P*)-**HeliDye3** and (*M*)-**HeliDye3** and (*rac*)-**HeliDye3** using five different oligonucleotides: ds($A_4T_4$)$_2$, ds($C_4G_4$)$_2$, ss($C_2AGT_2CGCGTAGTA_2C_3$) [ssDNA], ds($CA_2UCG_2AUCGA_2U_2CGAUC_2GAU_2G$) [dsRNA] and total RNA isolated from HeLa S3 cells (Fig. S12). Oligonucleotides were mixed with dyes in PBS buffer in wells of 96-well plate to reach final concentrations 5 μM for oligonucleotide and 10 μM for the dye. Light up was observed using ChemiDoc UV-transilluminator (BIO-RAD) imaging device using $\lambda_{excitation}$ = 302 nm. As predicted from ECD only (*P*)-enantiomer of **HeliDye3**, interacts and produce AT rich duplex DNA sensitive light-up. The selectivity of **HeliDyes** towards AT containing DNA duplex was shown by fluorescence measurements of each dye separately under its optimal exposure time.

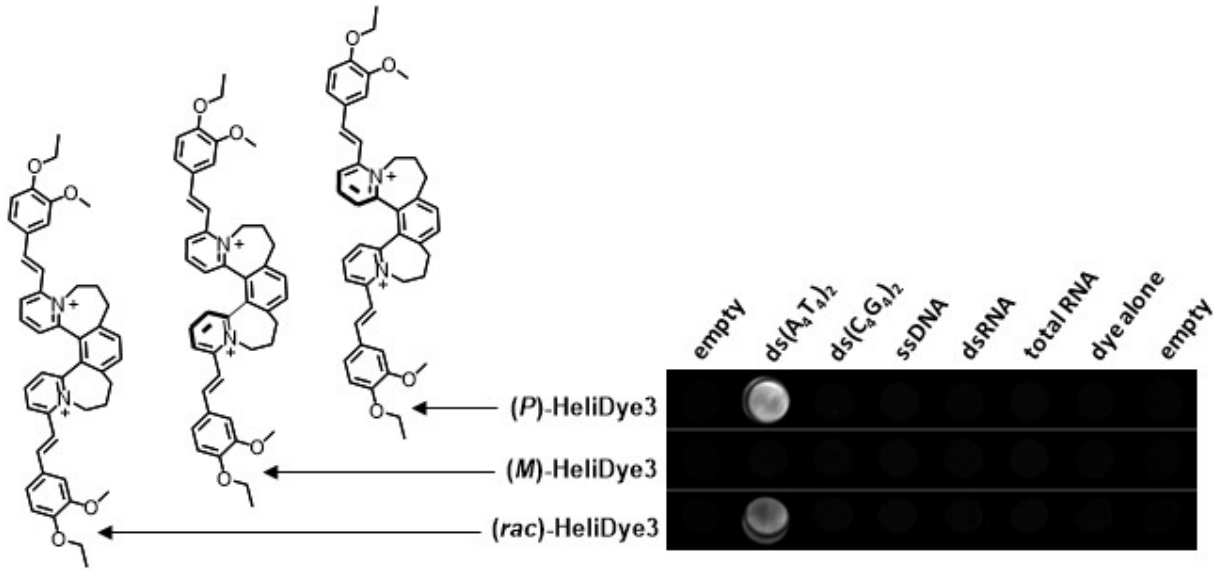


***Fig. S12*** *Sequence selectivity of enantiomericaly stable analogues of* ***HeliDye1****: (P)-****HeliDye3****, (M)-****HeliDye3*** *and their racemic mixture (rac)-****HeliDye3****.*

## 16. Cell-based assays and karyotyping

### 16.1. Cell lines and cell culture conditions:

For cell-based experiments U-2 OS and HeLa S3 cell lines were used. U-2 OS cell line (cat. no. ATCC HTB-96, ATCC®, USA) was cultured in DMEM-Dulbecco′s Modified Eagle′s Medium (cat. no. D5796, Sigma-Aldrich, USA) supplemented with 1.0 % of L-glutamine (cat. no. G7513, Sigma-Aldrich, USA) and 1 % of Penicillin-Streptomycin (cat. no. P0781, Sigma-Aldrich, USA). HeLa S3 cell line (cat. no. ATCC CCL-2.2™, ATCC®, USA) was cultured in RPMI-1640 Dutch Modification medium (cat. no. R7638 Sigma-Aldrich, USA) supplemented with 1 % of L-glutamine and 1.0 % of Penicillin-Streptomycin. All cell lines were cultivated in 10 % Fetal bovine serum (cat. no. F9665, Sigma-Aldrich, USA). Culture conditions of cell lines used for viability assay are indicated in Noskova *et al.* 2002[26].

## 16.2. Preparation of stock solutions and dilutions:

Compound **HeliDye1** was dissolved as a 10 mM stock solution in DMSO (Sigma-Aldrich, D2650) and several aliquots were prepared and frozen. For each experiment, new aliquot was used to produce desired concentration in PBS (maximum DMSO content was ≤ 1.0 % $_{vol}$).

## 16.3. Live / dead cell exclusion experiments:

For these experiments a mixture of dead and viable HeLa S3 cells was prepared in a ratio of approximately 1:1 for experiments with **HeliDye1** (Fig. S13A-C) and 2:1 for experiments with **HeliDye3** (Fig. S14A-C). Dead cells (Fig. S13A and Fig. S14A) were prepared by prolonged starvation. Subsequently the cell mixture was single stained with the **HeliDye1**, (*rac*)**-HeliDye3,** (*P*)**-HeliDye3** and (*M*)**-HeliDye3,** DAPI and Hoechst 33258 at the final concentration of 1 µM and PI at the final concentration of 1.5 µM (Fig. S13D-I and Fig. S14D-L). Only for co-staining of DAPI and **HeliDye1,** the concentration of **HeliDye1** was 5 µM (Fig. 6C in the manuscript). The cells for flow cytometry were stained for 15 min, measured by BD LSR Fortessa™ (Becton, Dickinson and Company, USA) and analyzed by Diva 8 software (v. 8.0 Becton, Dickinson and Company, USA). First, the forward scatter (FSC) and side scatter (SSC) were used to discriminate live and dead cells, then fluorescence signals of the stained cells were measured, stained populations were pseudo-coloured and back-gated to the dead population determined by FSC and SSC. By this, we could confirm that the single stained population is the same as the dead cell population (Fig. 6C in the manuscript). The same was done for all dyes (**HeliDye1**, (*rac*)**-HeliDye3,** (*P*)**-HeliDye3** and (*M*)**-HeliDye3,** DAPI, Hoechst 33258 and PI) and subsequently in co-staining experiments. The signals of co-staining experiments were checked for spill over in flow cytometry and bleed through in microscopy. The cells aimed for microscopy were visualized immediately after staining by confocal microscope (Zeiss LSM 780, Carl Zeiss, Germany) using the objective EC PlnN 10x/0.3 DICI. For settings and software that were used see section 16.5.

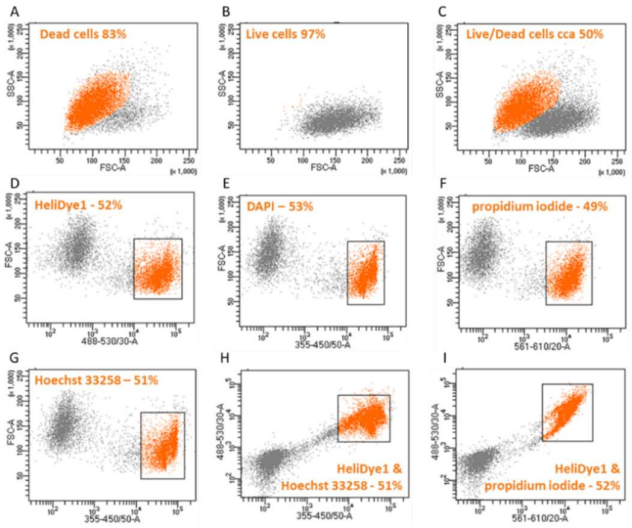


***Fig. S13*** *Preparation of a mixture of dead and live cells and single or co-staining of the mixture by various DNA dyes. Panel A: Dead cell population. Panel B: Viable cell population. Panel C: Mixed population of A and B such as a population of 50% live/dead cells arose. Panel D: Single staining with* ***HeliDye1*** *(1 µM). Panel E: Single staining with DAPI (1 µM). Panel F: Single staining with PI (1.5 µM). Panel G: Single staining with Hoechst 33258 (1 µM). Panel H: Co-staining of* ***HeliDye1*** *(1 µM) with Hoechst 33258 (1 µM). Panel I: Co-staining of* ***HeliDye1*** *(1 µM) with PI (1.5 µM). For panels D-I percentage corresponds to dead cells population in the dot-plot after gating.*

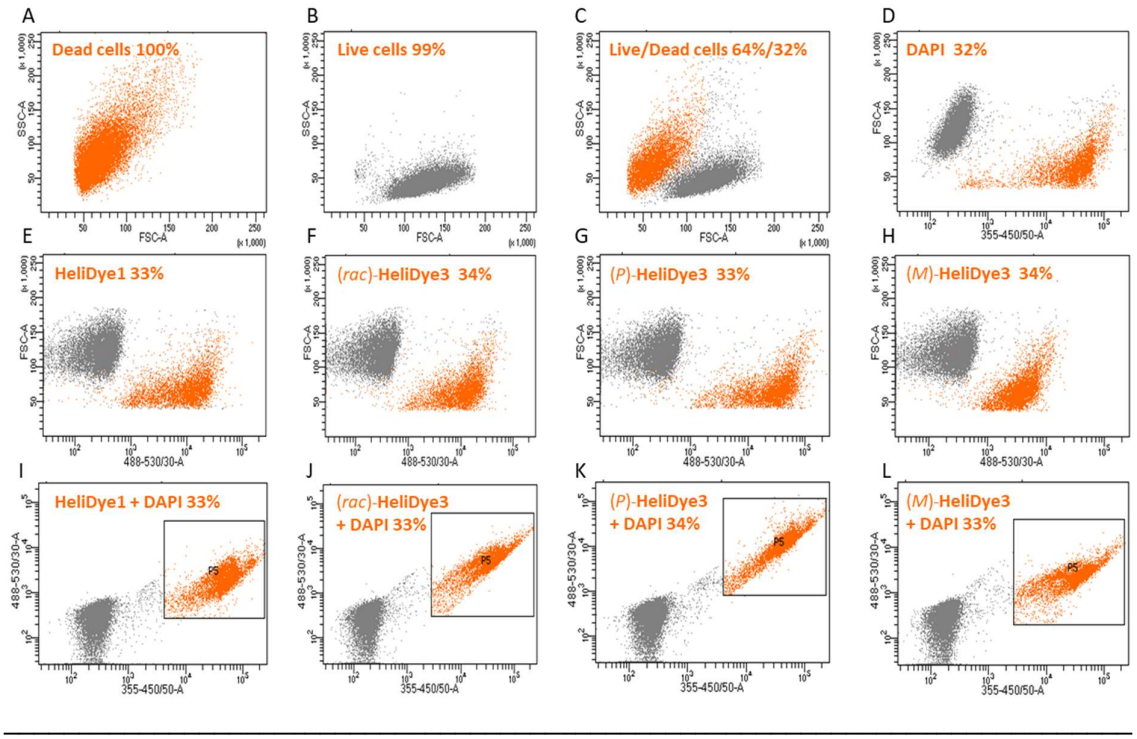


***Fig. S14*** *Preparation of a mixture of dead and live cells and single or co-staining of the mixture by various DNA dyes. Panel A: Dead cell population. Panel B: Viable cell population. Panel C: Mixed population of A and B – 33 % live / 64 % dead cells arose. Panel D: Single staining with DAPI (1 μM). Panel E: Single staining with* ***HeliDye1*** *(1 μM). Panel F: Single staining with (rac)-****HeliDye3*** *(1 μM). Panel G: Single staining with (P)-****HeliDye3*** *(1 μM). Panel H: Single staining with (M)-****HeliDye3*** *(1 μM). Panel I-L Co-staining of* ***HeliDye1*** *(1 μM), (rac)-****HeliDye3*** *(1 μM), (P)-****HeliDye3*** *(1 μM) and (M)-****HeliDye3*** *(1 μM) with DAPI (1 μM). Percentage correspond to dead cells and stained population in the dot-plot after gating. (M)-****HeliDye3*** *stains dead cells but its signal is much weaker as compared to the other dyes (Panel H) and the staining is not specific to DNA (as later shown by confocal microscopy Fig. S15).*

## 16.4. Cell cycle analysis:

For cell cycle analysis cca $10^6$ (1 million) HeLa S3 cells was used. The cells were counted, centrifuged, washed with PBS, fixed with ice cold EtOH (80 %) and left on ice for 30 minutes. Next the cells were washed with PBS and stained with **HeliDye1** or with PI at 37°C either in the presence of RNase (60 min treatment) or without RNase (3, 20 or 60 min treatment). The final concentration of **HeliDye1** was either 10 μM (for 20 and 60 min treatment) or 30 μM (for 3 min treatment). The final concentration of PI was 1.5 μM. The data were analyzed in FlowJo (v. 10.4, FLOWJO, LLC, USA). For cell cycle analysis, Watson (Pragmatic) model was used. The overlaid histograms show comparison of the treatments with and without RNase treatment for **HeliDye1** and PI (Fig. 6E in the manuscript). Comparison of quantifications of cell cycle phases is shown in Table S4.

***Table S4*** *Cell cycle analysis of HeLa S3 cells - Watson (Pragmatic) model.*

| Treatment | % of total cells in phase | | | $G_1$ CV |
|---|---|---|---|---|
| | $G_0/G_1$ | S | $G_2$/M | |
| **HeliDye1** | 42.7 | 31.1 | 13.4 | 5.86 |
| **HeliDye1** + RNase | 43.9 | 31.2 | 12.3 | 5.52 |
| propidium iodide (PI) | 47 | 31 | 12.8 | 10.2 |
| propidium iodide (PI) + RNase | 44.7 | 32 | 12.8 | 5.21 |

## 16.5. Confocal microscopy:

HeLa S3 cells were placed on a microscopic Petri dish (cat. no. D35C4-20-1.5-N, Cellvis, USA). After two days of growing the cells were washed with PBS, fixed with 4 % formaldehyde for 10 min., washed two times with PBS and double stained with **HeliDye1** and DAPI at the concentraion 5 µM and 1 µM, respectively (Fig. 6B in the manuscript), or with **HeliDye1,** (*rac*)**-HeliDye3,** (*P*)**-HeliDye3** and (*M*)**-HeliDye3** and DAPI all at the concentration 1 µM (Fig. S15). Stained cells were imaged with confocal microscope (Zeiss LSM 780, Carl Zeiss, Germany) using the water objective C-Apochromat 40x/1.2 W Korr FCS M27. 405 nm excitation and 410-465 nm emission wavelengths were used for DAPI. 488 nm excitation and 500-600 nm emission wavelengths were used for **HeliDye1,** (*rac*)**-HeliDye3,** (*P*)**-HeliDye3** and (*M*)**-HeliDye3**. Images were processed in Zen Black (v. 2.3, Carl Zeiss, Germany) and Image J. Presented picture is pseudo-colored with hot orange and blue colors for **HeliDye1,** (*rac*)**-HeliDye3,** (*P*)**-HeliDye3** and (*M*)**-HeliDye3** and DAPI, respectively (Fig. S15 and Fig. S16, and Fig. 6B in the manuscript). *(M)*-**HeliDye3** stains non-specifically and only very weakly the whole cell which is shown in overexposed image Fig. S16.

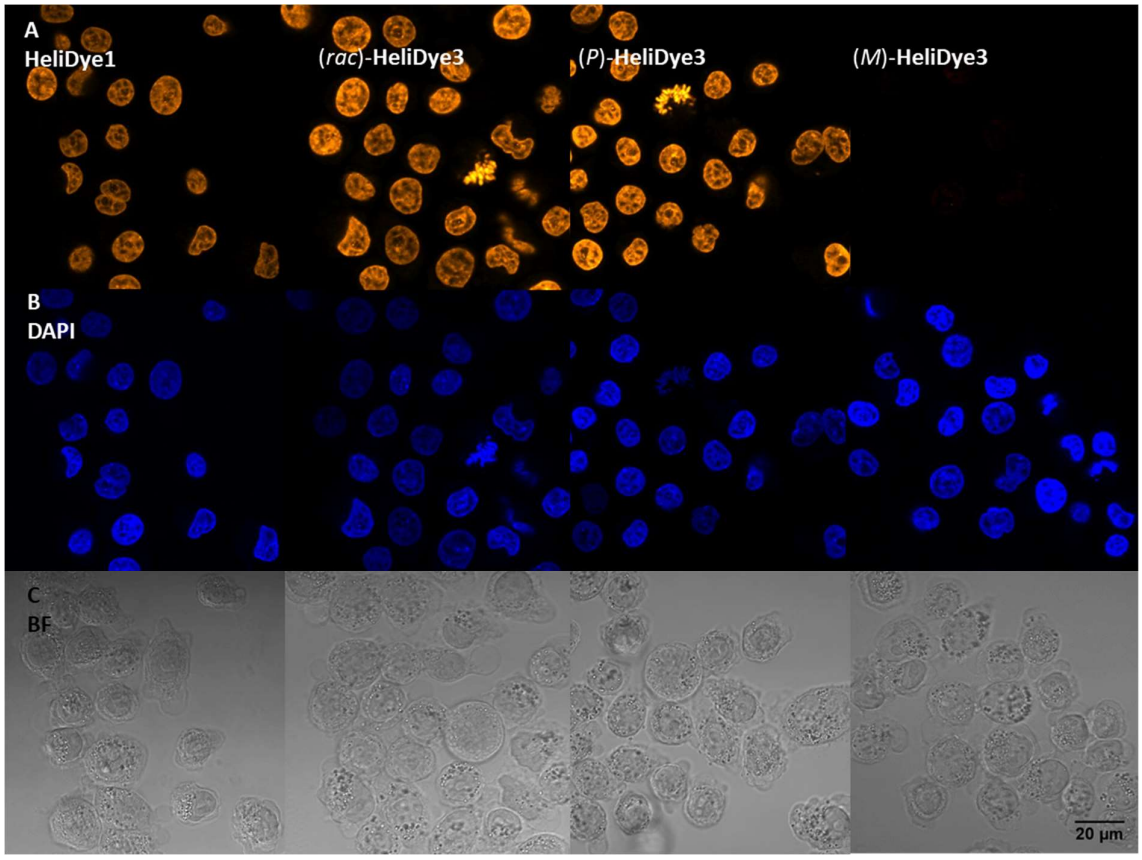


***Fig. S15*** *Confocal microscopy image shows co-staining of nuclei of fixed HeLa S3 cells with* ***HeliDye1****, (rac)-****HeliDye3****, (P)-****HeliDye3****, (M)-****HeliDye3*** *and DAPI at concentration 1 µM for all dyes. Panel A:* ***Helidye's*** *fluorescence channel Ex.488 nm (Em. 500-600 nm). Panel B: DAPI fluorescence channel Ex.405 nm (Em. 410-465 nm). Panel C: Bright field (BF). Scale bar 20 µm.* $c_{Helidyes}$ *= 1 µM and* $c_{DAPI}$ *= 1 µM. Settings for all* ***HeliDyes*** *and both channels are exactly the same to enable direct comparison of dye intensity and staining pattern. (M)-****HeliDye3*** *was not visible in* ***HeliDye's*** *fluorescence channel under given conditions.*

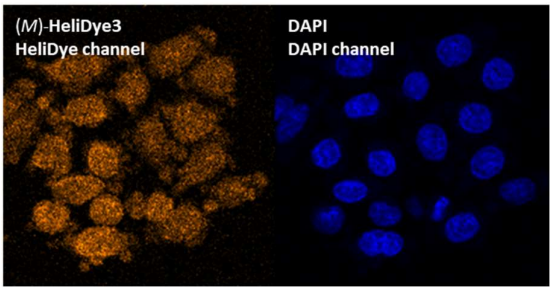


***Fig. S16*** *Confocal microscopy image shows co-staining of fixed HeLa S3 cells with (M)-**HeliDye3** and DAPI at concentration 1 µM for both dyes. Left: Overexposed (M)-**HeliDye3** fluorescence channel Ex.488 nm (Em. 500-600 nm). Right: DAPI fluorescence channel Ex.405 nm (Em. 410-465 nm). (M)-**HeliDye3** stains non-specifically and only very weakly the whole cell, in contrast to strong nuclear staining achieved by DAPI.*

## 16.6. Chromosomal staining, karyotyping:

**HeliDye1** was tested on mitotic spread preparates (Normal Metaphase CGH Slides, cat. no. 6J9601; Vysis, Abbott Molecular Inc.). The chromosome spreads were covered by the 5 µM solution of the **HeliDye1**, incubated for 5 min, washed (2 x SSC, pH 7.1), counter stained with DAPI (300 nM, cat no. 28718-90-3, Sigma Aldrich) and mounted in Mounting Medium (cat. no. PCN003, Cytocell). The samples were evaluated in epifluorescence microscope (exc. 480 nm; Olympus BX60), images were captured and karyotyped with ISIS, FISH Imaging System (Metasystems) containing CGH (comparative genomic hybridization) module. Magnification 1000x (Fig. 6D in the manuscript, Fig. S17).

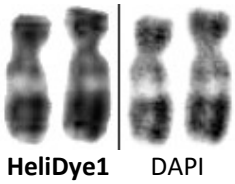


***Fig. S17*** *Chromosomal banding on chromosomes 17 observed in **HeliDye1** chanel (left) and DAPI chanel (right).*

## 16.7. Viability assay:

**HeliDye1** was evaluated for cytotoxic activity *in vitro* against a panel of human cancer and three non-cancer cell lines by using the standard 3-day MTS test[27]. The cancer cell lines were derived from acute T-lymphoblastic leukemia CCRF-CEM, chronic myeloid leukemia K562 and their multidrug resistant counterparts (CEM-DNR, K562-TAX) expressing the LRP and P-glycoprotein (P-gp) transporter proteins involved in tumor resistance, respectively. Additionally, solid tumor cell lines, including lung (A549) and colon (HCT116, HCT116p53-/-) adenocarcinomas, cervical tumor (HeLa) and osteosarcoma cell line (U-2 OS). For comparison, two human non-cancer fibroblast (BJ, MRC-5) and one endothelial (HUVEC) cell lines were included in the study.

## 17. Super-resolution microscopy

Bacteria *Staphylococcus Aureus* in the exponential growth were washed with PBS, centrifuged and fixed with 70% ethanol.The fixed bacteria were kept at -20 °C until further use. The bacterial suspension in 70% ethanol (0.5 μL) was stained by solution of **HeliDye1** in PBS (5 μM; 1 μL) so the resulted concetration of **HeliDye1** was 3.3 μM. Stained bacterial suspension (0.5 μL) was placed in a sterile and dast-free Petri dish (high performance cover glass; cat. no. D35-20-1.5H; Cellvis, USA). The sample was covered by thin (approximately 3 mm) pad of 1% low-melting agarose in PBS. The sample was imaged on super-resolution microscope Zeiss Elyra PS.1, 100x/1.46 Oil DIC M27 Elyra Objective alpha Plan-Apochromat, Tube Lens 1.6x, FWFOVPosition TIRF_HP, Axio Observer Andor1, excitatation laser: 488 nm HR Diode Laser 300 mW (100%), gain 300, frame interval 31.7 ms. For the analysis, 50 000 frames were recorded and the first 2 000 frames were disgarded due to higher fluorescence intensity (what caused mathematical problem for the analysis). Data were processed and analysed using ImageJ with a plug-in ThunderSTORM (the open-source software designed for interactive and automated processing, analysis and visualization of data acquired by single-molecule localization microscopy[28]). From resulted 48 000 images a median was calculated which was further subtracted from each image (subtraction of the background). From resulted 48 000 frames, the final image was reconstructed mathematicaly by following procedure. The single molecule localisations were firstly detected, then their accurate localizations were estimated and then processed mathematically (in the order: drift correction, merging, remove duplicates, density filter, second drift correction, uncertenity and offset filters, third drift correction, second density filter). The resulted set of processed localisations (75 000 pairs of x,y coordinates) was visualized by normalized Gaussian method (lateral uncertainty 20 nm; magnification 40; final pixel size 2.5 nm × 2.5 nm). Precise description of the procedure with all the settings is following:

{"version": "ThunderSTORM (dev-2016-09-10-b1)","imageInfo": {"title": "Substracted 1.000Median from substack 48k.tif"},
"cameraSettings": {"readoutNoise": 0.0, "offset": 414.0, "quantumEfficiency": 1.0,"isEmGain": true, "photons2ADU": 3.6,"pixelSize": 100.0,"gain": 100.0},
"analysisFilter": {"name": "Wavelet filter (B-Spline)","scale": 2.0,"order": 2},
"analysisDetector": {"name": "Local maximum","connectivity": 8,"threshold": "std(Wave.F1)*4"},
"analysisEstimator": {"name": "PSF: Gaussian","fittingRadius": 3,"method": "Maximum likelihood", "initialSigma": 1.6,"fullImageFitting": false,"crowdedField": {"name": "Multi-emitter fitting analysis", "mfaEnabled": false,"nMax": 0,"pValue": 0.0,"keepSameIntensity": false,"intensityInRange": false}},
"postProcessing": [{"name": "Drift correction","options": "magnification=10.0 method=[Cross correlation] ccsmoothingbandwidth=0.1 save=false steps=24 showcorrelations=false"},
{"name": "Merging","options": "zcoordweight=0.1 offframes=2 dist=20.0 framespermolecule=0"},
{"name": "Remove duplicates","options": "distformula=uncertainty_xy"},
{"name": "Density filter","options": "neighbors=5 radius=70.0 dimensions=2D"},
{"name": "Drift correction","options": "magnification=20.0 method=[Cross correlation] ccsmoothingbandwidth=0.1 save=false steps=36 showcorrelations=false"},
{"name": "Filter", "options": "formula=[(uncertainty_xy >7 & uncertainty_xy < 27) & (offset > 0.00001 & offset < 50) ]"},
{"name": "Drift correction","options": "magnification=20.0 method=[Cross correlation] ccsmoothingbandwidth=0.07 save=false steps=48 showcorrelations=false"},
{"name": "Density filter","options": "neighbors=5 radius=60.0 dimensions=2D"}],
"is3d": false,"isSet3d": true}

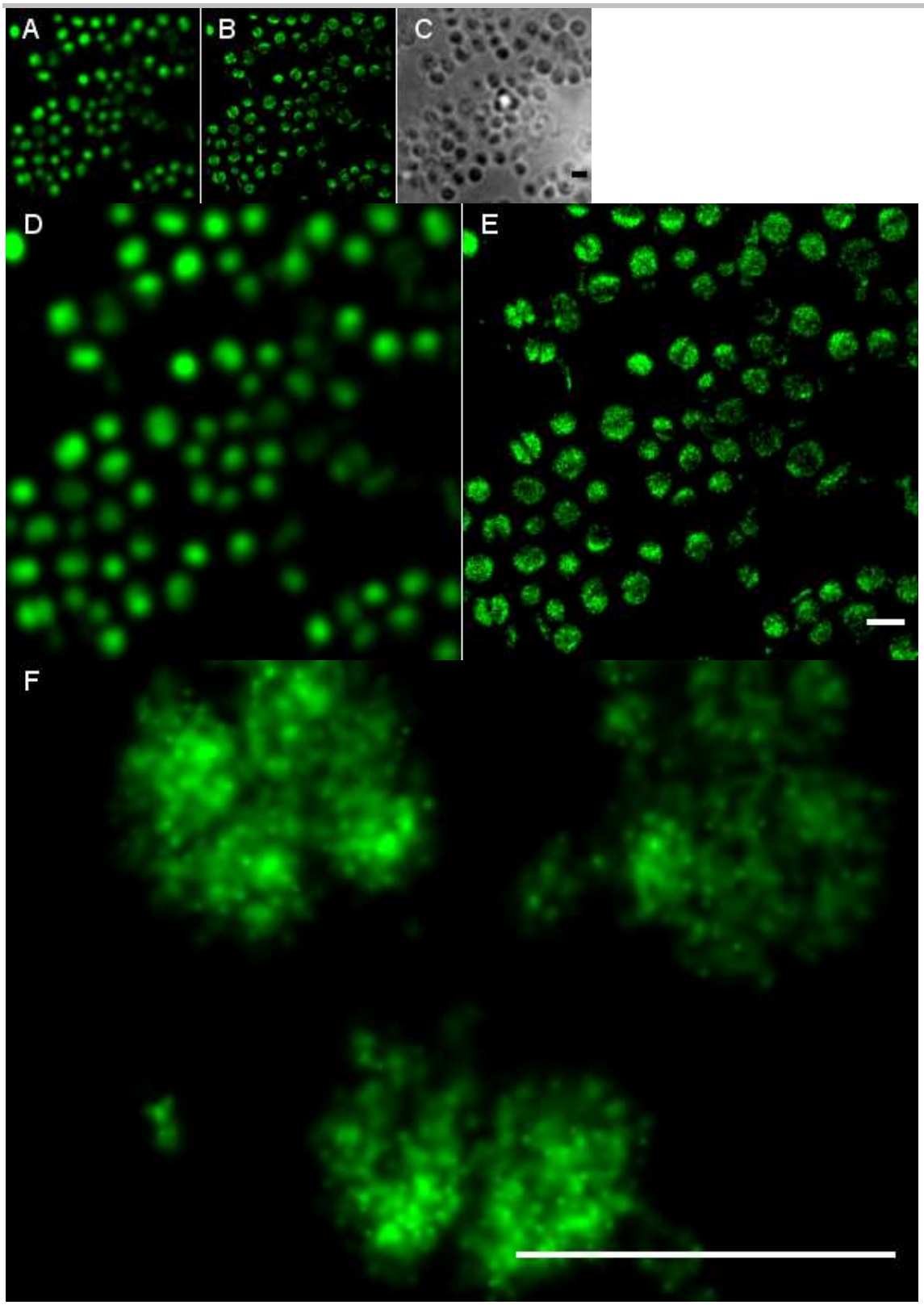


***Fig. S18*** *(A) Fluorescence microscopy image of Staphylococcus Aureus treated by HeliDye1 in original size and resolution. (B) Super-resolution image with the identical size is depicted for comparison reasons. (C) Bright field image. (D) Magnified (2.5 x) image A cannot reveal more information due to resolution of original image. (E) Super-reslution image shows more details than image B due to 2.5 x magnification. (F) Small part of the super-reslution image (part of 7B from manuscript) upon 25 x magnification reveals all details but can also contain artefacts. Scale bars in all images represent 1 μm.*

## 18. Notes and references


1. Amabilino, D. B., Ashton, P. R., Reder, A. S., Spencer, N. & Stoddart, J. F. Olympiadane. *Angew. Chem. Int. Ed. Engl.* **33**, 1286–1290 (1994).
2. Gray, A. P. *et al.* Approaches to Protection against Nerve Agent Poisoning. (Naphthylvinyl)pyridine Derivatives as Potential Antidotes. *J. Med. Chem.* **31**, 807–814 (1988).
3. Kasmi-Mir, S. *et al.* Synthesis of New Rhodacyanines Analogous to MKT-077 under Microwave Irradiation. *Synth. Commun.* **37**, 4017–4034 (2007).
4. Reyes-Gutiérrez, P. E. *et al.* Functional helquats: Helical cationic dyes with marked, switchable chiroptical properties in the visible region. *Chem. Commun.* **51**, 1583–1586 (2015).
5. Shen, Y. & Smith, R. D. High-resolution capillary isoelectric focusing of proteins using highly hydrophilic-substituted cellulose-coated capillaries. *J. Microcolumn Sep.* **12**, 135–141 (2000).
6. Koval, D., Kašička, V. & Cottet, H. Analysis of glycated hemoglobin A1c by capillary electrophoresis and capillary isoelectric focusing. *Anal. Biochem.* **413**, 8–15 (2011).
7. Sheldrick, G. M. A short history of SHELX. *Acta Crystallogr. Sect. A Found. Crystallogr.* **64**, 112–122 (2008).
8. QIAGEN. RNeasy Mini Handbook. *Sample Assay Technol.* 50–54 (2012).
9. Miller, J. M. *GraphPad PRISM*. *Analysis* vol. 52 (2003).
10. Sabnis, R. W. *Handbook of Fluorescent Dyes and Probes*. *Handbook of Fluorescent Dyes and Probes* (John Wiley & Sons, Inc, 2015).
11. Louis, S. Gold Biotechnology Protocol TD-P Revision 2.0 Creation GelRed™ Nucleic Acid Gel Stain, 10,000X Procedure for staining dsDNA, ssDNA or RNA in gels. 2017–2020 (2019).
12. Laboratories Bio-Rad. A Guide to Polyacrylamide Gel Electrophoresis and Detection. *Bio-Rad* 47 (2012).
13. www.molbiotools.com/dnacalculator.html.
14. M. J. Frisch *et al.* Gaussian 16, Revision A.03. *Gaussian, Inc., Wallingford CT* (2016).
15. Stephens, P. J., Devlin, F. J., Chabalowski, C. F. & Frisch, M. J. Ab Initio calculation of vibrational absorption and circular dichroism spectra using density functional force fields. *J. Phys. Chem.* **98**, 11623–11627 (1994).
16. Lee, C., Yang, W. & Parr, R. G. Development of the Colic-Salvetti correlation-energy formula into a functional of the electron density. *Phys. Rev. B* **37**, 36–39

(1988).

17. Becke, A. D. A new mixing of Hartree-Fock and local density-functional theories. *J. Chem. Phys.* **98**, 1372–1377 (1993).

18. Grimme, S., Antony, J., Ehrlich, S. & Krieg, H. A consistent and accurate ab initio parametrization of density functional dispersion correction (DFT-D) for the 94 elements H-Pu. *J. Chem. Phys.* **132**, (2010).

19. Scalmani, G. & Frisch, M. J. Continuous surface charge polarizable continuum models of solvation. I. General formalism. *J. Chem. Phys.* **132**, (2010).

20. Boese, A. D. & Martin, J. M. L. Development of density functional for thermochemical kinetics. *J. Chem. Phys.* **121**, 3405–3416 (2004).

21. Severa, L. *et al.* Resolution of a configurationally stable [5]helquat: Enantiocomposition analysis of a helicene congener by capillary electrophoresis. *New J. Chem.* **34**, 1063–1067 (2010).

22. Zgarbová, M. *et al.* Refinement of the Sugar-Phosphate Backbone Torsion Beta for AMBER Force Fields Improves the Description of Z- and B-DNA. *J. Chem. Theory Comput.* **11**, 5723–5736 (2015).

23. Wang, J., Wolf, R. M., Caldwell, J. W., Kollman, P. A. & Case, D. A. Development and testing of a general Amber force field. *J. Comput. Chem.* **25**, 1157–1174 (2004).

24. Berendsen, H. J. C., Postma, J. P. ., van Gunsteren, W. F. & Hermans, J. Interaction models for water in relation to protein hydatation. *Intermol. Forces* **3**, 331–334 (1981).

25. Berendsen, H. J. C., Postma, J. P. M., Van Gunsteren, W. F., Dinola, A. & Haak, J. R. Molecular dynamics with coupling to an external bath. *J. Chem. Phys.* **81**, 3684–3690 (1984).

26. Noskova, V. *et al.* In vitro chemoresistance profile and expression/function of MDR associated proteins in resistant cell lines derived from CCRF-CEM, K562, A549 and MDA MB 231 parental cells. *Neoplasma* **49**, 418–425 (2002).

27. Borkova, L. *et al.* Lupane and 18α-oleanane derivatives substituted in the position 2, their cytotoxicity and influence on cancer cells. *Eur. J. Med. Chem.* **121**, 120–131 (2016).

28. Ovesný, M., Křížek, P., Borkovec, J., Švindrych, Z. & Hagen, G. M. ThunderSTORM: A comprehensive ImageJ plug-in for PALM and STORM data analysis and super-resolution imaging. *Bioinformatics* **30**, 2389–2390 (2014).